STARS

Electronic Theses and Dissertations, 2004-2019

2015

Stability and Control in Complex Networks of Dynamical Systems

Saeed Manaffam
University of Central Florida

Part of the Engineering Commons

Find similar works at: https://stars.library.ucf.edu/etd

University of Central Florida Libraries http://library.ucf.edu

University of Central Florida

STARS
Showcase of Text, Archives, Research & Scholarship

STABILITY AND CONTROL IN COMPLEX NETWORKS OF DYNAMICAL SYSTEMS

by

SAEED MANAFFAM
M.Sc. in Electrical Engineering, University of Rochester, NY, 2012
M.Sc. in Digital Communications Systems, Sharif University of Technology, Iran, 2008
B.Sc. in Electrical Engineering, Amirkabir University of Technology, Iran, 2006

A dissertation submitted in partial fulfilment of the requirements
for the degree of Doctor of Philosophy
in the Department of Electrical Engineering and Computer Science
in the College of Engineering and Computer Science
at the University of Central Florida
Orlando, FL

Summer Term
2015

Major Professor: Azadeh Vosoughi

ABSTRACT

Stability analysis of networked dynamical systems has been of interest in many disciplines such as biology and physics and chemistry with applications such as LASER cooling and plasma stability. These large networks are often modeled to have a completely random (Erdös-Rényi) or semi-random (Small-World) topologies. The former model is often used due to mathematical tractability while the latter has been shown to be a better model for most real life networks.

The recent emergence of cyber physical systems, and in particular the smart grid, has given rise to a number of engineering questions regarding the control and optimization of such networks. Some of the these questions are: *How can the stability of a random network be characterized in probabilistic terms? Can the effects of network topology and system dynamics be separated? What does it take to control a large random network? Can decentralized (pinning) control be effective? If not, how large does the control network needs to be? How can decentralized or distributed controllers be designed? How the size of control network would scale with the size of networked system?*

Motivated by these questions, we began by studying the probability of stability of synchronization in random networks of oscillators. We developed a stability condition separating the effects of topology and node dynamics and evaluated bounds on the probability of stability for both Erdös-Rényi (ER) and Small-World (SW) network topology models. We then turned our attention to the more realistic scenario where the dynamics of the nodes and couplings are mismatched. Utilizing the concept of ε-synchronization, we have studied the probability of synchronization and showed that the synchronization error, ε, can be arbitrarily reduced using linear controllers.

We have also considered the decentralized approach of pinning control to ensure stability in such complex networks. In the pinning method, decentralized controllers are used to control a fraction of the nodes in the network. This is different from traditional decentralized approaches where all the nodes have their own controllers. While the problem of selecting the minimum number of pinning nodes is known to be NP-hard and grows exponentially with the number of nodes in the network we have devised a suboptimal algorithm to select the pinning nodes which converges linearly with network size. We have also analyzed the effectiveness of the pinning approach for the synchronization of oscillators in the networks with fast switching, where the network links disconnect and reconnect quickly relative to the node dynamics.

To address the scaling problem in the design of distributed control networks, we have employed a random control network to stabilize a random plant network. Our results show that for an ER plant network, the control network needs to grow linearly with the size of the plant network.

Every challenging work needs self efforts as well as guidance of elders especially those who are very close to our hearts. My humble effort, I dedicate to

my loving Mother & memory of my Father,

whose affection, love and encouragement made me to get such a success and honor.

In memory of

Prof. Alireza Seyedi

without whom this would not be possible.

ACKNOWLEDGMENTS

TABLE OF CONTENTS

LIST OF FIGURES

LIST OF TABLES

CHAPTER 1: LITERATURE REVIEW

The study of collective dynamics of networked systems has found significant interest and applications in a variety of disciplines including but not limited to social sciences (random gossip), biology (nervous system), physical sciences (plasma, laser cooling) and engineering (autonomous agents, communications networks and smart grids) [3–16].

Recently as the study of collective behavior of dynamical systems has reached some level of maturity [3], the stabilization and control of these complex networks have started to receive a great deal of attention by engineers and scientists [17–19].

In this chapter, we will introduce the basic concepts and review the significant contributions and literature relevant to the study of the collective behavior of these large complex networks as well as stabilization and control of these dynamics.

Background and Basic Concepts

There are two important aspects to the study of the collective dynamics in the networked systems. The first feature of networked systems is the dynamics of isolated systems, referred to as nodes. The second feature is the particular structure in which these nodes interact with each other. A brief introduction of the concepts related to these features is given below.

Dynamical Systems

Since systems which can be expressed with ordinary differential equations (ODE) constitutes a large class of dynamical systems, this introduction is limited to this class of systems. This

class of systems can be denoted as

$$\dot{\mathbf{x}} = \mathbf{f}(\mathbf{x}, t), \quad \mathbf{x}(t_0) = \mathbf{x}_0. \tag{1.1}$$

In particular we study an autonomous system where the function $\mathbf{f}$ does not depend explicitly on t

$$\dot{\mathbf{x}} = \mathbf{f}(\mathbf{x}). \tag{1.2}$$

$\mathbf{f} : \mathbb{R}^n \to \mathbb{R}^n$. We note that the study of autonomous systems can be generalized to non-autonomous systems via defining $\mathbf{y} = [\mathbf{x}^T, t]^T$ and $\mathbf{f}'(\mathbf{y}) = [\mathbf{f}^T(\mathbf{x}), 1]^T$.

One important concept in the study of dynamical systems is the concept of an *equilibrium point*, also called a *fixed point*.

Definition 1. *A point* $\mathbf{x} = \mathbf{x}^\star$ *is a fixed point of* (1.2), *if the state of the system starts at* $\mathbf{x}^\star$ *and remains at* $\mathbf{x}^\star$ *for all future time [20].*

Since for all future time the trajectory starting at $\mathbf{x}^\star$ stays there, $\mathbf{f}(\mathbf{x}^\star) = \mathbf{0}$. Therefore, fixed points are the solution of $\mathbf{f}(\mathbf{x}) = \mathbf{0}$.

Based on the behavior of the trajectories of the system in the neighborhood of $\mathbf{x}^\star$, fixed points are categorized as [2]:

1. **Attractors (sinks)**: fixed points which attract all the nearby trajectories.

2. **Repellors (sources)**: fixed points which repel all the nearby trajectories.

3. **Saddle points**: fixed points that attract trajectories on one side but repel them on the other.
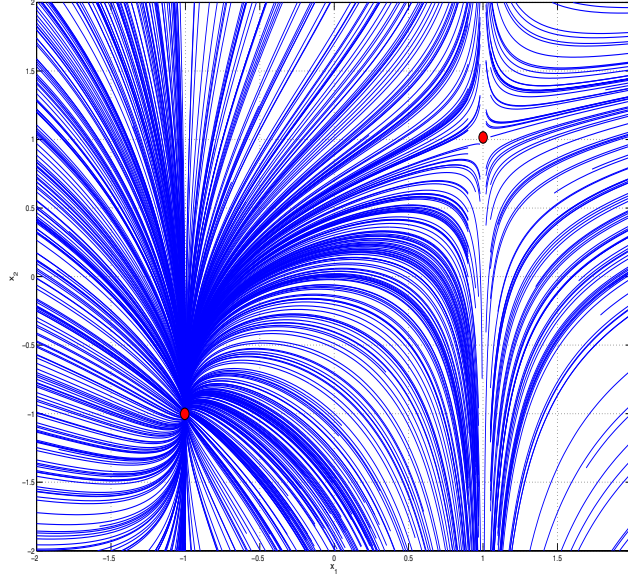
Figure 1.1: Behavior of trajectories near attracting (left) and repelling (right) fixed points, $c = 1$.

Definition 2. *The* basin of attraction *for a particular attractor is the set of initial points* $\{\mathbf{x}_0\}$ *such that the trajectories starting from each of these points approach the attractor as* $t \to \infty$ *[2].*

Theorem 1. *Let* $\mathbf{x}^\star$ *be a fixed point of* $\dot{\mathbf{x}} = \mathbf{f}(\mathbf{x})$, *i.e.,* $\mathbf{f}(\mathbf{x}^\star) = \mathbf{0}$, *and*

$$\mathbf{F} = \left. \frac{\partial}{\partial \mathbf{x}} \mathbf{f}(\mathbf{x}) \right|_{\mathbf{X} = \mathbf{X}^\star},$$

then the fixed point, $\mathbf{x}^\star$, *is exponentially stable if* $\mathbf{F} \prec \mathbf{0}$ *[2].*

The maximum eigenvalue of $\mathbf{F}$ is called the *characteristic value* of $\mathbf{x}^\star$.

Example 1. *Let*

$$\begin{bmatrix} \dot{x}_1 \\ \dot{x}_2 \end{bmatrix} = \begin{bmatrix} x_1^2 - c^2 \\ x_1 - x_2 \end{bmatrix},$$

then $\mathbf{x}_1^\star = (-|c|, -|c|)$ *and* $\mathbf{x}_2^\star = (|c|, |c|)$ *are two equilibrium points of the system with*

3

respective characteristic values of $\max(-|c|, -1)$ *and* $2|c|$. *Hence,* $\mathbf{x}_1^\star$ *is an attracting/stable fixed point and* $\mathbf{x}_2^\star$ *is repelling/unstable fixed points of the system. Fig. 1.1 illustrates the behavior of the trajectories near these fixed points.*

Oscillation or periodic behavior is another feature of dynamical systems.

Definition 3. *A system is said to have a nontrivial periodic solution or* limit cycle, *if*

$$\exists T > 0 \; \ni \; \mathbf{x}(t + T) = \mathbf{x}(t).$$

One example of such behavior can be found in van der Pol oscillator

$$
\begin{bmatrix} \dot{x}_1 \\ \dot{x}_2 \end{bmatrix} = \begin{bmatrix} -x_2 \\ -x_1 - \gamma(x_1^2 - 1)x_2 \end{bmatrix}
$$

Fig. 1.2 shows the oscillatory behavior of two trajectories in van der Pol system.

Another interesting behavior of nonlinear dynamical systems is *order determined* randomness, called *chaotic* behavior [2]. This order determinism comes from the fact that given the set of equations and initial conditions the evolution of the trajectories determines the subsequent behavior for future time [2]. One example of such systems is Rössler oscillator,

$$
\begin{bmatrix} \dot{x}_1 \\ \dot{x}_2 \\ \dot{x}_3 \end{bmatrix} = \begin{bmatrix} 0 & -1 & -1 \\ 1 & \alpha & 0 \\ 0 & 0 & -\beta \end{bmatrix} \begin{bmatrix} x_1 \\ x_2 \\ x_3 \end{bmatrix} + \begin{bmatrix} 0 \\ 0 \\ \gamma + x_1 x_3 \end{bmatrix},
$$

where $[\alpha, \; \beta, \; \gamma] \in \mathbb{R}^3$ are the set of known parameters. It is known that for certain ranges of these parameters, the system undergoes chaos [2].

Sample trajectories of Rössler oscillator are shown in Fig. 1.3.

4
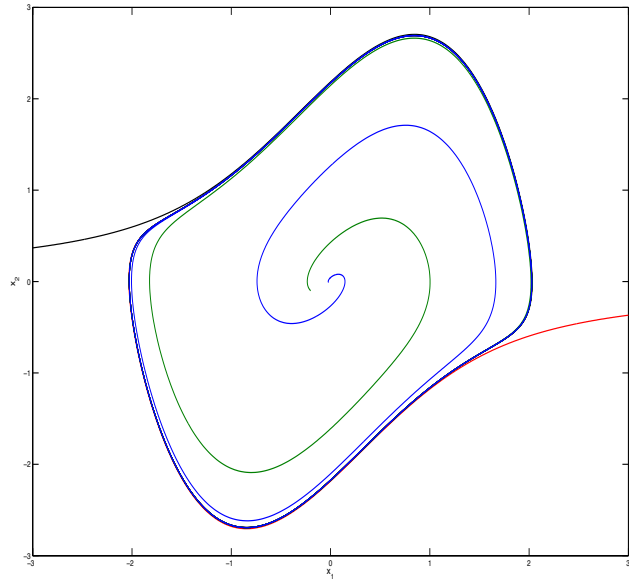
Figure 1.2: The van der Pol limit cycle, $\gamma = 1$.
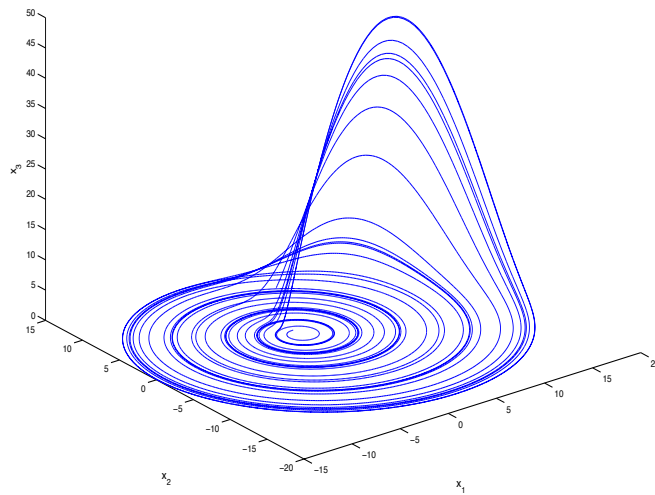
Figure 1.3: Sample trajectories of Rössler oscillator with chaotic behavior, $[\alpha, \ \beta, \ \gamma] = [0.165, \ 10, \ 0.2]$.

Stability

Here we will briefly review a central concept of systems theory known as *stability theory*.

Definition 4. *[20] The equilibrium point* $\mathbf{x} = \mathbf{0}$ *of system* (1.2)

- *is stable, if* $\forall \epsilon > 0$, *there exists* $\delta > 0$ *such that*

$$\|\mathbf{x}(0)\| < \delta \quad \Rightarrow \quad \|\mathbf{x}(t)\| < \epsilon, \quad \forall t \geq 0,$$

  and otherwise it is unstable.

- *is asymptotically stable, if the system is stable and* δ *can be chosen such that*

$$\|\mathbf{x}(0)\| < \delta \quad \Rightarrow \quad \lim_{t \to \infty} \mathbf{x}(t) = \mathbf{0}.$$

- *is exponentially stable, if the system is stable and there exists* $c, \alpha > 0$ *such that*

$$\|\mathbf{x}(0)\| < \delta \quad \Rightarrow \quad \|\mathbf{x}(t)\| \leq c\|\mathbf{x}(0)\|e^{-\alpha t}, \quad \forall t \geq 0.$$

Lyapunov Exponent

As linearization is proven to be a useful tool in the study of nonlinear dynamical systems, it is often used to determine the behavior of the trajectories near a certain set of points in the state space [2] [20]. Of course, one should be wary of the conditions under which linearization results in correct predictions. For instance, some of the justifications of using linearization are based on checking the regularity of the dynamics, Lipschitz condition [21].

By linearization of an autonomous system in (1.2), we have

$$\dot{\mathbf{x}} = \mathbf{F}\,\mathbf{x}, \quad \mathbf{x}(t_0) = \mathbf{x}_0, \tag{1.3}$$

where $\mathbf{F} = \partial\mathbf{f}/\partial\mathbf{x}$ is the Jacobian of the function $\mathbf{f}$ calculated on the set of points which the behavior is sought to be determined. In general, $\mathbf{F}$ is time varying, but for brevity of notation, argument t is omitted.

One measure to determine the behavior of trajectories in (1.3) is to calculate what is called *Lyapunov exponents* [2]. To calculate these exponents, one should first calculate the state transition matrix[1], $\Phi(t, t_0)$, for (1.3), then the ith Lyapunov exponent is

$$\sigma_i = \limsup_{t \to \infty} \frac{1}{2t}\mathrm{Real}\left\{\ln\left(\lambda_i\left(\Phi(t, t_0)^T\Phi(t, t_0)\right)\right)\right\}, \; i \in \{1, \cdots, n\} \tag{1.4}$$

where $\lambda_i(\cdot)$ returns the ith eigenvalue of the argument, and $\mathrm{Real}(\cdot)$ returns the real part of its argument.

Based on this measure, it is known that for a system to undergo chaos, at least one of the Lyapunov exponents should be positive. The set $\{\sigma_i, i = 1, \cdots, n\}$ is called *Lyapunov spectrum*. Based on signs and values of the Lyapunov exponents expected behavior of the system can be determined. Table 1.1 gives the possible behaviors expected for three dimensional systems based on the Lyapunov exponents.

Note that if all the Lyapunov exponents of an equilibrium point are negative then the equilibrium point is exponentially stable [2].

---

[1]The state transition matrix can be computed by Peano-Baker series [2].

Table 1.1: Spectra of Lyapunov exponents and the associated attractors for 3D state space [2].

signs of σ's	Types of attractors
$(-,-,-)$	Fixed points
$(0,-,-)$	Limit cycle
$(0,0,-)$	Quasi-periodic Torus
$(+,0,-)$	Chaotic attractor

Theorem 2. *[2] If the maximum Lyapunov exponent of* (1.3) *is negative, then* $\mathbf{x} = \mathbf{0}$ *is exponentially stable.*

Lyapunov Direct Method

Another method of investigating the behavior of dynamical systems is known as Lyapunov direct method.

Theorem 3. *[20] Let* $\mathbf{x} = \mathbf{0}$ *be an equilibrium point for* (1.2). *Let* $V : \Omega \to \mathbb{R}$, *be a continuously differentiable function on a neighborhood* Ω *of* $\mathbf{x} = \mathbf{0}$, *such that*

$$V(0) = 0 \quad and \quad V(\mathbf{x}) > 0 : \forall \mathbf{x} \in D - \{\mathbf{0}\},$$

$$\dot{V}(\mathbf{x}) \leq \mathbf{0}, \quad \forall \mathbf{x} \in D.$$

Then, $\mathbf{x} = \mathbf{0}$ *is stable. Moreover, if*

$$\dot{V}(\mathbf{x}) < 0, \quad \forall \mathbf{x} \in D - \{\mathbf{0}\}$$

then $\mathbf{x} = \mathbf{0}$ *is asymptotically stable.*

$V(\mathbf{x})$ in Theorem 3 is called Lyapunov function. One unique feature of Lyapunov direct method is that no differential equation is needed to be solved. Also, it is noteworthy that Theorem 3 only provides sufficient condition on the stability [20].

As it can be seen the Lyapunov theorem is only applicable to equilibrium points. To extend the theorem to study of limit cycles and/or chaotic attractors, *LaSalle invariant principle* has been introduced [22]. The following is the definition of an *invariant set* which is used in the principle.

Definition 5. *[20] The set $\mathcal{M}$ is called invariant set with respect to* (1.2) *if*

$$\mathbf{x}(0) \in \mathcal{M} \quad \Rightarrow \quad \mathbf{x}(t) \in \mathcal{M}, \quad \forall t \in \mathbb{R} \tag{1.5}$$

This means that if a solution belongs to $\mathcal{M}$ at some time instant, it belongs to $\mathcal{M}$ for all past and future time.

Theorem 4. *[20, LaSalle Invariance Principle] Let Ω be a compact (closed and bounded) set with the property that every solution of* (1.2) *which starts in Ω stays in Ω for all future time. Let $V : \Omega \to \mathbb{R}$ be a continuously differentiable function such that $\dot{V}(\mathbf{x}) \le 0, \forall \mathbf{x} \in \Omega$. Let $\mathcal{E}$ be the set of all points in Ω where $\dot{V}(\mathbf{x}) = 0$. Let $\mathcal{M}$ be the invariant set in $\mathcal{E}$. Then every solution starting in Ω approaches $\mathcal{M}$ as $t \to \infty$.*

Complex Networks

The mathematical notion of a complex network is a graph $\mathcal{G}$ consisting of a set of N nodes connected by a set of M links. This graph is uniquely represented by the adjacency matrix $\mathbf{A} = [a_{ij}]$, where entries $a_{ij} = 1$ if a directed link from j to i exists, and 0 otherwise. In the general case of a weighted network, a_{ij} represents the weight of the link from node j to

node i [23] [24]. The number of the links which connects node i to other nodes is called the degree of node i and is denoted by d_i.

Investigating the statistical properties of many real-world and artificial complex networks reveals that despite different network representations, some categorizations of these properties are possible. The most representative statistical property is the *degree distribution $P(d)$* which indicates the probability of a node having degree d. While historically, the degree distribution has been the first measure for studying the complex networks, several other measures are found to be more useful and effective [4]. Two of these prominent measures are the *average shortest path length*, ℓ^2, and the *clustering coefficient*, C. The average shortest path length is defined as

$$\ell = \frac{1}{(N-1)^2} \sum_{i,j=1}^{N} q_{ij},$$

where q_{ij} is the length of the shortest path[3] between node i and node j. The clustering coefficient is defined as "the fraction of actual triangles (three vertices forming a loop) over possible triangles in the graph". One way to calculate C is

$$C = \frac{1}{N} \sum_{i=1}^{N} C_i = \frac{1}{N} \sum_{i=1}^{N} \frac{2n_i}{d_i(d_i - 1)},$$

where n_i is the number of links between nearest neighbors of node i and d_i is its degree [3].

Another important property of a given network is its *spectra*, which refers to the eigenvalues

---

[2]Also known as characteristic path length.

[3]In case of the weighted networks, and this is minimal sum of the weights belonging to a path from node i to node j.

of the Laplacian matrix[4]. The Laplacian matrix of a network, $\mathbf{L} = [l_{ij}]$, is defined as

$$l_{ij} \triangleq \begin{cases} \sum_{m=1}^{N} a_{mi} & i = j \\ -a_{ij} & i \neq j \end{cases} . \tag{1.6}$$

Per definition, the Laplacian matrix is positive semidefinite. Since the entries on each row add up to zero, zero is an eigenvalue of the Laplacian matrix, with the all-one vector as its right eigenvector [24]. It has been shown that if the network is connected, i.e., there exists a path from each node to any other arbitrary node in the network, zero is a simple eigenvalue of the Laplacian matrix [24]. The second smallest eigenvalue of the Laplacian matrix is a measure of network's connectivity and is referred to as its *algebraic connectivity* [24] [25]. That is, a bigger algebraic connectivity implies a stronger connected network.

Classifying complex networks based on the degree distribution, $P(d)$, separates the networks to homogenous or heterogenous classes [3]. Homogeneity of the network is determined by the tail of the degree distribution. If the tail of the degree distribution rolls off exponentially with the degree, the network is referred to as *homogeneous*, otherwise, the network is called *heterogeneous* [3].

This classification can be improved upon by additionally taking the average shortest path length of the network into account. This parameter can be used as a measure of *smallness* of the network. That is, a smaller ℓ implies that the nodes in the network can be reached in smaller number of hops. This parameter is also referred to as small-world property [3]. Clustering coefficient, C, is another useful parameter in classification of the networks, where larger C values imply the existence of redundant paths and smaller C values imply otherwise.

---

[4]Also known as gradient matrix.
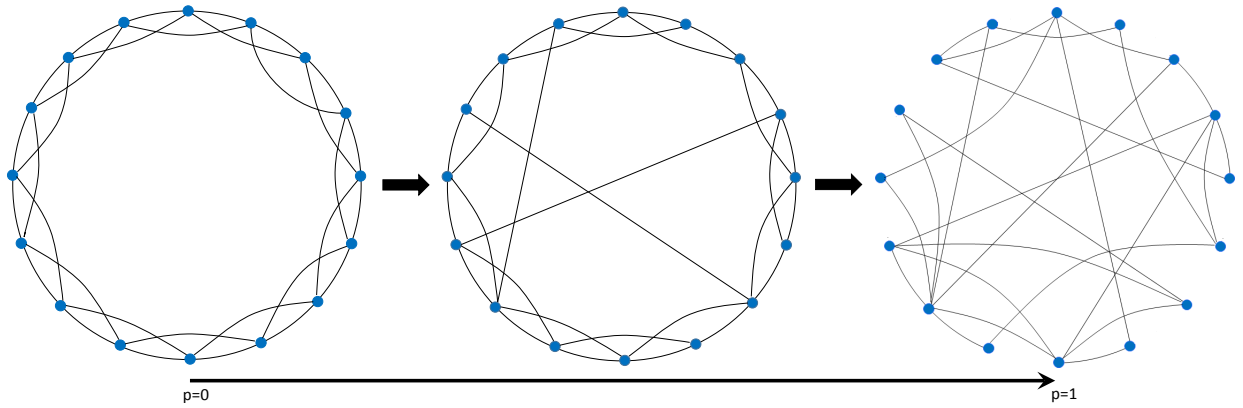
Figure 1.4: The transition from regular network to SW and random network.

Network Models

Here, three common structures of mathematical interest for the networks are briefly reviewed.

Regular network or lattice: a connected network which has the property of $d_i = d$ is called a regular network or lattice [4]. This is also known as d-regular networks. Fig. 1.4-left shows a lattice with $d = 4$. A regular network is homogeneous and its characteristic path length scales as $\ell \sim N^{1/d}$ and its clustering coefficient is

$$C = \frac{3(d-2)}{4(d-1)}.$$

Erdös-Rényi or random network: if the link between two arbitrary nodes exists with probability p, and otherwise nonexistent, the resulted network is called Erdös-Réyni network, and is denoted by $\mathcal{G}(N, p)$. Fig. 1.4-right shows an example of random network. An Erdös-Rényi network is also homogenous. . Its characteristic path length scales with logarithm of net-

work size given a constant average degree, $\ell \sim \ln(N)/\ln(\bar{d})$, where $\bar{d}$ is the average degree of the network, hence even when the network is large the average shortest path length is small [3] [23].

Small-worlds: one of the seminal works on the modeling of the networks has been done by Watts and Strogatz [4][5]. This work was intended to create a comprehensive model to understand the effect of substrate networks on the synchronization phenomena in real-world networks. The model predicts the highly correlated connections between the nodes as if there are invisible long range links between distant nodes in the network. This property in the real-world networks is known as *small-world* (SW) effect [3] [4] [6]. This model shows that if we start from a regular network and remove one end of a small number of links with probability p and reattach the free-end of these links with equal probability (in random) to other nodes, for $p \geq p_c$, the average distances between the nodes, ℓ, will be reduced drastically in the resulted network. As the number of rewired links increases the network becomes more and more random where for $p = 1$ the network is completely random. Fig. 1.4 shows this transition from regular networks to small-worlds and random networks.

A revision to the model came shortly after. In the revised model, instead of rewiring the existing connections, a small number of connections (with respect to the network order, M) is established in random to acquire the small-world [6]. This revision simplifies the original model, thus rendering it more suitable for analytical approaches [6]. In addition to having a small characteristic path length which scales logarithmically with the network size (like random networks), small-worlds also have the property of preserving the large clustering coefficients of the substrate regular network [6].

---

[5]Of course there were some experimental studies before this work, where *small-world* property was reported. Two instances of such studies are S. Milgram 's experiment of 1969 and "six degree of separation" concept by F. Karinthy in 1929 [3] [26, 27].

Even though the small-world models bridge the gap between regular and random networks, real-world networks prove to be more complex. Since the new model failed to give a comprehensive understanding of the behavior of the substrate network, a pragmatic model was introduced by Barbási and Albert [7]. In this model, the inherent nature for the formation of the real-world networks, such as preferential attachment and connectivity saturation[6], was also taken into account [3] [7] [25]. The real-world networks are usually a result of mechanism, whereby in the evolution of the network, new comers prefer to attach to the existing nodes with a higher number of links, also called *hubs*. The resultant networks have power-law degree distribution, $P(d) = d^{-\gamma}$ where γ is a positive constant. It has been shown that many real-world networks such as World Wide Web (WWW), electrical grids, etc. bear this property [7]. As it can be seen the degree distribution of power-law is independent of the network size, hence it does not scale with N and consequently, these networks are called "scale-free" (SF). Since the degree distribution is power-law, these networks have a small number of highly connected nodes, referred to as *hubs*, and a large number of nodes have very small number of links [7]. Since the degree distribution in scale-free networks has a heavy tail, these networks are classified as heterogeneous networks.

Synchronization in Complex Networks

One of the most intriguing collective behaviors found in complex network of dynamical systems is the phenomenon of synchronized states.

One of the earliest reports of the synchronization or "odd kind of sympathy" was reported by C. Huygens in 1665 where it was observed that two pendulum clocks with shared supporting

---

[6]That is, each node can handle/allow certain number/weight of connections, also called capacity constraint.

frame, swung with the same frequency in 180 degree phase difference [3]. The reported behavior would be also restored in case that the pendula were disturbed [3].

The problem formalization evolved with time and was first expressed in its current form by Wiener in his book, Cybernetics, to study and comprehend of synchrony between large groups of neurons, fireflies, or crickets at the same time [28].

It was not until A. T. Winfree's paper in 1967 work that the breakthrough in the study of this kind of collective behavior occurred [29]. Winfree's work was based on the mean field theory where the nodes (elements) in the network (population) were considered to be phase oscillators [3] [29]. In this formulation, only the synchronization of the phases in the oscillators was considered, while the amplitude of oscillators was ignored. Kuramoto 's oscillator is one of the common models used in this setup [3].

Following Winfree's work, there has been considerable efforts to study the structural and dynamical effects of the network on the emergence of the synchrony.

Parallel to the study of phase synchronization, there has been a lot of attention devoted to analysis of state synchronization in the network of identical oscillators [3]. A breakthrough in this research thrust was accomplished by Pecora and Carroll. When solving the problem of state-synchronization, they introduced the concept of master stability function (MSF) and chose the negativeness of the *maximum Lyapunov exponent* (MLE) of traverse modes as a measure of the stability for the synchronization status of the network [5].

One of the key benefits of the master stability condition (MSC) approach is that the impact of topological characteristics of the network on the stability of the synchronization can be assessed separately from the dynamical properties of the nodes in the network [3] [5] [30].

Let $\mathcal{N} = \{1, \cdots, N\}$ and let $\mathbf{x}_i \in \mathbb{R}^n$ be the state vector for node i, $i \in \mathcal{N}$, in the network of $|\mathcal{N}| = N$ identical nodes. Let the individual dynamics be $\dot{\mathbf{x}}_i = \mathbf{f}(\mathbf{x}_i)$ where $\mathbf{f} : \mathbb{R}^n \to \mathbb{R}^n$ [5]. Suppose $\mathbf{h} : \mathbb{R}^n \to \mathbb{R}^n$ is the inner coupling function of the states. Hence the dynamics of the network of N coupled oscillators can be expressed as

$$\dot{\mathbf{x}}_i = \mathbf{f}(\mathbf{x}_i) - c \sum_{j \in \mathcal{N}} a_{ij}(\mathbf{h}(\mathbf{x}_j) - \mathbf{h}(\mathbf{x}_i)), \quad \forall i \in \mathcal{N}$$

$$\mathbf{x}_i(t_0) = \mathbf{x}_i^0,$$

or equivalently,

$$\dot{\mathbf{x}}_i = \mathbf{f}(\mathbf{x}_i) - c \sum_{j \in \mathcal{N}} l_{ij}\mathbf{h}(\mathbf{x}_j), \quad \forall i \in \mathcal{N} \tag{1.7}$$

$$\mathbf{x}_i(t_0) = \mathbf{x}_i^0,$$

where c is the coupling strength, a_{ij} indicates the weight of the connection from node j to node i, and, $\mathbf{L} = [l_{ij}]$ is the Laplacian matrix of the network. If the network is assumed to be connected, then zero is a simple eigenvalue of the Laplacian matrix of the network with the all-one vector as its corresponding eigenvector. Also in this section we assume that network is symmetric/bidirectional, hence the Laplacian is diagonalizable by the unitary matrix [31].

Let $N - 1$ constraints $\mathbf{x}_1 = \cdots = \mathbf{x}_N$ define the synchronization manifold, and $\mathbf{s}$ to be the synchronization state. Also, let the error vector of node i from the synchronization manifold be

$$\mathbf{e}_i \triangleq \mathbf{x}_i - \mathbf{s}.$$

16

Then the variational equation corresponding to (1.7) is

$$\dot{\mathbf{e}}_i = \mathbf{F}\,\mathbf{e}_i - c \sum_{j \in \mathcal{N}} l_{ij}\,\mathbf{H}\,\mathbf{e}_j, \quad \forall i \in \mathcal{N}, \tag{1.8}$$

$$\mathbf{e}_i(t_0) = \mathbf{e}_i^0,$$

where $\mathbf{F} = \partial\mathbf{f}/\partial\mathbf{x}|_{\mathbf{x}=\mathbf{s}}$ and $\mathbf{H} = \partial\mathbf{h}/\partial\mathbf{x}|_{\mathbf{x}=\mathbf{s}}$ are the Jacobians of the vector-functions $\mathbf{f}$ and $\mathbf{h}$ calculated on the trajectory, $\mathbf{s}$, respectively. Note that $\mathbf{F}$ and $\mathbf{H}$ are in general time varying, but we have dropped the notation for the sake of brevity.

Equation (1.8), can also be represented as

$$\dot{\mathbf{e}} = (\mathbf{I} \otimes \mathbf{F} - c\,\mathbf{L} \otimes \mathbf{H})\,\mathbf{e}, \tag{1.9}$$

$$\mathbf{e}(t_0) = \mathbf{e}^0,$$

where $\mathbf{e} = [\mathbf{e}_1^T, \cdots, \mathbf{e}_N^T]^T$.

As it will be shown in the following chapters, equation (1.9) is equivalent to

$$\dot{\boldsymbol{\eta}} = (\mathbf{I} \otimes \mathbf{F} - c\,\boldsymbol{\Lambda} \otimes \mathbf{H})\,\boldsymbol{\eta}, \tag{1.10}$$

$$\boldsymbol{\eta}(t_0) = \boldsymbol{\eta}^0,$$

where $\boldsymbol{\eta} = (\mathbf{U}^H \otimes \mathbf{I})\mathbf{e}$ and $\mathbf{U}$ is the unitary matrix which diagonalizes the Laplacian matrix, $\mathbf{L} = \mathbf{U}\boldsymbol{\Lambda}\mathbf{U}^H$, and $\boldsymbol{\Lambda}$ is a diagonal matrix, with eigenvalues of the Laplacian matrix as its diagonal entries [5] [24] [31].

As it is noted in [5], $\boldsymbol{\eta}_N$ corresponding to $\mu_N = 0$ gives the variations parallel to the synchronization manifold, $\mathbf{s}$, which will be ignored in this section. To study this term we identify the

synchronization manifold in Chapter 3. As $\boldsymbol{\eta}_i$, $i = 1, \cdots, N-1$ are traverse to the manifold, for the realization of synchronization state, it is necessary that these traverse modes to be damped out. In other words, $\mathbf{0}$ should be a stable equilibrium point of

$$\dot{\boldsymbol{\eta}}' = (\mathbf{I} \otimes \mathbf{F} - c\,\boldsymbol{\Lambda}' \otimes \mathbf{H})\,\boldsymbol{\eta}', \tag{1.11}$$

$$\boldsymbol{\eta}'(t_0) = \boldsymbol{\eta}^{0'},$$

where $\boldsymbol{\eta}' = [\boldsymbol{\eta}_1^T, \cdots, \boldsymbol{\eta}_{N-1}^T]^T$ and $\boldsymbol{\Lambda}' = \mathrm{diag}([\mu_1, \cdots, \mu_{N-1}])$. Hence the synchronization is achievable if $\mathbf{0}$ is the stable equilibrium of the following

$$\dot{\boldsymbol{\eta}}_i = (\mathbf{F} - c\,\mu_i\,\mathbf{H})\boldsymbol{\eta}_i, \quad \forall i \in \mathcal{N} - \{N\}, \tag{1.12}$$

$$\boldsymbol{\eta}_i(t_0) = \boldsymbol{\eta}_i^0,$$

where μ_i is the ith largest eigenvalue of the Laplacian matrix of the network.

From Theorem 2, we know if the MLE of $(\mathbf{F} - c\,\mu_i\,\mathbf{H})$ is negative for $i \in \mathcal{N} - \{N\}$, the synchronization would be achieved [5].

Calculation of MLE for the generic equation of

$$\dot{\mathbf{z}} = (\mathbf{F} - c\lambda\mathbf{H})\mathbf{z}$$

as a function of λ gives the *master stability function* (MSF) of the network [5].

Based on the definition of MSF, $\sigma(\cdot)$, can be defined as

$$\sigma(\lambda) \triangleq \mathrm{MLE}(\mathbf{F} - c\lambda\mathbf{H}), \tag{1.13}$$

where MLE($\cdot$) returns the maximum Lyapunov exponent of the argument. Three types of MSFs of interest are [1]:

1. Type I: monotonically increasing MSF (e.g. $\mathbf{H}$ is negative definite) where the stability region is $c\lambda(\mathbf{L}) \in (0, \alpha_1)$, with α_1 being the positive root of the MSF.

2. Type II: monotonically decreasing MSF (e.g. $\mathbf{H}$ is positive definite) where the stability region is $c\lambda(\mathbf{L}) \in (\alpha_1, +\infty)$, with α_1 being the positive root of the MSF.

3. Type III: MSF which returns negative values in the finite interval (α_1, α_2) (e.g. $\mathbf{H}$ is positive semidefinite), where $\alpha_1 < \alpha_2$ are the positive roots of the MSF.

Fig. 1.5 shows the MSF types of practical interest.
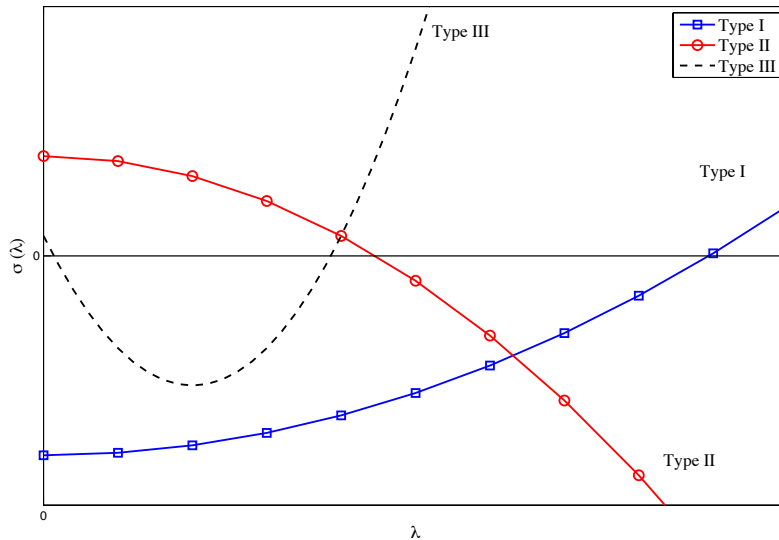
Figure 1.5: Three types of master stability function of interest [1].

19

Literature Review on Synchronization in Complex Networks

Following Pecora's work, the vast majority of the existing literature on the subject have adopted the negativeness of the largest traversal Lyapunov exponent as a measure of stability of the synchronization. Of course, as noted in [5] and [21], the negativity of Lyapunov exponents, *in general*, is neither a necessary nor a sufficient condition on the stability of the synchronization manifold itself and it does not stop the manifold from *bubbling* and *bursting* [5]. The condition of having MSF to be negative is called master stability condition (MSC).

Since MSC leads to useful bounds on structural properties of the network, especially the eigenvalues of its Laplacian matrix, scientists have been more focused on studying ways to relate the bounds on the eigenvalues of the Laplacian matrix imposed by the MSC to other properties of the network, such as minimum or maximum degree of the nodes, average degree, etc. [5] [6] [11] [12] [30] [32] [33] [34]. These studies have been extended to understand the relation of synchronizability of the network to its macroscopic and/or qualitative characteristics such as regularity, smallness, randomness or scalability [30] [32] [33].

Even though the random networks are of limited practical interest, their study helps to pave the path to understand dynamical flow in the networks with some degree of randomness such as small-worlds or scale-free networks. Although, it has been numerically shown in [11] [35] [36] that in large random networks, the average degree is the parameter directly linked to the stability of the synchronization, rigorous analytical treatment has been lacking.

Due to practical interest in small-worlds, the synchronizability analysis in such networks has drawn a lot of attention in many disciplines [3] [30] [32] [33] [34] [37]. It has been shown that the synchronization is easier to achieve in small-worlds compared to regular

networks [30] [34]. It has been also shown that in addition to small characteristic path in small-worlds, homogeneity of these networks contributes to their enhanced synchronizability [33] [38]. That is, as the network becomes more heterogeneous, e.g., scale-free networks, the synchronization is harder to achieve [33] [38]. Furthermore, it has been shown that the synchronizability of the network is closely related to the spectra of the Laplacian matrix of the network. Along this line, there have been some attempts to approximate the distribution of the spectra for different network types, such as random networks [11], and small-worlds [39]. The approximations of the Laplacian spectra in these studies have been performed using low orders of moments of the Laplacian matrix specially in the case of small-worlds [39].

Most of these studies consider the networks to be unweighted and undirected, however, there have been some attempts in analysis of weighted-undirected and binary directed networks [40–42]. In [5], it has been shown that for directed networks, where the eigenvalues of the Laplacian matrix of the network are not real, the short and long wavelength bifurcation phenomena can happen in regular networks (lattices). Also, the stability of the synchronization in the context of time-varying or switching networks has been studied in [43–45].

Even though the study of the synchronization in the networks of identical nodes appears to be matured, there have been a few attempts made to study the networks under more realistic assumptions. One such assumption is to consider inner couplings and isolated dynamics being mismatched. One of the reports on the synchronization of slightly different oscillators is given in [46]. The authors report that even in the networks where the oscillator dynamics and their couplings vary slightly from each other, the network can be almost synchronized. That is, the states will converge to the vicinity of a certain synchronization state. In [47] and [48], a sensitivity analysis of synchronization has been performed for the network of mismatched oscillators. It has been shown that near-synchronization behavior can occur in a network of mismatched oscillators using master stability function. The general stability

of the synchronization in the network of dynamical systems with nonidentical dynamics for each node is studied in [49] and [50] using the Lyapunov direct method. However, in most of these studies the effects of uncertainties in the weights of the links and inner couplings have been ignored [51]. Also to the best of the author 's knowledge, there has been no attempt to investigate the phase transition in which the network undergoes this type of synchronization (neighborhood synchronization).

Switching Networks

Although the majority of the synchronization literature study static networks, where the links are considered to be fixed in time, in most applications the network evolves with time [52]. One of the interesting models of the time varying networks is the one with switching structure, where existing links are removed or new links are established through a deterministic or stochastic process. The use of non-conservative methods, such as MSF, for analysis of the switching networks requires simultaneous (joint) upper-triangularization of the Laplacian matrix of the set of networks which switching is chosen from[7]. This substantially limits the scope of the study of this kind of networks [53] [54]. Also the joint upper-triangularization of the matrix set guarantees the existence of common quadratic Lyapunov function (CQLF) for the *linear time-invariant* (LTI) systems [53]. Since CQLF is conservative, switched quadratic Lyapunov functions (SQLF) has attracted some attentions [55]. The idea is that if all the networks in the switching set are synchronizable, the Lyapunov function of each network can be concatenated based on the switching signal to form a global Lyapunov function. Alternatively, the synchronizability of the network-set under arbitrary switching can be checked by examining a set of linear matrix inequalities (LMI) [54]. Another method in analysis of the

---

[7]The simultaneous upper-triangularization of any set of matrices is only possible if the Lie algebra produced by the matrix set is solvable (nilpotent) [53] [54].

synchronization/stability of the network is called multiple Lyapunov function (MLF) [56]. In this method, for each network in the set a Lyapunov function is found with negative definite derivative. The concatenation of these multiple Lyapunov functions constructs a positive semidefinite function, with guaranteed negative definite derivative everywhere with the exception of the switching instances[8]. Now if the values of the concatenated function at the switching instances are descending, then negative definiteness of the derivatives of all consisting Lyapunov functions the ensures stability of the synchronization [54]. Unlike SQLF[9], MLF can correspond to different regions of the state space, which renders it useful in designing of the switching control signal [53]. The result for synchronization under arbitrary switching can be found in [54] and references therein.

Under the particular condition of deterministic (or stochastic) fast switching, it has been shown that the results obtained for the static network can be applied to the time-average (stochastic average, i.e., expected value) of the architecture of the network [52] [57]. The network is considered to be fast switching if the establishment and removal of connections are faster than the dynamics of individual nodes. Examples of such networks can be found in moving particles in plasma, mobile agents in wireless sensor networks, UAVs and etc. [43] [52] [58].

---

[8]Hence MLF is not a Lyapunov function.

[9]SQLF only partitions the time domain while MLF can partition state space as well.

Control of complex networks

In control theory, the controllability of a dynamical system is defined as the following [59] [60]

A system with a suitable choice of inputs is controllable if it can be driven from any arbitrary initial state to a certain target state within a finite time.

Although control theory is mathematically matured in many applications, its advance in complex networked systems is hindered [60]. The issue is that the controllability of such systems is determined by two independent factors, the first factor is the topology of the system, i.e., how the subsystems interact with each other; and the second factor is the governing dynamics of each individual subsystems [60]. With the availability of deeper understanding of structural/topological properties of complex networks, recently there have been profound results regarding the controllability of these networks (see [60–62] and the references therein).

The need to regulate the behavior of systems consisting of many interconnected components is a common feature for most applications in social, biological sciences and engineering. Hence, designing a network of controllers (control network) that can guarantee a specific behavior of a given network of plants is of utmost importance. Examples include but not limited to synchronous heart beat cells, synchronization of neurons in nervous systems, flight formation of unmanned aerial vehicle (UAV), networked control systems in industrial plants, opinion dynamics in social networks by leaders, and cell cycles in biology [62–64].

Historically, the first controllers designed for networks were centralized, where all the state information was known at a central point and control laws were determined using all that information [61]. Even though the optimal control is possible with this kind of controller

design, the scalability and complexity issues and the requirement of the availability of perfect state information of the whole network at all times forced engineers to trade-off the optimality of such controllers to overcome some of the obstacles in the implementation process [61].

To alleviate some of the issues regarding centralized control design, an extreme alternative is decentralized control. In this approach controllers use only the local state information to form a control law for each node. This way the complexity of the controller design is reduced and thus, the solution can be easily scaled. Decentralized control is more effective in a network of sparsely or weakly coupled subsystems [65–67]. Even though the simplicity and scalability of the design is achieved with this method, the performance drastically suffers. Pinning control is an example of decentralized control.

In pinning control, the set of nodes is divided into two subsets, one subset consists of nodes that have self-feedback and knowledge of the target set. These nodes are called pinned nodes. The nodes without any controllers form the other subset. The pinned nodes play the role of leaders or pacemakers in the network. The desired action is initiated only from these nodes and propagates to the rest of the network [62] [63].

Pinning Control

As this study will mostly focus on the analysis of synchronization and its stability in complex networks, the effects of pinning on the synchronizability of such networks will be reviewed here. Since first proposed in [68], pinning control has been a viable candidate to achieve stability in complex networks. This technique is utilized to compensate for spectral requirement of the architecture of the original network and/or to achieve the robustness of the stability of the synchronization in the event of link failures and other sources of disturbances [17] [18] [34] [60] [62] [63]. Sometimes pinning is used when the network is expected

to reflect a predetermined behavior. For instance in opinion networks, such a predetermined behavior/opinion comes from leaders, the synchronous beats of heart cells which is generated by pacemaker cells in sinoatrial node, or following a reference trajectory in a group of UAVs, etc. [62] [63].

The pinning controllability has been defined in [62] and has been shown to be equivalent to the synchronizability of an augmented system. The augmented system includes an additional node which is the reference signal in the local controller and its connections are directed from that node to the pinned set and zero to the rest of nodes [58].

It has been shown in [17] that a network of oscillators can be stabilized by a single controller. Clearly, pinning a network in this manner requires a very large controller gain, which is practically undesirable if not impossible. This idea has been evolved to use multiple controllers with smaller controller gains to obtain a practical design of controllers with utilizing a small number of controllers [19] [49] [69]. In [69], pinning of higher degree nodes has been investigated which has been shown to be effective in scale-free networks. As it was pointed out previously, when the network evolves based on preferential attachment of new comers, controlling the hubs, where the arriving nodes are likely to be connected, helps the scalability and efficiency of the control. In [19], assuming that the inner coupling matrix is positive definite (MSF type II), it is proposed to pin the lower degree nodes to stabilize the network globally. It has been shown that this approach outperforms that of [69]. In [70], the condition of positive definiteness of the coupling matrix has been relaxed to positive definiteness of symmetric part of its product with another positive definite matrix. It has been also shown that the number of pinning controllers is inversely related to feedback gain. The adaptive pinning control is used in [17], [19] and [71], where the controller gains are evolved by a differential equation. This approach provides robustness in the presence of possible uncertainties and perturbations.

In most of these studies, controllers' gains are considered to be equal, which makes the design of controllers conservative. Also these designs use the Lyapunov direct method, to form a control law and assign of the controllers, which adds another layer to their conservativeness. While this enhances the robustness of the controllers in the event of failures in the connections, the other approaches, in general, result in a fewer number of pinned nodes [63].

The optimal gains of controllers and their locations have been analyzed in [63]. The problem has been converted to a combinatorial and continuous optimization problem and solved by *particle swarm optimization.* This approach, even though effective in avoiding local optima compared to generic particle swarm optimization techniques, is computationally complex.

In [72], the cost optimization of pinning control and its effectiveness in several special networks such as, lattices, complete networks, cluster of star shaped sub-networks have been studied. Using MSF, it has been shown that pinning lower degree nodes yields in minimal cost of pinning for MSF-type II. In this work, cost function is assumed to be the sum of the controllers' gains.

In [43], the idea of "spatial pinning" has been introduced, where depending on the application, the individual assignments of the controllers is either impossible (e.g. plasma) or undesirable (e.g. mobile agents). The proposed method applies controllers to any mobile agent located in a fraction of the total deployed area. It is assumed that if two nodes are in certain distance of each other they become neighbors, i.e., coupled. If the nodes move adequately fast or if the density of the nodes is sufficiently large, a fast switching network emerges and the results of [52] or [57] can be applied to control the network. It has been shown that by choosing a sufficiently large controller area, i.e., pinning area, the network is synchronizable.

Node-to-node pinning control has been proposed in [58]. In this strategy, only one node is

pinned at any time instant but the controller (pinning point) switches in faster rate than the dynamics of individual nodes, hence the controller is *passed around* among the nodes. Even though the authors in [?] assumed a time-invariant network, the result is very similar to that of [43]. Considering the cost function to be the aggregate controllers' gains, the authors in [?] proved that the optimal gain assignment is to pin the nodes with uniform controller gains as it was conjectured by the extensive numerical results in [62].

Most of these studies assume that the inner coupling matrix, $\mathbf{H}$, is positive definite which means the MSF of the network is of type II form (see Fig. 1.5). Moreover, the methods of analysis in these literatures are mostly conservative (the Lyapunov direct method). Furthermore, these results, like pinning a lower degree nodes, are primarily based on extensive numerical simulations and not analytical. Also, the main part of these analyses is based on using a single controller to pin the network which usually results in a very large controller gain.

To mitigate some of the drawbacks in decentralized control, distributed control has been introduced. In these controllers the state information of other (neighboring) nodes is combined with the local state information to form the control law which increases the performance of the controllers. Distributed control can be used in a wide range of networks to achieve the stability of the entire network [61] [73]. Since this method uses the information from a wider subset of the network nodes, it can be much more effective than the decentralized approach. However, this approach attains the stability goal by increasing the size of the control network, which directly increases the cost by introducing communications of the state in the control network. Another drawback for this networked control method is that the availability and the proper estimation of the states at given time has been proven to be challenging in the implementation process [61].

Distributed Control

Here, the concept of distributed control is briefly described and the existing results are reviewed. Networked control systems are defined as [74]:

> "*Networked control systems (NCSs) are spatially distributed systems in which the communications between sensors, actuators, and controllers occur through a shared band-limited digital communication network.*"

As the controllability of arbitrary distributed networks is still to be determined, the impact of topological characteristics of the network on its stability is largely under-studied [73–76]. One major step in this direction has been accomplished in [60] ,where the structural controllability in complex networks of LTI systems has been studied.

To address some of the issues such as imperfect communications and structural uncertainties, different types of controllers are proposed to be used in distributed networks. Adaptive controllers are used to cope with the architectural changes and also to compensate for noisy data where quantizations of states, noise in observation, and errors in estimation of the recovered data's contribute to those uncertainties [74, 77].

Since the important feature of the implementation of distributed algorithms is communication and controller actuation, the event/time triggered controllers are commonly used in NCSs. These controllers, in most cases, relax the requirement of continuous transmission of data and they can operate on centralized or decentralized triggering rules [74] [78] [79]. In centralized type of triggering, the time sequence of information updates is calculated and communicated by a central entity, based on a global measure in the network, hence

the sampling is performed in a synchronous fashion in the nodes. However, as the limitation of communication and processing power gets contingent then the distributed, i.e., asynchronous, implementations are favorable. As an extension to event-triggering, a self-triggering is considered in [78] [80], where each node calculates the next update time at the current time. In this approach, the measurements are not needed to be tracked between two consecutive updates.

Although, there have been great strides made in the subject of distributed control, the question of scalability of the size of the controller network, also known as communication network, have received very little attention. That is, if the order and/or size of the network increase by some factors how does that effect the order and/or size of the control network?

Contributions of Thesis

As it is known the spectra of the Laplacian matrix is a major factor in determining the stability of the dynamical networks. However, there has been small progress on this subject. In chapter 2, we will provide asymptotic analysis of the spectra of the Laplacian matrix for random networks as well as small-worlds. Then in chapter 3, we will take on the synchronization problem in complex networks with uncertainties in isolated node dynamics, inner coupling and weights of the links. Additionally, with calculating the probability of the stability we will assess the transition of the mismatched network to synchrony.

Chapter 4 will provide the study of the pinning control with multiple pinning controllers under the assumption of the positive inner coupling matrices and constrained controllers' gains. The analysis will be performed by MSF like methods and a heuristic algorithm will be presented to identify the pinning set and the corresponding controllers' gains. It will be

shown that the algorithm results in improved performance in the sense of the number of pinning controllers, compared to existing methods. In chapter 5, by removing the condition of positive definiteness of the inner coupling matrices, the pinning problem will be studied in the network of moving agents where it is assumed that coupling/linkage of the agents changes faster than the dynamics of the isolated nodes.

In chapter 6, the problem of scalability of the controller network in the network of LTI nodes will be analyzed. Here it will be assumed that the controller network is Erdös-Rényi. We will show that the best controller network should be a subnetwork of the substrate network, called the plant network. The scalability factor of the controller network will be calculated as a function of the average degree of the plant network. Chapter 7 is dedicated to networks of linear-time varying systems which are partially observable. Finally, chapter 8 will conclude this study.

CHAPTER 2: PROBABILITY OF SYNCHRONIZATION IN LARGE COMPLEX NETWORKS

In this chapter, we use an alternative master stability condition (MSC) derived from Lyapunov direct method to obtain a sufficient condition on the stability of the network, based on the eigenvalues of symmetric part of local and coupling dynamics. We perform our analysis in a generalized framework where the linkage matrices are not limited to be diagonal and/or binary components), allowing multi-state and cross-state linkages, possibly with different strengths [81] [82]. We then use the derived MSC to calculate a lower bound on the probability of stability for large Erdös-Rényi and Newman-Watts small-world networks.

System Model

Consider a network of N identical nodes with identical coupling dynamics

$$\dot{\mathbf{x}}_i = \mathbf{f}(\mathbf{x}_i) - \sum_{j=1}^{N} l_{ij}\mathbf{h}(\mathbf{x}_j), \tag{2.1}$$

where $\mathbf{x}_i \in \mathbb{R}^n, 1 \leq i \leq N$ denote the state vector of node i, and $\mathbf{f}(\cdot)$ and $\mathcal{H}(\cdot)$ denote the node and coupling dynamics, respectively. $\mathbf{L} = [l_{ij}]$ is the Laplacian matrix of the network. We assume that the network is undirected, i.e. $l_{ij} = l_{ji}$ for all i, j. Since $\mathbf{L}$ has zero row-sum, this network has a synchronization state, $\mathbf{x}_0$, which is the solution of local state equation, $\dot{\mathbf{x}}_0 = \mathbf{f}(\mathbf{x}_0)$. This equation also defines the synchronization manifold. To maintain the synchrony throughout the network, all $\mathbf{x}_i$ should converge to a synchronous state, $\mathbf{x}_0$. This means that all the modes traverse to the synchronization manifold should be damped out [5]. Denote the deviation of the state of each node from the synchronous state by $\mathbf{e}_i = \mathbf{x}_i - \mathbf{x}_0$.

If $\mathbf{e}_i$ are small, (2.1) can be linearized around $\mathbf{x}_0$ as

$$\dot{\mathbf{e}}_i = \mathbf{F}\mathbf{e}_i - \sum_{j=1}^{N} l_{ij}\mathbf{H}\mathbf{e}_j, \tag{2.2}$$

where $\mathbf{F}$ and $\mathbf{H}$ are Jacobian matrices of $\mathbf{f}(\cdot)$ and $\mathcal{H}(\cdot)$ around $\mathbf{x}_0$, respectively. Note that in general, $\mathbf{x}_0$ is time dependent and so are $\mathbf{F}$ and $\mathbf{H}$. For cleaner notation, we have dropped their explicit dependence. Stacking (2.2) yields

$$\dot{\mathbf{e}} = (\mathbf{I} \otimes \mathbf{F} - \mathbf{L} \otimes \mathbf{H})\mathbf{e} = \tilde{\mathbf{F}}\mathbf{e}, \tag{2.3}$$

where $\mathbf{I}$ is the identity matrix, $\otimes$ denotes the Kronecker product, and $\mathbf{e} = [\mathbf{e}_1^T \ \cdots \mathbf{e}_N^T]^T$ is the error vector with respect to $\mathbf{1} \otimes \mathbf{x}_0$, where $\mathbf{1} = [1 \ \cdots \ 1]^T$.

Network stability condition

The network synchronization is exponentially stable, if $\tilde{\mathbf{F}}$ is exponentially stable. Since $\mathbf{L}$ has zero row sum, its smallest eigenvalue, μ_N, is zero [24]. The mode for $\mu_N = 0$ in (2.3) represents the variations parallel to manifold and hence should be omitted in the study of stability for traversal exponents [5]. Furthermore, multiplicity of zero in the set of network eigenvalues is one, if and only if the the graph is connected [24]. The remaining modes in (2.3) are traverse to the synchronization manifold and decay exponentially if and only if the remaining modes of (2.3) are exponentially stable. Considering (2.3), norm of $\mathbf{e}$ can be bounded by ([21] Thms. 1 and 2)

$$\|\mathbf{e}(t)\| \leq \|\mathbf{e}(t_0)\| \exp\left[\frac{1}{2}\int_{t_0}^{t} \lambda_1\left(\tilde{\mathbf{F}}(\tau) + \tilde{\mathbf{F}}^T(\tau) + \epsilon\mathbf{I}\right) d\tau\right],$$

33

for $t \geq t_0$ and $\epsilon > 0$, where $\lambda_i(.)$ denotes the ith largest eigenvalue of the argument. If $\tilde{\mathbf{F}} + \tilde{\mathbf{F}}^T + \epsilon\mathbf{I} \prec \mathbf{0}$ for all $t \geq t_0$, this bound approaches zero as t grows and the system is exponentially stable. Thus, a sufficient condition on stability is

$$\exists\,\epsilon > 0 \ \text{s.t.} \ \tilde{\mathbf{F}}(t) + \tilde{\mathbf{F}}^T(t) + \epsilon\mathbf{I} \prec \mathbf{0}, \ \forall t \geq t_0. \tag{2.4}$$

Since $\mathbf{L}$ is real and symmetric, it can be unitarily diagonalized as $\mathbf{L} = \mathbf{Q}\boldsymbol{\Lambda}\mathbf{Q}^T$. Consequently, $\tilde{\mathbf{F}}$ can be block diagonalized, using transform $\mathbf{Q}^T \otimes \mathbf{I}$. That is

$$(\mathbf{Q}^T \otimes \mathbf{I})\tilde{\mathbf{F}}(\mathbf{Q} \otimes \mathbf{I}) = (\mathbf{Q}^T \otimes \mathbf{I})(\mathbf{I} \otimes \mathbf{F})(\mathbf{Q} \otimes \mathbf{I}) - (\mathbf{Q}^T \otimes \mathbf{I})(\mathbf{Q}\boldsymbol{\Lambda}\mathbf{Q}^T \otimes \mathbf{H})(\mathbf{Q} \otimes \mathbf{I})$$

$$= \mathbf{I} \otimes \mathbf{F} - \boldsymbol{\Lambda} \otimes \mathbf{H}.$$

The diagonal block elements are $\mathbf{F} + \mu_i\mathbf{H}$, where μ_i is the ith largest eigenvalue of $\mathbf{L}$. Hence (2.4) can be replaced by

$$\exists\,\epsilon > 0 \ \text{s.t.} \ \mathbf{F} + \mathbf{F}^T - \mu_i\left(\mathbf{H} + \mathbf{H}^T\right) + \epsilon\mathbf{I} \prec 0, \ \forall t \geq t_0, \tag{2.5}$$

for $1 \leq i \leq N - 1$. Note that since $\mathbf{L}$ is symmetric, μ_i are real and non-negative.

Now we can use Weyl's inequalities to further explore (2.5). Assume that $\mathbf{B}$ and $\mathbf{C}$ are $n \times n$ Hermitian matrices, and $1 \leq j, k, j + k - n \leq n$, then Weyl's inequalities state that ([83] Thm. 1.3)

$$\lambda_{j+k-1}(\mathbf{B} + \mathbf{C}) \leq \lambda_j(\mathbf{B}) + \lambda_k(\mathbf{C}) \tag{2.6}$$

$$\lambda_{j+k-n}(\mathbf{B} + \mathbf{C}) \geq \lambda_j(\mathbf{B}) + \lambda_k(\mathbf{C}). \tag{2.7}$$

34

Utilizing (2.6) with $j + k = 2$ and (2.7) with $j + k - n = 1$ yields

$$\lambda_j(\mathbf{B}) + \lambda_{n-j+1}(\mathbf{C}) \leq \lambda_1(\mathbf{B} + \mathbf{C}) \leq \lambda_1(\mathbf{B}) + \lambda_1(\mathbf{C}), \tag{2.8}$$

for $1 \leq j \leq n$. Now, since $\mathbf{F} + \mathbf{F}^T$ and $-\mu_i(\mathbf{H} + \mathbf{H}^T)$ are Hermitian, we can use (2.8) to bound $\lambda_1(\mathbf{F} + \mathbf{F}^T - \mu_i\mathbf{H} - \mu_i\mathbf{H}^T) + \epsilon$ from both sides:

$$\begin{aligned} \lambda_1(\mathbf{F} + \mathbf{F}^T - \mu_i\mathbf{H} - \mu_i\mathbf{H}^T) + \epsilon \\ \leq \lambda_1(\mathbf{F} + \mathbf{F}^T) + \lambda_1(-\mu_i\mathbf{H} - \mu_i\mathbf{H}^T) + \epsilon \\ = \lambda_1(\mathbf{F} + \mathbf{F}^T) - \mu_i\lambda_n(\mathbf{H} + \mathbf{H}^T) + \epsilon, \end{aligned} \tag{2.9}$$

and

$$\begin{aligned} \lambda_1(\mathbf{F} + \mathbf{F}^T - \mu_i\mathbf{H} - \mu_i\mathbf{H}^T) + \epsilon \\ \geq \lambda_j(\mathbf{F} + \mathbf{F}^T) + \lambda_{n-j+1}(-\mu_i\mathbf{H} - \mu_i\mathbf{H}^T) + \epsilon \\ = \lambda_j(\mathbf{F} + \mathbf{F}^T) - \mu_i\lambda_j(\mathbf{H} + \mathbf{H}^T) + \epsilon, \end{aligned} \tag{2.10}$$

for $1 \leq j \leq n$.

To obtain a sufficient condition on stability we now force the upper bound in (2.9), to be negative

$$\lambda_1(\mathbf{F} + \mathbf{F}^T) - \min_{1 \leq i \leq N-1}\{\mu_i\lambda_n(\mathbf{H} + \mathbf{H}^T)\} + \epsilon < 0. \tag{2.11}$$

for some $\epsilon > 0$. Based on the sign of $\lambda_n(\mathbf{H} + \mathbf{H}^T)$, condition (2.11) reduces to

$$\begin{aligned} \mu_{N-1} > \mu^\dagger \quad \text{if } \lambda_n(\mathbf{H} + \mathbf{H}^T) > 0 \\ \mu_1 < \mu^\dagger \quad \text{if } \lambda_n(\mathbf{H} + \mathbf{H}^T) < 0, \end{aligned} \tag{2.12}$$

where $\mu^\dagger = (\lambda_1(\mathbf{F} + \mathbf{F}^T) + \epsilon)/\lambda_n(\mathbf{H} + \mathbf{H}^T)$. This means that, using the terminology introduced in [84], we can say that the *synchronizability set* of the network is $\{\mathbf{L}|\mathbf{L}$ satisfies (12)$\}$.

We can also derive a necessary condition for (2.5) by forcing the lower bound in (2.10) to be negative, or

$$\max_{i,j}\left\{\lambda_j(\mathbf{F}+\mathbf{F}^T) - \mu_i\lambda_j(\mathbf{H}+\mathbf{H}^T)\right\} + \epsilon \leq 0. \tag{2.13}$$

Let k_+ be the index of smallest positive eigenvalue of $\mathbf{H}+\mathbf{H}^T$. Then (2.13) reduces to

$$
\begin{aligned}
\mu_{N-1} &\geq \mu^\ddagger_{N-1} \triangleq \max_{j \geq k_+} \frac{\lambda_j\left(\mathbf{F}+\mathbf{F}^T\right)+\epsilon}{\lambda_j\left(\mathbf{H}+\mathbf{H}^T\right)} \\
\mu_1 &\leq \mu^\ddagger_1 \triangleq \max_{j < k_+} \frac{\lambda_j\left(\mathbf{F}+\mathbf{F}^T\right)+\epsilon}{\lambda_j\left(\mathbf{H}+\mathbf{H}^T\right)}
\end{aligned}
\qquad . \tag{2.14}
$$

In the case that $\lambda_j(\mathbf{H}+\mathbf{H}^T) = 0$, if $\lambda_j(\mathbf{F}+\mathbf{F}^T) > 0$ then the condition (2.5) is not satisfied, and if $\lambda_j(\mathbf{F}+\mathbf{F}^T) < 0$, the corresponding condition can be eliminated.

We note that, (2.14) is a necessary condition on (2.5), which itself is a sufficient condition on stability. Therefore (2.14) does not reveal anything about the stability of the network. However, since (2.12) and (2.14) sandwich (2.5), condition (2.14) provides information regarding how close (2.5) and (2.12) are.

Having developed the bounds on condition (2.5), namely (2.12) and (2.14), we now proceed to relate them to the degree properties of the network. To do this, we employ following inequalities known for symmetric Laplacian matrices [24]

$$\mu_{N-1} \leq \frac{N}{N-1}d_{\min} \;\; \text{and} \;\; \mu_1 \leq \frac{N}{N-1}d_{\max},$$

where $d_{\min}$ and $d_{\max}$ denote the minimum and maximum node degrees, respectively. Using

these, and (2.12), the stability condition can be also expressed as

$$
\begin{aligned}
d_{\min} \geq d_{\min}^{\dagger} &\triangleq \tfrac{N-1}{N}\mu_{N-1}^{\dagger} && \text{if } \lambda_n(\mathbf{H}+\mathbf{H}^T) > 0 \\
d_{\max} \leq d_{\max}^{\dagger} &\triangleq \tfrac{N-1}{N}\mu_{1}^{\dagger} && \text{if } \lambda_n(\mathbf{H}+\mathbf{H}^T) < 0
\end{aligned}.
$$

Similarly, necessary conditions for (2.5) become

$$
\begin{aligned}
d_{\min} \geq d_{\min}^{\ddagger} &\triangleq \tfrac{N-1}{N}\mu_{N-1}^{\ddagger} \\
d_{\max} \leq d_{\max}^{\dagger} &\triangleq \tfrac{N-1}{N}\mu_{1}^{\ddagger}
\end{aligned}
\tag{2.15}
$$

From (2.12) one can draw the conclusion that in the network with low algebraic connectivity, μ_{N-1}, synchronization is difficult to achieve. This behavior is caused by the fact that the coupling is not strong enough to push/pull the oscillators to synchronous state. And from (2.15) we can see the other case of non-synchronization behavior occurs when (some) nodes have too many connections (condition on $d_{\max}$). This phenomenon is known as synchronization quenching, where the coupling is so strong that eliminates the self-drive of (some of) the oscillators and consequently, the network cannot achieve synchrony [85].

Probability of Stability

Erdös-Rényi networks

In the following, we investigate probability of stability of Erdös-Rényi networks [23]. For large Erdös-Rényi networks with randomness parameter p, we can use (2.12) and (2.14) to calculate the lower and upper bounds on the probability of (2.5) being satisfied. We recall that (2.12) provides a lower bound on the probability of stability, whereas (2.14) describes

the closeness of this lower bound and the probability of (2.5).

Since eigenvalues of any large randomly generated symmetric matrix follows the Wigner's semi-circular distribution [86], we can approximate the distribution of eigenvalues of Laplacian for an Erdös-Rényi network. By definition, $\mathbf{L} = \text{diag}(\mathbf{d}) - \mathbf{A}$, where $\mathbf{A}$ is the adjacency matrix of the network, and $\mathbf{d}$ is the degree sequence of the nodes. Also in large Erdös-Rényi network, we can approximate $\text{diag}(\mathbf{d})$ by $Np\,\mathbf{I}$ [23]. Hence, $\mathbf{L} \approx Np\,\mathbf{I} - \mathbf{A}$. Thus the pdf of the eigenvalues of $\mathbf{L}$ is approximately [86]

$$
p_\mu(x) = \begin{cases} \frac{1}{\pi\sqrt{Np(1-p)}}\sqrt{1-X^2} & |X| < 1 \\ 0 & \text{elsewhere} \end{cases},
$$

where $X = \frac{x - Np}{2\sqrt{Np(1-p)}}$. The order statistics μ_{N-1} and μ_1 have densities

$$
p_{\mu_{N-1}}(x) = (N-1)[1 - P_\mu(x)]^{N-2}p_\mu(x),
$$

$$
p_{\mu_1}(x) = (N-1)P_\mu^{N-2}(x)p_\mu(x),
$$

where

$$
P_\mu(x) = \int_{(N-1)p-2\sqrt{Np(1-p)}}^{x} p_\mu(y)dy
$$

$$
= 1 - \frac{1}{\pi}\cos^{-1} X + \frac{1}{\pi}X\sqrt{1-X^2}.
$$

Now, we can evaluate the probability of occurrence of each conditions given in (2.12) and (2.14). The lower bound on the probability of stability attained from Wigner's approximation for (2.12) is

$$
P_{\text{W,LB}} = \begin{cases} 1 - \left[1 - P_\mu\left(\mu^\dagger\right)\right]^{N-1} & \lambda_n(\mathbf{H} + \mathbf{H}^T) > 0 \\ P_\mu^{N-1}\left(\mu^\dagger\right) & \lambda_n(\mathbf{H} + \mathbf{H}^T) < 0 \end{cases} \tag{2.16}
$$

Similarly, an upper bound on the probability of (2.5) can be derived by applying Wigner's approximation to (2.14) is

$$P_{\text{W,UB}} = \left[P_\mu \left(\mu_1^\ddagger \right) - P_\mu \left(\mu_{N-1}^\ddagger \right) \right]^{N-1}. \tag{2.17}$$

Since these probabilities have relatively sharp roll-offs as a function of N (see numerical results), we can use randomness values, p_{L} and p_{U}, which yield $P_{\text{W,LB}}(p_{\text{L}}) = 1/2$ and $P_{\text{W,UB}}(p_{\text{U}}) = 1/2$, to study the synchrony trends as network parameters change. From (2.16) and (2.17), we have

$$p_{\text{L}} \approx \frac{1}{N+4} \left[\frac{\lambda_1(\mathbf{F} + \mathbf{F}^T) + \epsilon}{\lambda_n(\mathbf{H} + \mathbf{H}^T)} + 4 \right],$$
$$p_{\text{U}} \approx \frac{1}{N+4} \left[\max_{j>k} \frac{\lambda_j(\mathbf{F} + \mathbf{F}^T) + \epsilon}{\lambda_j(\mathbf{H} + \mathbf{H}^T)} \right].$$

Thus, the value of randomness, p, required to have stable synchronous state decreases as $O(1/N)$.

Small-World Networks

Consider a small-world network based on the Newman-Watts model [6] constructed by randomly adding links, with probability p, to a k-regular ring network. This is equivalent to the superimposition of a ring network and an Erdös-Rényi network on the same node set. Thus, the Laplacian matrix of the small-world network is

$$\mathbf{L}_{\text{SW}} = \mathbf{L}_{\text{R}_k} + \mathbf{L}_{\text{ER}} - \mathbf{L}_{\text{overlap}},$$

where $\mathbf{L}_{\mathrm{R}_k}$, $\mathbf{L}_{\mathrm{ER}}$ and $\mathbf{L}_{\mathrm{overlap}}$ denote the Laplacian matrices of a k-regular ring, an Erdös-Rényi network, and their overlap of edges, respectively. Let us denote the ith largest eigenvalues of these matrices by μ_i^{SW}, $\mu_i^{\mathrm{R}_k}$, μ_i^{ER} and μ_i^{overlap}, respectively. Weyls' inequalities yield

$$\mu_1^{\mathrm{SW}} \leq \mu_1^{\mathrm{R}_k} + \mu_1^{\mathrm{ER}} - \mu_1^{\mathrm{overlap}} \leq \mu_1^{\mathrm{R}_k} + \mu_1^{\mathrm{ER}}. \tag{2.18}$$

Define $\mathbf{L}_1 = \mathbf{L}_{\mathrm{ER}} - \mathbf{L}_{\mathrm{overlap}}$ and $\mathbf{L}_2 = \mathbf{L}_{\mathrm{R}_k} - \mathbf{L}_{\mathrm{overlap}}$. Since the overlap is always a subnetwork of both the random network as well as the ring network, $\mathbf{L}_1$ and $\mathbf{L}_2$ are Laplacian matrices. Thus, their smallest eigenvalues are zero. Hence, once again we can use the Weyls' inequalities to get

$$\mu_{N-1}^{\mathrm{SW}} \geq \max\{\mu_{N-1}^{\mathrm{R}_k}, \mu_{N-1}^{\mathrm{ER}}\}. \tag{2.19}$$

For even N the eigenvalues of a k-regular ring network are

$$\mu_l^{\mathrm{R}_k} = 2\left(k - \frac{\sin\frac{k\pi l}{N}\cos\frac{(k+1)\pi l}{N}}{\sin\frac{\pi l}{N}}\right)$$

Thus, the pdfs of the upper bound on μ_1^{SW} and the lower bound on μ_{N-1}^{SW} are

$$p_1^{\mathrm{SW},UB}(x) = (N-1)P_\mu^{N-2}(x - \mu_1^{\mathrm{R}_k})p_\mu(x - \mu_1^{\mathrm{R}_k})$$

$$p_{N-1}^{\mathrm{SW},LB}(x) = \left(1 - \left[1 - P_\mu\left(\mu_{N-1}^{\mathrm{R}_k}\right)\right]^{N-1}\right)\delta\left(x - \mu_{N-1}^{\mathrm{R}_k}\right)$$

$$+ (N-1)[1 - P_\mu(x)]^{N-2}p_\mu(x)u\left(x - \mu_{N-1}^{\mathrm{R}_k}\right),$$

where $\delta(\cdot)$ and $u(\cdot)$ are the impulse and step functions. Thus, the lower bound on the probability of stability is given by

$$P_{\text{SW,LB}} = \left(1 - \left[1 - P_\mu\left(\mu_{N-1}^{R_k}\right)\right]^{N-1}\right) u\left(\mu^\dagger - \mu_{N-1}^{R_k}\right)$$
$$+ \left[1 - P_\mu\left(\mu^{R_k}\right)\right]^{N-1} - \left[1 - P_\mu\left(\mu^\dagger\right)\right]^{N-1} \tag{2.20}$$

if $\lambda_n(\mathbf{H} + \mathbf{H}^T) > 0$, and

$$P_{\text{SW,LB}} = P_\mu^{N-1}\left(\mu^\dagger - \mu_{N-1}^{R_k}\right) \tag{2.21}$$

if $\lambda_n(\mathbf{H} + \mathbf{H}^T) < 0$.

Numerical Results

For a numerical example, we consider a network of Rössler oscillators (with parameters $a_1 = 0.165$, $a_2 = 0.2$, and $a_3 = 10$) coupled through all of their states. This set of parameters results in a coherent chaotic oscillation, since $a_1 < 0.21$ [85]. Therefore, the Jacobian of the oscillator can be computed as

$$\mathbf{F} = \begin{bmatrix} 0 & -1 & -1 \\ 1 & 0.165 & 0 \\ x_3 & 0 & x_1 - 10 \end{bmatrix}$$

We also assume

$$\mathbf{H} = \frac{c}{\sqrt{6} + \sqrt{3} + \sqrt{2}} \begin{bmatrix} \sqrt{2} & \sqrt{2} & \sqrt{2} \\ 0 & \sqrt{3} & \sqrt{3} \\ 0 & 0 & \sqrt{6} \end{bmatrix}.$$

41

where $c = \text{trace}(\mathbf{H})$, is the coupling strength.
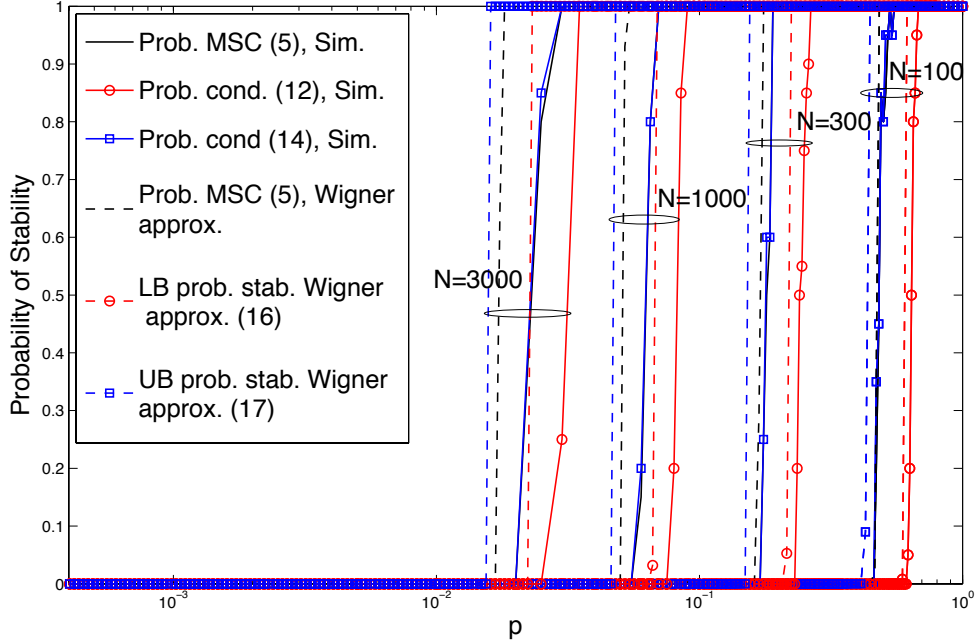
Figure 2.1: Probability of stability of Erdös-Rényi networks as a function of p.

With this setting we first consider an Erdös-Rényi network and calculate our results on the probability of stability of the network for different values of N, p, and c. To this end, we have considered N trajectories starting from initial point $[s_i \ s_j \ 0]^T$ where s_j's are selected uniformly from interval $[0.95, \ 1.05]$ and all the corresponding eigenvalues are calculated over average of 20 cycles of initiated trajectories.

Fig. 2.1 shows the probability of the stability of the network as a function of network randomness, p, for different network size, N, and with coupling strength $c = 1$. As it can be seen, probabilities of (2.12) and (2.14) are close to that of (2.5). Moreover, we observe that the approximated probabilities provided by the Wigner's distribution of eigenvalues of

the network are also reasonably close. As Fig. 2.1 shows for positive definite $\mathbf{H} + \mathbf{H}^T$ in a large network if the average degree, pN, is above some *threshold*, $p_L N \approx \lambda_1(\mathbf{F} + \mathbf{F}^T)/\lambda_n(\mathbf{H} + \mathbf{H}^T)$, (in this example approximately 50) the network becomes stable. Note that in this particular numerical example, due to positive definiteness of $\mathbf{H} + \mathbf{H}^T$, only the transition from asynchrony to synchrony is observed.

The behavior of the network in the sense of its stability versus network size for several values of p is shown in Fig. 2.2. Once again we observe that the probability of stability suddenly increases as pN crosses the threshold above.
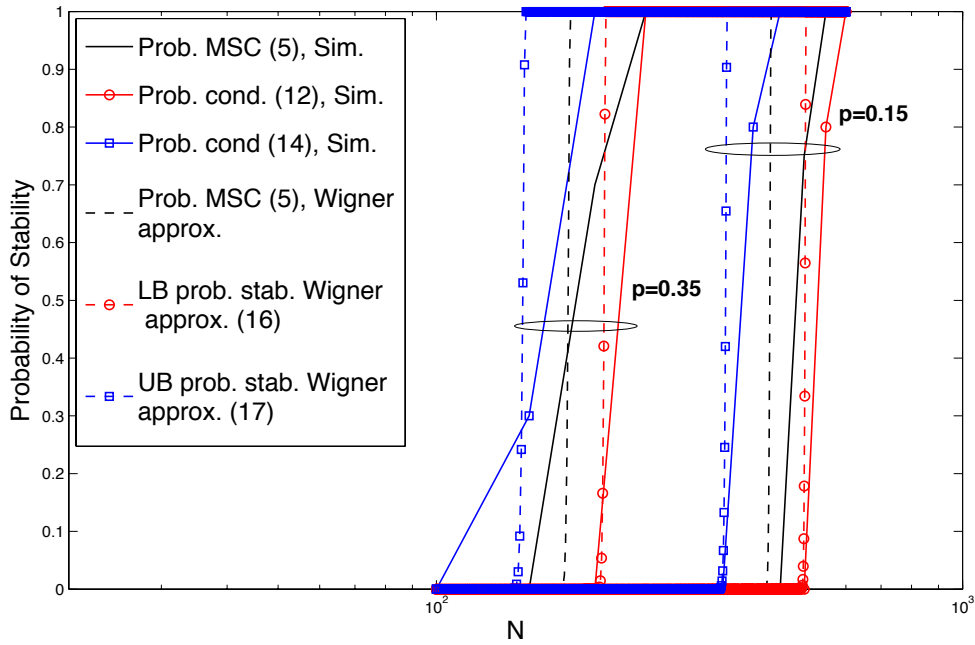
Figure 2.2: Probability of stability of Erdös-Rényi networks as a function of N.
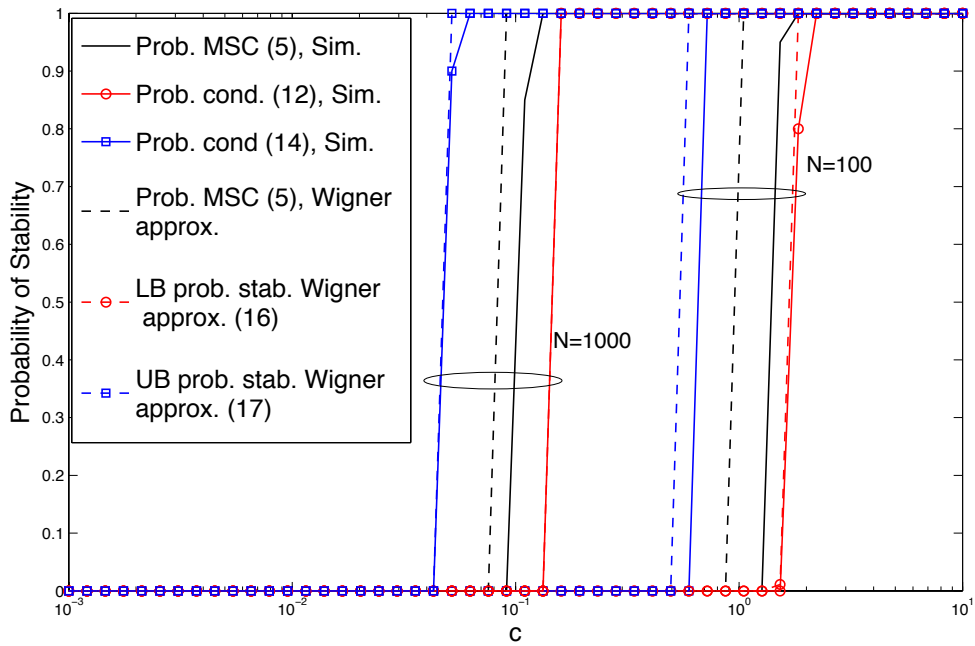
Figure 2.3: Probability of stability of Erdös-Rényi networks as a function of c.

44

Fig. 2.3 shows that the stability of the network grows as the network size and coupling factor increase. Of course this is due to our choice of coupling dynamics which is positive definite and by increasing coupling strength, it provides stronger negative feedback to stabilize the network.

For small-world networks with Newman-Watts method, we start with a regular ring network with coordination number $k = 20$. In other words, each node is connected to its nearest $2k = 40$ neighbors. Other parameters are kept the same as the Erdös-Rényi case.

Figs. 2.5, 2.4 and 2.6 depict the probability of stability as functions of randomness parameter, p, network size, N, and coupling strength, c, respectively. We observe that the lower bound on the probability of stability derived from (2.19) are close to the simulated results, as well as (2.20). Also, similar to the Erdös-Rényi case, we can observe the sharp transition from asynchrony to synchrony state as p, N or c change. We can also see that as pN, which is directly related to the *smallness* of the network, passes a certain value (in our example 30) network becomes stable.
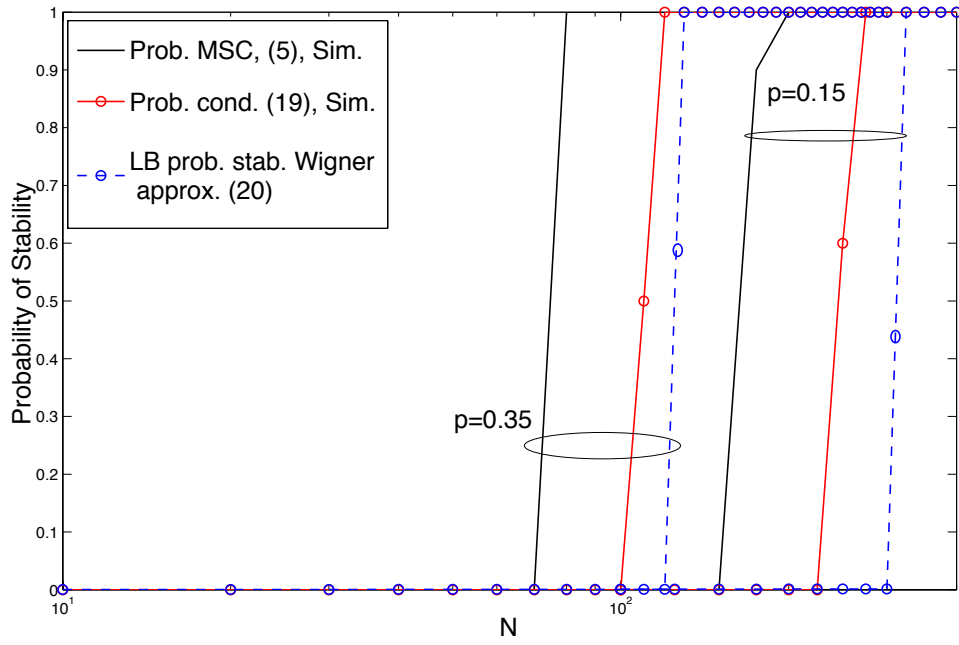
Figure 2.4: Probability of stability of small-world networks as a function of N.
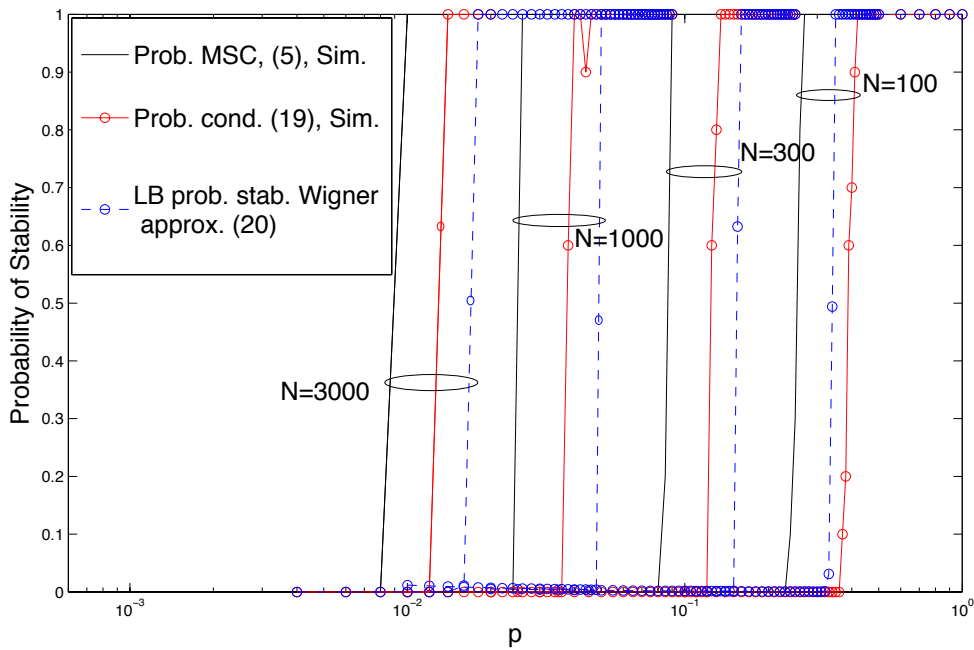
Figure 2.5: Probability of stability of small-world networks as a function of p.

46
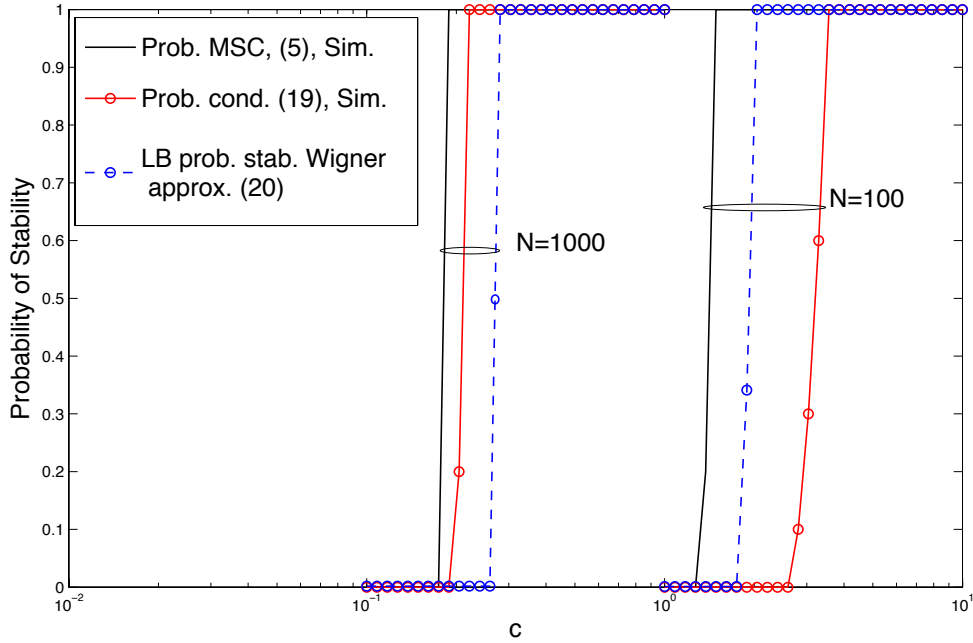
Figure 2.6: Probability of stability of small-world networks as a function of c.

Conclusion

In conclusion, considering an alternative master stability condition, we have derived a suf-
ficient condition of stability which is a function of the eigenvalues of network structure and
symmetric parts of linearized local and coupling dynamics. Our condition relates the largest
eigenvalues of the symmetric parts of coupling and local dynamics to the stability of the
networks. For both Erdös-Rényi and Newman-Watts small-world networks we have calcu-
lated a lower bound on the probability of stability. We have also show that a *threshold* value
of randomness exists, where the system sharply becomes stable as p increases beyond this
threshold. The reason for this phenomenon is that below the certain threshold, all or some

47

of the nodes cannot achieve sufficient information exchange. As a result, those nodes cannot synchronize themselves with the rest of the network. Our approach and results can be extended to the case of randomly changing network topology, if the eigenvalues of instantaneous networks satisfy our stability criterion stochastically.

CHAPTER 3: PROBABILITY OF STABILITY OF SYNCHRONIZATION IN NETWORK OF MISMATCHED OSCILLATORS

Here, we investigate the synchronization of a network of mismatched oscillators with mismatched couplings. Our formulation also allows the consideration of uncertainties in network link weights, thus generalizing [48] in addition to its main contributions. Since in presence of mismatch there is no unique synchronization state in the network, we use the concept of ε-synchronization [47], where the steady states of the nodes in the network fall into an ε-neighborhood of a certain trajectory (synchronization manifold). We then use a generalized master stability function to study the behavior of the network around the synchronization state. The proposed generalized master stability function bounds the oscillator states to a neighborhood of average synchronization trajectory as a function of Lyapunov exponents of the dynamical network. These Lyapunov exponents, in turn, are related to eigenvalues of the Laplacian matrix of the network. We then provide a probabilistic treatment of synchronization behavior in terms of mismatch parameters for regular and random network models. We calculate probability of stability of synchronization, and use it to investigate phase transitions of the synchronization in the network as the network and node parameters vary. Finally, we verify our analytical results by a numerical example for a network of van der Pol oscillators [87] with mismatched oscillators and couplings.

Notation and Main Variables

The set of real (column) n-vectors is denoted by $\mathbb{R}^n$ and the set of real $m \times n$ matrices is denoted by $\mathbb{R}^{m \times n}$. We refer to the set of non-negative real numbers by $\mathbb{R}_+$. Matrices and vectors are denoted by capital and lower-case bold letters, respectively. Identity matrix is shown by $\mathbf{I}$. The Euclidean $(\mathcal{L}_2)$ vector norm is represented by $\|\cdot\|$. When applied to a matrix, $\|\cdot\|$ denotes the $\mathcal{L}_2$ induced matrix norm, $\|\mathbf{A}\| = \sqrt{\lambda_{\max}(\mathbf{A}^T \mathbf{A})}$. Table 3.1 summarizes the main variables used.

Table 3.1: Main variables

Variable	Description
$\mathbf{x}_i$	State vector of node i
$\boldsymbol{\gamma}_i$	Parameters vector of node i
$\boldsymbol{\theta}_{ji}$	Parameter vector of coupling from node j to node i
$\mathbf{f}(\mathbf{x}_i, \boldsymbol{\gamma}_i)$	Dynamics function of node i
$\mathbf{h}(\mathbf{x}_j, \mathbf{x}_i, \boldsymbol{\theta}_{ji})$	Coupling function from node j to node i
$\mathbf{u}_i$	Input vector for node i
$\mathbf{F_X}$	Jacobian of vector $\mathbf{f}$ with respect to $\mathbf{x}$
$\mathbf{F_\gamma}$	Jacobian of vector $\mathbf{f}$ with respect to $\boldsymbol{\gamma}$
$\mathbf{H_X}$	Jacobian of coupling vector $\mathbf{h}$ with respect to $\mathbf{x}$
$\mathbf{H_y}$	Jacobian of coupling vector $\mathbf{h}$ with respect to $\mathbf{y}$
$\mathbf{H_\theta}$	Jacobian of coupling vector $\mathbf{h}$ with respect to $\boldsymbol{\theta}$

System Description

Consider a network of N oscillators, indexed by $\mathcal{N} = \{1 \cdots N\}$. Assume that the dynamics of each isolated oscillator is governed by

$$\dot{\mathbf{x}}_i = \mathbf{f}(\mathbf{x}_i, \boldsymbol{\gamma}_i),$$

where $\mathbf{x}_i \in \mathbb{R}^n$ and $\boldsymbol{\gamma}_i \in \mathcal{P} \subseteq \mathbb{R}^p$ are the state and parameter vectors of local dynamics of node i, respectively. $\mathcal{P}$ denotes the set of possible parameter vectors, and $\mathbf{f} : \mathbb{R}^{n+p} \to \mathbb{R}^n$ describes the local dynamics of an isolated node.

The dynamics of coupled oscillators are given as

$$\dot{\mathbf{x}}_i = \mathbf{f}(\mathbf{x}_i, \boldsymbol{\gamma}_i) + \sum_{i,j \in \mathcal{N}} a_{ij} \mathbf{h}(\mathbf{x}_j, \mathbf{x}_i, \boldsymbol{\theta}_{ij}), \tag{3.1}$$

where $\boldsymbol{\theta}_{ij} \in \mathcal{Q} \subseteq \mathbb{R}^q$ is the parameter vector of coupling dynamics from node j to node i, $\mathcal{Q}$ denotes the set of possible parameter values for couplings. The adjacency matrix of the network is $\mathbf{A} = [a_{ij}]$, where $a_{ij} \in \mathbb{R}_+$ is the weight of the link from node j to node i. There is no connection if $a_{ij} = 0$. Note that we allow the more general case of directed and wighted networks. Moreover, $\mathbf{h} : \mathbb{R}^{2n+q} \to \mathbb{R}^n$ models the coupling from node j to node i. We assume that $\mathbf{h}(\mathbf{x}, \mathbf{y}, \boldsymbol{\theta})$ is Hamiltonian. That is, we assume that $\mathbf{H_X} = -\mathbf{H_Y}$, where $\mathbf{H_X}$ and $\mathbf{H_Y}$ denotes the Jacobians of $\mathbf{h}(\mathbf{x}, \mathbf{y}, \boldsymbol{\theta})$ with respect to $\mathbf{x}$ and $\mathbf{y}$, respectively. This is a very general assumption and encompasses the *diffusive coupling* model predominantly used in the literature [33, 48, 51], where it is assumed that $\mathbf{h}(\mathbf{x}_1, \mathbf{x}_2, [\boldsymbol{\theta}_1\ \boldsymbol{\theta}_2]) = \tilde{\mathbf{h}}(\mathbf{x}_1, \boldsymbol{\theta}_1) - \tilde{\mathbf{h}}(\mathbf{x}_2, \boldsymbol{\theta}_2)$.

Note that this generalized model also incorporates uncertainties in the adjacency matrix of the network, $\mathbf{A} = [a_{ij}] + [\delta a_{ij}]$, considered in [48], by absorbing δa_{ij} into θ_{ij}, i.e., $\boldsymbol{\theta}'_{ij} = [\boldsymbol{\theta}_{ij}^T\ \delta a_{ij}]^T$.

Let $\mathbf{s}$ be a weighted average of the trajectories of all oscillators

$$\mathbf{s} = \sum_{i \in \mathcal{N}} \alpha_i \mathbf{x}_i, \tag{3.2}$$

where $\sum_{i \in \mathcal{N}} \alpha_i = 1$. Define the deviation of the trajectory of oscillator i from $\mathbf{s}$ as

$$\mathbf{e}_i = \mathbf{x}_i - \mathbf{s}. \tag{3.3}$$

Moreover, let $\mathbf{L} = [l_{ij}]$ be the Laplacian matrix of the network [24],

$$\mathbf{L} = \text{diag}([d_1^{\text{in}} \cdots d_N^{\text{in}}]) - \mathbf{A},$$

where $d_i^{\text{in}} = \sum_{j \in \mathcal{N}} a_{ij}$ is the in-degree of node i.

Lemma 1. $\mathbf{s} = \sum_{i \in \mathcal{N}} \alpha_i \mathbf{x}_i$ *is an invariant synchronization manifold of the network if* $\boldsymbol{\alpha} = [\alpha_1 \cdots \alpha_N]^T$ *is a null vector of* $\mathbf{L}^T$.

Proof. Taking derivative of (3.2) yields

$$\dot{\mathbf{s}} = \sum_{i \in \mathcal{N}} \alpha_i \dot{\mathbf{x}}_i$$
$$= \sum_{i \in \mathcal{N}} \alpha_i \mathbf{f}(\mathbf{s} + \mathbf{e}_i, \bar{\boldsymbol{\gamma}} + \delta\boldsymbol{\gamma}_i) + \sum_{i,j \in \mathcal{N}} a_{ij} \alpha_i \mathbf{h}(\mathbf{s} + \mathbf{e}_j, \mathbf{s} + \mathbf{e}_i, \bar{\boldsymbol{\theta}} + \delta\boldsymbol{\theta}_{ij}), \tag{3.4}$$

where $\bar{\boldsymbol{\gamma}} = \sum_{i \in \mathcal{N}} \alpha_i \boldsymbol{\gamma}_i$, $\delta\boldsymbol{\gamma}_i = \boldsymbol{\gamma}_i - \bar{\boldsymbol{\gamma}}$, $\bar{\boldsymbol{\theta}} = \frac{1}{\bar{d}_{\text{in}}} \sum_{i,j \in \mathcal{N}} \alpha_i a_{ij} \boldsymbol{\theta}_{ij}$, $\delta\boldsymbol{\theta}_{ij} = \boldsymbol{\theta}_{ij} - \bar{\boldsymbol{\theta}}$, and $\bar{d}_{\text{in}} = \sum_{i \in \mathcal{N}} \alpha_i d_i^{\text{in}}$ is the weighted average in-degree of the network. Linearization of (3.4)

around $(\mathbf{s}, \bar{\boldsymbol{\gamma}}, \bar{\boldsymbol{\theta}})$ results in

$$\dot{\mathbf{s}} = \sum_{i \in \mathcal{N}} \alpha_i \mathbf{f}(\mathbf{s}, \bar{\boldsymbol{\gamma}}) + \mathbf{F}_{\boldsymbol{\gamma}} \sum_{i \in \mathcal{N}} \alpha_i \delta \boldsymbol{\gamma}_i + \sum_{i,j \in \mathcal{N}} a_{ij} \alpha_i \mathbf{h}(\mathbf{s}, \mathbf{s}, \bar{\boldsymbol{\theta}}) + \mathbf{H}_{\mathbf{X}} \sum_{i,j \in \mathcal{N}} a_{ij} \alpha_i (\mathbf{e}_j - \mathbf{e}_i)$$

$$+ \mathbf{H}_{\boldsymbol{\theta}} \sum_{i,j \in \mathcal{N}} a_{ij} \alpha_i \delta \boldsymbol{\theta}_{ji},$$

where $\mathbf{H}_{\mathbf{X}}$ and $\mathbf{H}_{\boldsymbol{\theta}}$ are Jacobians of $\mathbf{h}$ with respect to its first and third variable, respectively. Recalling that $\sum_{i \in \mathcal{N}} \alpha_i = 1$, we have

$$\dot{\mathbf{s}} = \mathbf{f}(\mathbf{s}, \bar{\boldsymbol{\gamma}}) + \mathbf{h}(\mathbf{s}, \mathbf{s}, \bar{\boldsymbol{\theta}}) \sum_{i \in \mathcal{N}} d_i^{\text{in}} \alpha_i$$

$$+ \mathbf{H}_{\mathbf{X}} \sum_{i,j \in \mathcal{N}} a_{ij} \alpha_i (\mathbf{e}_j - \mathbf{e}_i).$$

For $\mathbf{s}$ to be an invariant manifold, the last term in the above equation must be zero. This is achieved if α_i are chosen to satisfy

$$\sum_{i,j \in \mathcal{N}} a_{ij} \alpha_i (\mathbf{e}_j - \mathbf{e}_i) = \sum_{i \in \mathcal{N}} \left[\sum_{j \in \mathcal{N}} (a_{ji} \alpha_j - a_{ij} \alpha_i) \right] \mathbf{e}_i = \mathbf{0}. \tag{3.5}$$

Equation (3.5), in turn, will be satisfied if $\sum_{j \in \mathcal{N}} (a_{ij} \alpha_j - a_{ij} \alpha_i) = 0$ for all $i \in \mathcal{N}$, which in matrix form can be represented as

$$\mathbf{A}^T \boldsymbol{\alpha} = \text{diag}([d_1^{\text{in}} \cdots d_N^{\text{in}}]) \boldsymbol{\alpha},$$

where $\boldsymbol{\alpha} = [\alpha_1 \cdots \alpha_N]$, or

$$\left[\mathbf{A}^T - \text{diag}([d_1^{\text{in}} \cdots d_N^{\text{in}}]) \right] \boldsymbol{\alpha} = \mathbf{0} = \mathbf{L}^T \boldsymbol{\alpha}.$$

That is, $\boldsymbol{\alpha}$ is a null vector of $\mathbf{L}^T$. □

Remark 1. *We note that, by definition, $\mathbf{L}$ has zero row sum. Thus, it is singular. Consequently, $\mathbf{L}^T$ always has a null vector, $\boldsymbol{\alpha}$. This means that any network has at least one invariant manifold.*

Remark 2. *If the the network is connected, the invariant synchronization manifold is unique. This is due to the fact that for connected networks the nullity of $\mathbf{L}$ is one. Thus, $\boldsymbol{\alpha}$ and, therefore, $\mathbf{s}$ are unique.*

Remark 3. *In the special case where the network is undirected, $\mathbf{L}$ is symmetric. Thus, it also has zero column-sum. Consequently, $\boldsymbol{\alpha} = \frac{1}{N}[1 \ \cdots \ 1]$ is its null vector, and the invariant manifold, $\mathbf{s}$, is the simple average of the trajectories.*

With α_i chosen such that $\mathbf{s}$ is an invariant manifold, we have

$$\dot{\mathbf{s}} = \mathbf{f}(\mathbf{s}, \bar{\boldsymbol{\gamma}}) + \bar{d}_{\text{in}} \, \mathbf{h}(\mathbf{s}, \mathbf{s}, \bar{\boldsymbol{\theta}}), \tag{3.6}$$

$$\mathbf{s}(0) = \sum_{i \in \mathcal{N}} \alpha_i \mathbf{x}_i(0),$$

where $\mathbf{s}(0)$ and $\mathbf{x}(0)$ are initial states.

Generalized Master Stability Function

In this section we introduce a master stability function which generalizes those in [47] and [48] by taking into account the parameter mismatch in the links and applies to directed and weighted networks.

As it has been shown in previous section, every connected network has a unique invariant manifold. Hence, we can define ε-synchronization as

Definition 6. *A network of oscillators is ε-synchronized if there exists $\varepsilon > 0$ such that*

$$\limsup_{t \to \infty} \|\mathbf{e}\| \leq \varepsilon,$$

where $\mathbf{e} = [\mathbf{e}_1 \ ... \ \mathbf{e}_N]^T$.

This definition means that the error from the manifold is contained in a ball of radius ε. We note that our definition is different but closely related to that given in [50].

Substituting (3.1) and (3.2) in (3.3), and using Taylor series, the dynamics of the error with respect to the synchronization manifold, $\mathbf{e}_i$, is given by

$$\dot{\mathbf{e}}_i = \mathbf{F_X}\mathbf{e}_i - \sum_{j=1}^{N} l_{ij}\mathbf{H_X}\mathbf{e}_j + \mathbf{F}_{\boldsymbol{\gamma}}\delta\boldsymbol{\gamma}_i + \sum_{j=1}^{N} \mathbb{1}_{i \neq j} l_{ij}\mathbf{H}_{\boldsymbol{\theta}}\delta\boldsymbol{\theta}_{ij} + (d_i^{\text{in}} - \bar{d}_{\text{in}})\mathbf{h}(\mathbf{s}, \mathbf{s}, \bar{\boldsymbol{\theta}}), \quad (3.7)$$

where $\mathbb{1}_X$ is the indicator function of X. Stacking (3.7) for all i yields the dynamics of the deviation of node trajectories from $\mathbf{s}$:

$$\dot{\mathbf{e}} = (\mathbf{I} \otimes \mathbf{F_X} - \mathbf{L} \otimes \mathbf{H_X})\,\delta\mathbf{x} + (\mathbf{I} \otimes \mathbf{F}_{\boldsymbol{\gamma}})\,\delta\boldsymbol{\gamma}$$

$$+ (\boldsymbol{\mathcal{A}} \otimes \mathbf{H}_{\boldsymbol{\theta}})\,\delta\boldsymbol{\theta} + (\mathbf{d}^{\text{in}} - \bar{d}_{\text{in}}\mathbf{1}_N^T) \otimes \mathbf{h}(\mathbf{s}, \mathbf{s}, \bar{\boldsymbol{\theta}}), \quad\quad (3.8)$$

where

$$\delta\boldsymbol{\gamma} = [\delta\boldsymbol{\gamma}_1^T \cdots \delta\boldsymbol{\gamma}_N^T]^T,$$

$$\delta\boldsymbol{\theta} = [\delta\boldsymbol{\theta}_{11}^T \cdots \delta\boldsymbol{\theta}_{1N}^T \ \delta\boldsymbol{\theta}_{21}^T \cdots \delta\boldsymbol{\theta}_{2N}^T \ \cdots \ \boldsymbol{\theta}_{N1}^T \cdots \delta\boldsymbol{\theta}_{NN}^T]^T,$$

$$\mathbf{d}^{\text{in}} = [d_1^{\text{in}} \cdots d_N^{\text{in}}]^T,$$

$$\boldsymbol{\mathcal{A}} = \text{diag}([\mathbf{a}_1 \cdots \mathbf{a}_N]),$$

and $\mathbf{a}_i$ is the ith row of $\mathbf{A}$.

Let $\mathbf{L} = \mathbf{PJP}^{-1}$ be the Jordan decomposition of $\mathbf{L}$, where $\mathbf{P} = [p_{ij}]$ is a similarity transform and $\mathbf{J}$ is in Jordan form. Then, (3.8) can be rewritten as

$$\dot{\mathbf{e}} = (\mathbf{P} \otimes \mathbf{I}) (\mathbf{I} \otimes \mathbf{F_X} - \mathbf{J} \otimes \mathbf{H_X}) (\mathbf{P}^{-1} \otimes \mathbf{I}) \mathbf{e} + (\mathbf{I} \otimes \mathbf{F_\gamma}) \delta\boldsymbol{\gamma}$$
$$+ (\boldsymbol{\mathcal{A}} \otimes \mathbf{H_\theta}) \delta\boldsymbol{\theta} + (\mathbf{d}^{\text{in}} - \bar{d}_{\text{in}} \mathbf{1}_N^T) \otimes \mathbf{h}(\mathbf{s}, \mathbf{s}, \bar{\boldsymbol{\theta}}).$$

Using the similarity transform

$$\boldsymbol{\eta} = (\mathbf{P}^{-1} \otimes \mathbf{I}) \mathbf{e},$$

where $\boldsymbol{\eta} = [\boldsymbol{\eta}_1^T \cdots \boldsymbol{\eta}_N^T]^T$, we obtain

$$\dot{\boldsymbol{\eta}} = (\mathbf{I} \otimes \mathbf{F_X} - \mathbf{J} \otimes \mathbf{H_X}) \boldsymbol{\eta} + (\mathbf{P}^{-1} \otimes \mathbf{I}) (\mathbf{I} \otimes \mathbf{F_\gamma}) \delta\boldsymbol{\gamma}$$
$$+ (\mathbf{P}^{-1} \otimes \mathbf{I}) (\boldsymbol{\mathcal{A}} \otimes \mathbf{H_\theta}) \delta\boldsymbol{\theta}$$
$$+ (\mathbf{P}^{-1} \otimes \mathbf{I}) ((\mathbf{d} - \bar{d}_{\text{in}} \mathbf{1}_N^T) \otimes \mathbf{h}(\mathbf{s}, \mathbf{s}, \bar{\boldsymbol{\theta}}))$$
$$= (\mathbf{I} \otimes \mathbf{F_X} - \mathbf{J} \otimes \mathbf{H_X}) \boldsymbol{\eta} + (\mathbf{P}^{-1} \otimes \mathbf{F_\gamma}) \delta\boldsymbol{\gamma}$$
$$+ (\mathbf{P}^{-1} \boldsymbol{\mathcal{A}} \otimes \mathbf{H_\theta}) \delta\boldsymbol{\theta}$$
$$+ (\mathbf{P}^{-1} (\mathbf{d} - \bar{d}_{\text{in}} \mathbf{1}_N^T)) \otimes \mathbf{h}(\mathbf{s}, \mathbf{s}, \bar{\boldsymbol{\theta}}).$$
$$= (\mathbf{I} \otimes \mathbf{F_X} - \mathbf{J} \otimes \mathbf{H_X}) \boldsymbol{\eta} + \mathbf{v}, \tag{3.9}$$

where $\mathbf{v} = [\mathbf{v}_1 \cdots \mathbf{v}_N]$,

$$\mathbf{v}_i = \sum_{j \in \mathcal{N}} q_{ij} \left[\mathbf{F_\gamma} \delta\boldsymbol{\gamma}_j + \sum_{k=1, k \neq j}^{N} a_{jk} \mathbf{H_\theta} \delta\boldsymbol{\theta}_{jk} \right.$$
$$\left. + \mathbf{h}(\mathbf{s}, \mathbf{s}, \bar{\boldsymbol{\theta}})(d_i^{\text{in}} - \bar{d}_{\text{in}}) \right],$$

and q_{ij} are the elements of $\mathbf{Q} = \mathbf{P}^{-1}$. It is clear that stability of $\boldsymbol{\eta}$ and $\mathbf{e}$ are equivalent.

To study the stability of (3.9), let us first consider the simpler case where $\mathbf{J}$ consists of a single Jordan block, i.e.

$$
\mathbf{J} = \mathbf{J}_N(\mu) =
\begin{bmatrix}
\mu & 1 & 0 & \cdots & 0 & 0 \\
0 & \mu & 1 & \cdots & 0 & 0 \\
0 & 0 & \mu & \cdots & 0 & 0 \\
\vdots & \vdots & \vdots & \ddots & \vdots & \vdots \\
0 & 0 & 0 & \cdots & \mu & 1 \\
0 & 0 & 0 & \cdots & 0 & \mu
\end{bmatrix}.
$$

Lemma 2. *For system*

$$
\dot{\boldsymbol{\eta}} = \left(\mathbf{I} \otimes \mathbf{F_X} - \mathbf{J}_N(\mu) \otimes \mathbf{H_X}\right)\boldsymbol{\eta} + \mathbf{v},
$$

there exists $\phi > 0$ such that

$$
\limsup_{t \to \infty} \|\boldsymbol{\eta}_i\| \leq \sum_{j=i}^{N} \left(\frac{\phi}{\lambda}\right)^{N-j+1} \limsup_{t \to \infty} \|\mathbf{F_X} - \mathbf{H_X}\|^{N-j} \times \limsup_{t \to \infty} \|\mathbf{v}_j\|,
$$

for all i, if $\lambda > 0$, where $\lambda = MLE(\mathbf{F_X} - \mu\mathbf{H_X})$, and $MLE(.)$ returns the maximum Lyapunov exponent of the argument.

Proof. The state space equation for the $\boldsymbol{\eta}_i$ can be written as

$$
\dot{\boldsymbol{\eta}}_i = \left(\mathbf{F_X} - \mu\mathbf{H_X}\right)\boldsymbol{\eta}_i + \left(\mathbf{F_X} - \mathbf{H_X}\right)\boldsymbol{\eta}_{i+1} + \mathbf{v}_i(t), \tag{3.10}
$$

for $i \neq N$, and

$$\dot{\boldsymbol{\eta}}_N = \left(\mathbf{F_X} - \mu \mathbf{H_X}\right)\boldsymbol{\eta}_N + \mathbf{v}_N(t). \tag{3.11}$$

The solution of (3.10) and (3.11) are

$$\boldsymbol{\eta}_i(t) = \boldsymbol{\Phi}(t,0)\boldsymbol{\eta}_i(0) + \int_0^t \boldsymbol{\Phi}(t,\tau)\mathbf{v}_i(\tau)d\tau + \int_0^t \boldsymbol{\Phi}(t,\tau)(\mathbf{F_X} - \mathbf{H_X})\boldsymbol{\eta}_{i+1}(\tau)d\tau,$$

for $i \neq N$ and

$$\boldsymbol{\eta}_N(t) = \boldsymbol{\Phi}(t,0)\boldsymbol{\eta}_N(0) + \int_0^t \boldsymbol{\Phi}(t,\tau)\mathbf{v}_N(\tau)d\tau,$$

where $\boldsymbol{\Phi}(t,\tau) = \mathbf{Z}(t)\mathbf{Z}^{-1}(\tau)$, and $\mathbf{Z}$ is the normal fundamental matrix of $\mathbf{F_X} - \mu \mathbf{H_X}$ [88].

Applying triangle inequality yields

$$\|\boldsymbol{\eta}_i(t)\| \leq \|\boldsymbol{\Phi}(t,0)\|\|\boldsymbol{\eta}_i(0)\|$$
$$+ \int_0^t \|(\mathbf{F_X} - \mathbf{H_X})\boldsymbol{\eta}_{i+1}(\tau) + \mathbf{v}_i(\tau)\|\|\boldsymbol{\Phi}(t,\tau)\|d\tau,$$

for $i \in \{1, ..., N-1\}$, and

$$\|\boldsymbol{\eta}_N(t)\| \leq \|\boldsymbol{\Phi}(t,0)\|\|\boldsymbol{\eta}_N(0)\| + \int_0^t \|\mathbf{v}_N(\tau)\|\|\boldsymbol{\Phi}(t,\tau)\|d\tau,$$

which, as $t \to \infty$, yields

$$\limsup_{t\to\infty}\|\boldsymbol{\eta}_i\| \leq \|\boldsymbol{\eta}_i(0)\|\limsup_{t\to\infty}\|\boldsymbol{\Phi}(t,0)\|$$

$$+ \limsup_{t\to\infty}\|\mathbf{v}_i\|\limsup_{t\to\infty}\int_0^t\|\boldsymbol{\Phi}(t,\tau))\|d\tau$$

$$+ \limsup_{t\to\infty}\|\mathbf{F_X} - \mathbf{H_X}\|\limsup_{t\to\infty}\|\boldsymbol{\eta}_{i+1}\|$$

$$\times \limsup_{t\to\infty}\int_0^t\|\boldsymbol{\Phi}(t,\tau)\|d\tau, \qquad (3.12)$$

and

$$\limsup_{t\to\infty}\|\boldsymbol{\eta}_N\| \leq \|\boldsymbol{\eta}_N(0)\|\limsup_{t\to\infty}\|\boldsymbol{\Phi}(t,0)\|$$

$$+ \limsup_{t\to\infty}\|\mathbf{v}_N\|\limsup_{t\to\infty}\int_0^t\|\boldsymbol{\Phi}(t,\tau)\|d\tau. \qquad (3.13)$$

We know that there exists positive real ϕ such that [88]

$$\|\boldsymbol{\Phi}(t,\tau)\| \leq \phi e^{-\lambda(t-\tau)},$$

where λ is the maximum Lyapunov exponent of $\mathbf{F_X} - \mu\mathbf{H_X}$. If $\lambda > 0$ this yields

$$\limsup_{t\to\infty}\|\boldsymbol{\Phi}(t,0))\| = 0,$$

$$\limsup_{t\to\infty}\int_0^t\|\boldsymbol{\Phi}(t,\tau))\|d\tau \leq \frac{\phi}{\lambda}.$$

Substituting in (3.12) and (3.13) yields,

$$\limsup_{t\to\infty}\|\boldsymbol{\eta}_i\| \leq \frac{\phi}{\lambda}\limsup_{t\to\infty}\|\mathbf{F_X} - \mathbf{H_X}\|\|\boldsymbol{\eta}_{i+1}\| + \frac{\phi}{\lambda}\limsup_{t\to\infty}\|\mathbf{v}_i\|,$$

and

$$\limsup_{t\to\infty}\|\boldsymbol{\eta}_N\| \le \frac{\phi}{\lambda}\limsup_{t\to\infty}\|\mathbf{v}_N\|.$$

Solving the recursive inequalities we get

$$\limsup_{t\to\infty}\|\boldsymbol{\eta}_i\| \le \sum_{j=i}^{N}\left(\frac{\phi}{\lambda}\right)^{N-j+1}\limsup_{t\to\infty}\|\mathbf{F_X}+\mathbf{H_X}\|^{N-j}\times\limsup_{t\to\infty}\|\mathbf{v}_j\|.$$

$\square$

Now, let us assume that $\mathbf{J}$ consists of M Jordan blocks with eigenvalues μ_m and sizes n_m, $m \in \{1,\cdots,M\}$, where $\sum_{m=1}^{M}n_m = N$. Then $N_m = \sum_{m=1}^{j}n_m$ will be the index of the last row of the mth Jordan block. Define $J(i)$ to be the index of the Jordan block that contains the ith row of $\mathbf{J}$. In other words, $J(i) = m$, if $N_{m-1} < i \le N_m$.

Theorem 5. *A network of oscillators is ε-synchronized if $\lambda_m = MLE(\mathbf{F_X}-\mu_m\mathbf{H_X}) > 0$ and*

$$\|\mathbf{P}\|^2\sum_{j=1}^{N-1}\left(\sum_{k=1}^{n_{J(j)}}\left(\frac{\phi_{J(j)}}{\lambda_{J(j)}}\right)^{n_{J(j)}-k+1}\limsup_{t\to\infty}\|\mathbf{F_X}-\mathbf{H_X}\|^{n_{J(j)}-k}\limsup_{t\to\infty}\|\mathbf{v}_j\|\right)^2 \le \varepsilon^2, \qquad (3.14)$$

where ϕ_m satisfies

$$\forall t,\tau, \quad \|\boldsymbol{\Phi}_m(t,\tau)\| \le \phi_m e^{-\lambda_m(t-\tau)}.$$

and $\boldsymbol{\Phi}_m(t,\tau)$ is the state transition matrix of $\mathbf{F_X}-\mu_m\mathbf{H_X}$.

Proof. We have

$$\limsup_{t\to\infty}\|\mathbf{e}\|^2 = \limsup_{t\to\infty}\boldsymbol{\eta}^T(\mathbf{P}^T\otimes\mathbf{I})(\mathbf{P}\otimes\mathbf{I})\boldsymbol{\eta}$$

$$\leq \|\mathbf{P}^T\mathbf{P}\|\limsup_{t\to\infty}\|\boldsymbol{\eta}\|^2$$

$$= \|\mathbf{P}\|^2\limsup_{t\to\infty}\|\boldsymbol{\eta}\|^2. \tag{3.15}$$

For any Laplacian matrix, we have $\mu_M = 0$. If the network is connected, we further have $n_M = 1$. Thus,

$$\boldsymbol{\eta}_N = \sum_{j=1}^{N}\alpha_j\mathbf{e}_j = \sum_{j=1}^{N}\alpha_j(\mathbf{x}_j - \mathbf{s}) = \left(\sum_{j=1}^{N}\alpha_j\mathbf{x}_j\right) - \mathbf{s} = \mathbf{0},$$

which together with (3.15) yields

$$\limsup_{t\to\infty}\|\mathbf{e}\|^2 \leq \|\mathbf{P}\|^2\sum_{i=1}^{N-1}\limsup_{t\to\infty}\|\boldsymbol{\eta}_i\|^2. \tag{3.16}$$

Lemma 2 upper bounds the right hand side of (3.16) by the left hand side of (3.14). □

Corollary 1. *A symmetric network of oscillators is ε-synchronized if $\lambda_j = MLE(\mathbf{F_X} - \mu_j\mathbf{H_X}) > 0$ and*

$$\sum_{j=1}^{N-1}\left(\frac{\phi_j}{\lambda_j}\right)^2\limsup_{t\to\infty}\|\mathbf{v}_j(t)\|^2 \leq \varepsilon^2, \tag{3.17}$$

where ϕ_j satisfies

$$\forall t,\tau, \quad \|\boldsymbol{\Phi}_j(t,\tau)\| \leq \phi_j e^{-\lambda_j(t-\tau)},$$

and $\boldsymbol{\Phi}_j(t,\tau)$ is the state transition matrix of $\mathbf{F_X} - \mu_j\mathbf{H_X}$.

Proof. Since $\mathbf{L}$ is symmetric, it can be diagonalized by unitary matrix $\mathbf{P} = \mathbf{U} = [u_{ij}]$, where

$\mathbf{U}^H\mathbf{U} = \mathbf{I}$. Thus, each Jordan block will be of size 1. This means that $M = N$, $n_m = 1$, and $J(i) = i$. Thus, (3.14) reduces to

$$\sum_{j=1}^{N-1} \left(\frac{\phi_j}{\lambda_j}\right)^2 \limsup_{t\to\infty} \|\mathbf{v}_j\|^2 \le \varepsilon^2.$$

$\square$

Remark 4. *In proof of Corollary 1, since unitary transformation preserves Euclidean norm, (3.16) holds with equality. Thus, Corollary 1 is relatively less conservative than Theorem 5.*

Probability of Stability

In the remaining of the paper, we make the following assumptions:

Assumption 1. *The network is symmetric.*

This implies that $\mathbf{L}$ is diagonalizable by a unitary matrix, $\mathbf{U} = [u_{ij}]$.

Assumption 2. *Mismatch parameters, $\delta\boldsymbol{\gamma}_i$ and $\delta\boldsymbol{\theta}_{ij}$, are independent zero mean Gaussian random vectors with covariance matrices, $\boldsymbol{\Sigma_\gamma} = E[(\boldsymbol{\gamma}_i - \bar{\boldsymbol{\gamma}})(\boldsymbol{\gamma}_i - \bar{\boldsymbol{\gamma}})^T]$ and $\boldsymbol{\Sigma_\theta} = E[(\boldsymbol{\theta}_{ij} - \bar{\boldsymbol{\theta}})(\boldsymbol{\theta}_{ij} - \bar{\boldsymbol{\theta}})^T]$, respectively.*

Under Assumption 2, $\mathbf{v}_i$ are linear combination of independent Gaussian random variables. Thus, they are jointly Gaussian. To calculate the probability of (3.17) being satisfied, we need to find the probability density function of $\mathbf{v} = [\mathbf{v}_1^T \cdots \mathbf{v}_N^T]^T$.

Lemma 3. *The covariance matrix of $\mathbf{v}$ is $\boldsymbol{\Sigma_V} = [\boldsymbol{\Sigma}_{ij}]$ where*

$$\boldsymbol{\Sigma}_{ij} = \mathbf{F_\gamma}\boldsymbol{\Sigma_\gamma}\mathbf{F_\gamma}^T \mathbb{1}_{i=j} + \sum_{l=1}^{N} u_{il}u_{jl}^* \sum_{k=1}^{N} a_{lk}^2 \mathbf{H_\theta}\boldsymbol{\Sigma_\theta}\mathbf{H_\theta}^T.$$

Proof. The covariance of $\mathbf{v}$ is

$$\boldsymbol{\Sigma}_{\mathbf{V}} = E[(\mathbf{v} - \bar{\mathbf{v}})(\mathbf{v} - \bar{\mathbf{v}})^T] = [\boldsymbol{\Sigma}_{ij}],$$

where $\bar{\mathbf{v}} = \mathbf{h}(\mathbf{s}, \mathbf{s}, \bar{\boldsymbol{\theta}}) \otimes (\mathbf{D}^{\mathrm{in}} - \bar{d}_{\mathrm{in}}\mathbf{I})$ and $\mathbf{D}^{\mathrm{in}} = \mathrm{diag}([d_1^{\mathrm{in}} \cdots d_N^{\mathrm{in}}])$. Thus, the ijth block of $\boldsymbol{\Sigma}_{\mathbf{V}}$ is

$$
\begin{aligned}
\boldsymbol{\Sigma}_{ij} &= \sum_{k,l\in\mathcal{N}} u_{ik} u_{jl}^{\star} E\left[\left(\mathbf{F}_{\boldsymbol{\gamma}}\delta\boldsymbol{\gamma}_k + \sum_{m\in\mathcal{N}} a_{mk}\mathbf{H}_{\boldsymbol{\theta}}\delta\boldsymbol{\theta}_{mk}\right)\left(\mathbf{F}_{\boldsymbol{\gamma}}\delta\boldsymbol{\gamma}_l + \sum_{n\in\mathcal{N}} a_{ln}\mathbf{H}_{\boldsymbol{\theta}}\delta\boldsymbol{\theta}_{nl}\right)^T\right] \\
&= \sum_{k,l\in\mathcal{N}} u_{ik} u_{jl}^{\star} \mathbf{F}_{\boldsymbol{\gamma}}\boldsymbol{\Sigma}_{\boldsymbol{\gamma}}\mathbf{F}_{\boldsymbol{\gamma}}^T + \sum_{k,l,m,n\in\mathcal{N}} u_{ik} u_{jl}^{\star} a_{km} a_{ln} \mathbf{H}_{\boldsymbol{\theta}}\boldsymbol{\Sigma}_{\boldsymbol{\theta}}\mathbf{H}_{\boldsymbol{\theta}}^T \mathbb{1}_{k=l}\mathbb{1}_{m=n} \\
&= \mathbf{F}_{\boldsymbol{\gamma}}\boldsymbol{\Sigma}_{\boldsymbol{\gamma}}\mathbf{F}_{\boldsymbol{\gamma}}^T 1_{i=j} + \sum_{k,m\in\mathcal{N}} u_{ik} u_{jk}^{\star} |a_{km}|^2 \mathbf{H}_{\boldsymbol{\theta}}\boldsymbol{\Sigma}_{\boldsymbol{\theta}}\mathbf{H}_{\boldsymbol{\theta}}^T.
\end{aligned}
$$

$\square$

We now provide upper bounds on the probability of stable synchronization for unweighted regular, Erdös-Rényi, and Newman-Watts networks.

Theorem 6. *Under Assumptions 1 and 2, the probability of stable synchronization of an unweighted K-regular network of oscillators is lower bounded by*

$$P_{stab}^{LB}(\varepsilon) = \left[\prod_{i=2}^{N-1}\left(\frac{\phi_1\,\lambda_i}{\lambda_1\,\phi_i}\right)^n\right] \times \sum_{j=0}^{\infty} a_j^{(N-1)} P\left(\frac{(N-1)n}{2} + j, \frac{\lambda_1^2\varepsilon^2}{\phi_1^2\sigma^2}\right), \qquad (3.18)$$

63

where $P(\cdot, \cdot)$ is the regularized gamma function,

$$a_j^{(i)} = \sum_{k=0}^{j} a_k^{(i-1)} \frac{n_{j-k}}{(j-k)!} (1 - \frac{\phi_1^2 \, \lambda_i^2}{\lambda_1^2 \, \phi_i^2})^{j-k},$$

$$a_k^{(2)} = \frac{n_k}{k!} \left(1 - \frac{\phi_1^2 \, \lambda_2^2}{\lambda_1^2 \, \phi_2^2}\right)^k,$$

$$n_k = \prod_{l=0}^{k-1} \left(\frac{n}{2} + l\right),$$

and

$$\sigma = \limsup_{t \to \infty} \|\mathbf{F}_{\boldsymbol{\gamma}} \Sigma_{\boldsymbol{\gamma}} \mathbf{F}_{\boldsymbol{\gamma}}^T + K \mathbf{H}_{\boldsymbol{\theta}} \Sigma_{\boldsymbol{\theta}} \mathbf{H}_{\boldsymbol{\theta}}^T\|^{1/2}. \qquad (3.19)$$

Proof. Since the network is unweighted and K-regular, we have $d_i = \sum_{k=1}^{N} a_{ik}^2 = K$. According to Lemma 3 the blocks of the covariance matrix, $\Sigma_{\mathbf{V}}$, are

$$\Sigma_{ij} = \mathbf{F}_{\boldsymbol{\gamma}} \Sigma_{\boldsymbol{\gamma}} \mathbf{F}_{\boldsymbol{\gamma}}^T \mathbb{1}_{i=j} + K \mathbf{H}_{\boldsymbol{\theta}} \, \Sigma_{\boldsymbol{\theta}} \mathbf{H}_{\boldsymbol{\theta}}^T \sum_{l=1}^{N} u_{il} u_{jl}^*.$$

$$= (\mathbf{F}_{\boldsymbol{\gamma}} \Sigma_{\boldsymbol{\gamma}} \mathbf{F}_{\boldsymbol{\gamma}}^T + K \mathbf{H}_{\boldsymbol{\theta}} \Sigma_{\boldsymbol{\theta}} \mathbf{H}_{\boldsymbol{\theta}}^T) \mathbb{1}_{i=j}. \qquad (3.20)$$

Hence, $\mathbf{v}_i$ are uncorrelated. The mean value of $\mathbf{v}_i$ can be computed as

$$E[\mathbf{v}_i] = \sum_{j \in \mathcal{N}} q_{ij} \left(\mathbf{F}_{\boldsymbol{\gamma}} E[\delta\boldsymbol{\gamma}_j] + \sum_{k=1, k \neq j}^{N} a_{jk} \mathbf{H}_{\boldsymbol{\theta}} E[\delta\boldsymbol{\theta}_{jk}] + \mathbf{h}(\mathbf{s}, \mathbf{s}, \bar{\boldsymbol{\theta}})(K - \bar{d}_{\text{in}}) \right) = \mathbf{0},$$

which follows noting that $\delta\boldsymbol{\gamma}_i$ and $\delta\boldsymbol{\theta}_{ij}$ have zero mean and $\bar{d}_{\text{in}} = K$. Since $\mathbf{v}_i$ are jointly Gaussian, uncorrelated, and have zero mean, they are independent.

64

Now, let us define the whitened Gaussian random vectors

$$\mathbf{z}_i = \boldsymbol{\Sigma}_{ii}^{-\frac{1}{2}} \mathbf{v}_i.$$

Since Euclidean norm is sub-multiplicative, we have

$$\|\mathbf{v}_i\| \le \|\mathbf{z}_i\| \left\| \boldsymbol{\Sigma}_{ii}^{\frac{1}{2}} \right\|.$$

$$\limsup_{t\to\infty} \|\mathbf{v}_i\| \le \limsup_{t\to\infty} \left(\|\mathbf{z}_i\| \left\| \boldsymbol{\Sigma}_{ii}^{\frac{1}{2}} \right\| \right).$$

$$\le \limsup_{t\to\infty} \|\mathbf{z}_i\| \limsup_{t\to\infty} \left\| \boldsymbol{\Sigma}_{ii}^{\frac{1}{2}} \right\|.$$

$$= \|\mathbf{z}_i\| \limsup_{t\to\infty} \left\| \boldsymbol{\Sigma}_{ii}^{\frac{1}{2}} \right\|,$$

The last equality is due to the fact that with the whitening of $\|\mathbf{v}_i\|$, $\|\mathbf{z}_i\|$ is no longer time variable. In other words, $\|\mathbf{z}_i\|$ is a random variable (not a random process). Since $\|\mathbf{z}_i\|^2$ is the norm squared of a white Gaussian n-vector, it has a chi-squared distribution with n degrees of freedom. Applying the result of Corollary 1,

$$\|\mathbf{e}\|^2 = \sum_{i=1}^{N-1} \|\boldsymbol{\eta}_i\|^2$$

$$\le \sum_{i=1}^{N-1} \left(\frac{\phi_i}{\lambda_i} \right)^2 \limsup_{t\to\infty} \|\mathbf{v}_i\|^2$$

$$\le \sum_{i=1}^{N-1} \left(\frac{\phi_i \sigma}{\lambda_i} \right)^2 \|\mathbf{z}_i\|^2.$$

where σ is defined in (3.19).

Now we have

$$\Pr\left(\limsup_{t\to\infty}\|\mathbf{e}\| < \varepsilon\right) = \Pr\left(\limsup_{t\to\infty}\|\mathbf{e}\|^2 < \varepsilon^2\right)$$

$$\geq \Pr\left(\sum_{i=1}^{N-1}\left(\frac{\phi_i\sigma}{\lambda_i}\right)^2\|\mathbf{z}_i\|^2 \leq \varepsilon^2\right)$$

$$= \left[\prod_{i=2}^{N-1}\left(\frac{\phi_1\,\lambda_i}{\lambda_1\,\phi_i}\right)^n\right] \times \sum_{j=0}^{\infty}a_j^{(N-1)}\int_0^{\varepsilon^2}f_j(y)dy,$$

where

$$f_j(y) = \left(\frac{\lambda_1^2}{2\phi_1^2\sigma^2}\right)^{\frac{(N-1)n}{2}+j}\frac{y^{\frac{(N-1)n}{2}+j-1}}{\Gamma\left(\frac{(N-1)n}{2}+j\right)}e^{-\frac{\lambda_1^2}{2\phi_1^2\sigma^2}y}.$$

which using the results in [89] yields (6.23). □

Theorem 7. *Under Assumptions 1 and 2, the limiting probability of stable synchronization of an unweighted Erdös-Rényi (ER) network of oscillators, with parameter p, as $N \to \infty$, is lower bounded by*

$$P_{stab}^{LB}(\varepsilon|\boldsymbol{\lambda}) = \left[\prod_{i=2}^{N-1}\left(\frac{\phi_1\,\lambda_i}{\lambda_1\,\phi_i}\right)^n\right]\times\sum_{j=0}^{\infty}a_j^{(N-1)}P\left(\frac{(N-1)n}{2}+j,\frac{\lambda_1^2\varepsilon^2}{\phi_1^2\sigma^2}\right), \tag{3.21}$$

where $\sigma = \limsup_{t\to\infty}\ \|\mathbf{F}_{\boldsymbol{\gamma}}\boldsymbol{\Sigma}_{\boldsymbol{\gamma}}\mathbf{F}_{\boldsymbol{\gamma}}^T + pN\mathbf{H}_{\boldsymbol{\theta}}\boldsymbol{\Sigma}_{\boldsymbol{\theta}}\mathbf{H}_{\boldsymbol{\theta}}^T\|^{1/2}$ and $\boldsymbol{\lambda} = [\lambda_1\cdots\lambda_{N-1}]$.

Proof. The largest eigenvalue of the Laplacian matrix of any symmetric network is bounded below by the maximum degree of the network. For large ER networks ($N \to \infty$), it is also bounded above by $Np + \sqrt{Np(1-p)}$ (see eq. (2.15)). Thus

$$d_{\max} \leq \mu_{\max} \leq Np + \sqrt{Np(1-p)}.$$

66

Similarly, the smallest non-zero eigenvalue of ER network can be bounded as

$$d_{\min} \geq \mu_{\min} \geq Np - \sqrt{Np(1-p)}.$$

According to Lemma 3, the diagonal blocks of covariance matrix of $\mathbf{v}$ are

$$\begin{aligned}
\boldsymbol{\Sigma}_{ii} &= \mathbf{F}_{\boldsymbol{\gamma}}\boldsymbol{\Sigma}_{\boldsymbol{\gamma}}\mathbf{F}_{\boldsymbol{\gamma}}^T + \mathbf{H}_{\boldsymbol{\theta}}\boldsymbol{\Sigma}_{\boldsymbol{\theta}}\mathbf{H}_{\boldsymbol{\theta}}^T \sum_{l=1}^{N} |u_{il}|^2 d_l \\
&= \mathbf{F}_{\boldsymbol{\gamma}}\boldsymbol{\Sigma}_{\boldsymbol{\gamma}}\mathbf{F}_{\boldsymbol{\gamma}}^T + Np\mathbf{H}_{\boldsymbol{\theta}}\boldsymbol{\Sigma}_{\boldsymbol{\theta}}\mathbf{H}_{\boldsymbol{\theta}}^T,
\end{aligned}$$

as $N \to \infty$, and the off diagonal entries are

$$\begin{aligned}
\boldsymbol{\Sigma}_{ij} &= \mathbf{H}_{\boldsymbol{\theta}}\boldsymbol{\Sigma}_{\boldsymbol{\theta}}\mathbf{H}_{\boldsymbol{\theta}}^T \sum_{l=1}^{N} u_{il}u_{jl}^* d_l \\
&= \mathbf{H}_{\boldsymbol{\theta}}\boldsymbol{\Sigma}_{\boldsymbol{\theta}}\mathbf{H}_{\boldsymbol{\theta}}^T \sum_{l=1}^{N} u_{il}u_{jl}^* (d_l - Np) \\
&\leq \sqrt{Np(1-p)}\mathbf{H}_{\boldsymbol{\theta}}\boldsymbol{\Sigma}_{\boldsymbol{\theta}}\mathbf{H}_{\boldsymbol{\theta}}^T.
\end{aligned}$$

Therefore,

$$\lim_{N \to \infty} \frac{\|\boldsymbol{\Sigma}_{ij}\|}{\|\boldsymbol{\Sigma}_{ii}\|} = 0.$$

Consequently, as $N \to \infty$, $\mathbf{v}_i$ become independent. The remaining of the proof is similar to that of Theorem 6 and is omitted in the interest of brevity. $\square$

To study the synchronization in small-world networks, we consider the Newman-Watts model [6]. This model constructs a small-world network by starting from a K-regular ring network substrate, then randomly adds new links with probability p.

Theorem 8. *Under assumptions 1 and 2, the limiting probability of stable synchronization*

of an unweighted Newman-Watts small-world network of oscillators, with parameters p and K, as $N \to \infty$, is lower bounded by

$$P_{stab}^{LB}(\varepsilon|\boldsymbol{\lambda}) = \left[\prod_{i=2}^{N-1} \left(\frac{\phi_1 \; \lambda_i}{\lambda_1 \; \phi_i} \right)^n \right] \times \sum_{j=0}^{\infty} a_j^{(N-1)} P \left(\frac{(N-1)n}{2} + j, \frac{\lambda_1^2 \varepsilon^2}{\phi_1^2 \sigma^2} \right), \qquad (3.22)$$

where

$$\sigma = \limsup_{t \to \infty} \; \|\mathbf{F}_{\boldsymbol{\gamma}} \boldsymbol{\Sigma}_{\boldsymbol{\gamma}} \mathbf{F}_{\boldsymbol{\gamma}}^T + (K + Np)\mathbf{H}_{\boldsymbol{\theta}} \boldsymbol{\Sigma}_{\boldsymbol{\theta}} \mathbf{H}_{\boldsymbol{\theta}}^T \|^{1/2}.$$

Proof. The Laplacian matrix of a Newman-Watts small world network is

$$\mathbf{L}_{\mathrm{NW}} = \mathbf{L}_{\mathrm{Ring}} + \mathbf{L}_{\mathrm{ER}},$$

where $\mathbf{L}_{\mathrm{Ring}}$ and $\mathbf{L}_{\mathrm{ER}}$ are the laplacians of a K-regular ring and an Erdös-Rényi network with parameter p. Using Weyl's inequalities we can bound the minimum and maximum eigenvalues of the small-world [24]

$$\max\{\mu_{\mathrm{min}}^{\mathrm{Ring}}, \mu_{\mathrm{min}}^{\mathrm{ER}}\} \leq \mu_{\mathrm{min}}^{\mathrm{NW}} \leq d_{\mathrm{min}},$$

$$\mu_{\mathrm{max}}^{\mathrm{Ring}} + \mu_{\mathrm{max}}^{\mathrm{ER}} \geq \mu_{\mathrm{max}}^{\mathrm{NW}} \geq d_{\mathrm{max}},$$

where the eigenvalues of a K-regular ring is [24]

$$\mu_i^{\mathrm{Ring}} = K - 2 \frac{\sin \frac{iK\pi}{2N} \cos \frac{(K+2)i\pi}{2N}}{\sin \frac{i\pi}{N}},$$

and subscripts min and max refer to smallest non-zero and maximum eigenvalue of $\mathbf{L}$ in corresponding configurations, respectively. The remaining of the proof is similar to that of Theorem 7 and is omitted in the interest of brevity. $\square$

Numerical Example

In this section we verify our analytical results using numerical examples. We consider the van der Pol oscillator [87] which has the following dynamics

$$\mathbf{f}(\mathbf{x}_i, \boldsymbol{\gamma}_i) = \begin{bmatrix} x_{i2} \\ -x_{1i} - \gamma_i(x_{i1}^2 - 1)x_{i2} \end{bmatrix}.$$

We note that since the van der Pol oscillator has a limit cycle, as $t \to \infty$, $\mathbf{s}$ is a periodic trajectory. Hence, the Jacobians are also periodic. We can, therefore, solve (3.6) analytically using Fourier series [87].

We assume that the nodes are coupled through their first states by

$$\mathbf{h}(\mathbf{x}_j, \mathbf{x}_i, \boldsymbol{\theta}_{ij}) = \begin{bmatrix} \theta_{ij1}(x_{1j} - x_{1i}) + \theta_{ij2} \\ 0 \end{bmatrix}.$$

Thus, the Jacobians of $\mathbf{f}(.)$ and $\mathbf{h}(.)$ around $(\mathbf{s}, \bar{\boldsymbol{\gamma}}, \bar{\boldsymbol{\theta}})$ are

$$\mathbf{F_X} = \begin{bmatrix} 0 & 1 \\ -1 - 2\bar{\gamma}s_1s_2 & \bar{\gamma}(1 - s_1^2) \end{bmatrix},$$

$$\mathbf{H_X} = \begin{bmatrix} \bar{\theta}_1 & 0 \\ 0 & 0 \end{bmatrix},$$

$$\mathbf{F}_\gamma = \begin{bmatrix} 0 \\ (1 - s_1^2)s_2 \end{bmatrix},$$

$$\mathbf{H}_{\boldsymbol{\theta}} = \begin{bmatrix} 0 & 1 \\ 0 & 0 \end{bmatrix},$$

69

where $\mathbf{s} = [s_1 \ s_2]^T$. Fig. 3.1 depicts the maximum Lyapunov exponent of $\mathbf{F_X} - \mu\mathbf{H_X}$ as a function of μ, where μ is the eigenvalue of Laplacian matrix of the network.
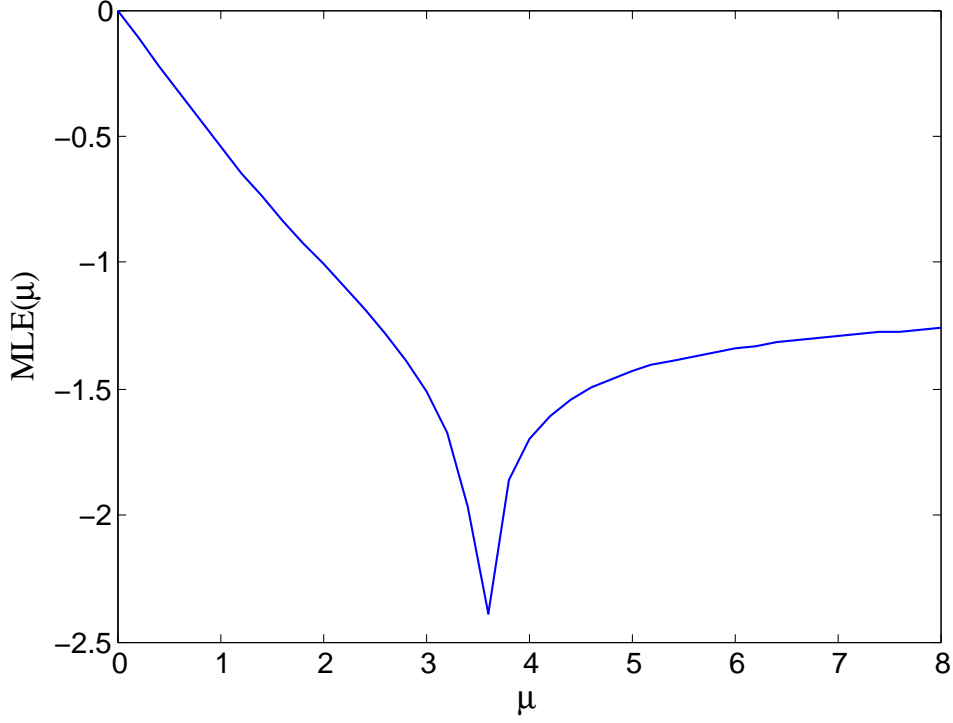
Figure 3.1: Maximum Lyapunov Exponent (MLE) as a function of eigenvalues of Laplacian matrix of the network, μ.

Furthermore,

$$\mathbf{v}_i = \left[\begin{array}{c} \sum_{j=1}^{N} u_{ji}^* \sum_{k=1}^{N} a_{jk} \delta\theta_{kj2} \\ (1 - s_1^2)s_2 \sum_{j=1}^{N} u_{ji}^* \delta\gamma_j \end{array} \right].$$

It is clear that $\mathbf{v}_i$ are independent of $\delta\theta_{ij1}$. Also, covariance matrix of $\mathbf{v}_i$ of a K-regular ring

network for $\bar{\gamma} = 1$ can be calculated from (3.20) as

$$
\Sigma_{ii} =
\begin{bmatrix}
K\bar{\theta}_1^2 \sigma_{\theta 2}^2 & 0 \\
0 & \sigma_\gamma^2 ((1 - s_1^2) s_2)^2
\end{bmatrix},
$$

and

$$
\sup \Sigma_{ii} =
\begin{bmatrix}
K\bar{\theta}_1^2 \sigma_{\theta 2}^2 & 0 \\
0 & 9.93 \sigma_\gamma^2
\end{bmatrix},
\tag{3.23}
$$

where $\sup((1 - s_1^2) s_2)^2$ is determined by simulation to be 9.93 and the supremums are calculated over one period of the limit cycle. Hence, $\sigma = \max(\sqrt{K}\bar{\theta}_1 \sigma_{\theta_2}, 3.15 \sigma_\gamma)$.

Now, consider a 6-regular ring network of size $N = 100$, where $\gamma \sim \mathcal{N}(1, 0.01)$ and $\boldsymbol{\theta} \sim \mathcal{N}([1\ 0]^T, 0.01\mathbf{I})$. Fig. 3.2 depicts the synchronization manifold, $\mathbf{s}$, and a sample trajectory, $\mathbf{x}_1$, converging to $\mathbf{s}$. Fig. 3.3 presents the analytical lower bound on the probability of stable ε-synchronization in the considered ring network, as a function of σ_{θ_2} and σ_γ for $\varepsilon = 0.40$. As it can be seen, the probability of synchronization falls sharply as the variances of mismatches increase. Moreover, we observe that the range of σ_γ and σ_{θ_2} for which the network is stable with high probability is rectangular. This is explained by noting that σ is related to the maximum of σ_γ and σ_{θ_2}, as it can be seen in (3.23). Another observation from Fig. 3.3 is that even small mismatches leads to instability of the synchronization state even with a relatively large tolerance of $\varepsilon = 0.40$.
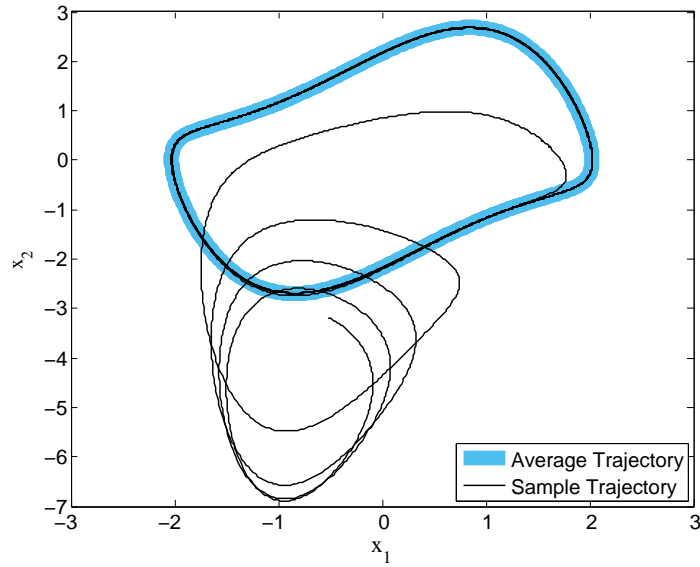
Figure 3.2: Synchronization manifold, $\mathbf{s}$, and a sample trajectory, $\mathbf{x}_1$, for a ring network of van der Pol oscillators.
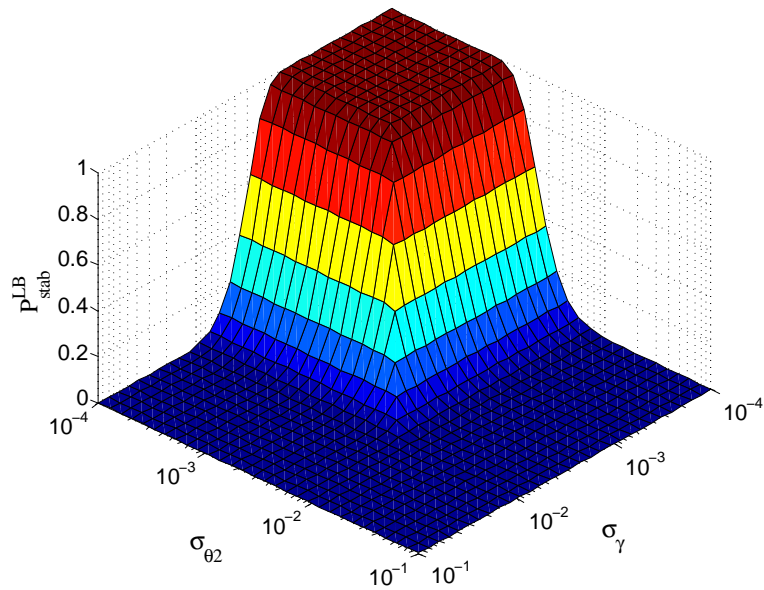
Figure 3.3: $P_{\text{stab}}^{\text{LB}}$ in the ring network as a function of σ_{θ_2} and σ_γ for $\varepsilon = 0.4$.
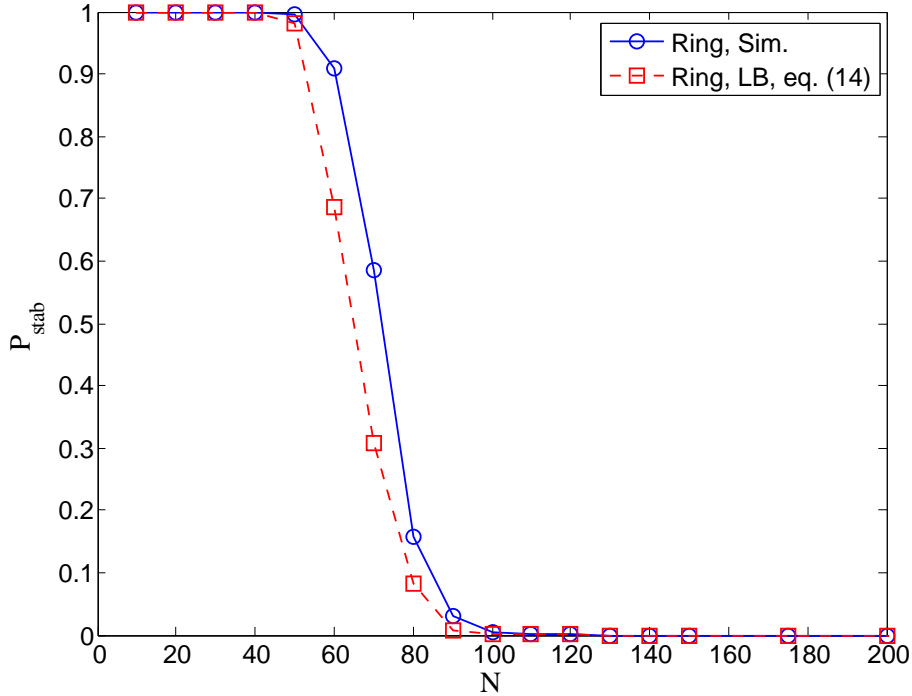
Figure 3.4: Probability of stability as a function N, for the ring network.

We now proceed to compare a ring network, an Erdös-Rényi network and a Newman-Watts (small-world) network. For a fair comparison, we choose the network parameters such that all networks have the same number of nodes and the same average node degree. That is, we consider a $N = 100$ node, 10-regular ring, an Erdös-Rényi network with $N = 100$ and randomness parameter $p = 0.1$, and a Newman-Watts network generated from a $N = 100$ node, 6-regular ring and link addition probability $p = 0.4 \times 100/94 = 0.4167$. Fig.s 3.4 through 3.6 present the probability of stability versus network size, N, for these three networks with $\varepsilon = 0.4$. As it can be seen for the Ring network (Fig. 3.4), as N increases, even though the variance of the mismatch input is constant, $\sigma = 3.15\sigma_\gamma$, the ε-synchronization of the network deteriorates. This is because as the degree of the nodes are kept constant and

network size increases, the algebraic connectivity of the network,

$$\mu_{N-1}^{\mathrm{ring}} = k - 2\frac{\sin(k\pi/2N)\cos((k+2)\pi/2N)}{\sin(\pi/N)},$$

decreases. For large N, in our example, smaller algebraic connectivity means smaller MLE (See Fig. 3.1), hence the probability of ε-synchronization falls sharply.

Fig. 3.5 presents the probability of ε-stability of the Erdös-Rényi network. It is interesting to note that since the network is disconnected for smaller network sizes, the network is not synchronized. As network size continues to grow, the network becomes connected and synchronization behavior emerges. This behavior continues until the growth in the network size, increases the variance of the mismatch input, $\mathbf{v}$, to the extent that the network falls out of ε-stability.
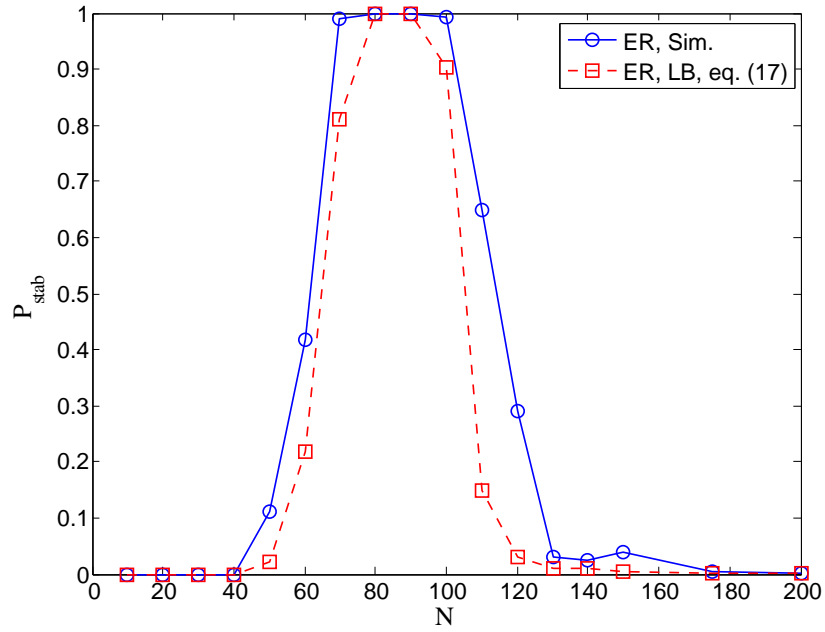
Figure 3.5: Probability of stability as a function N, for the Erdös-Réyni network.
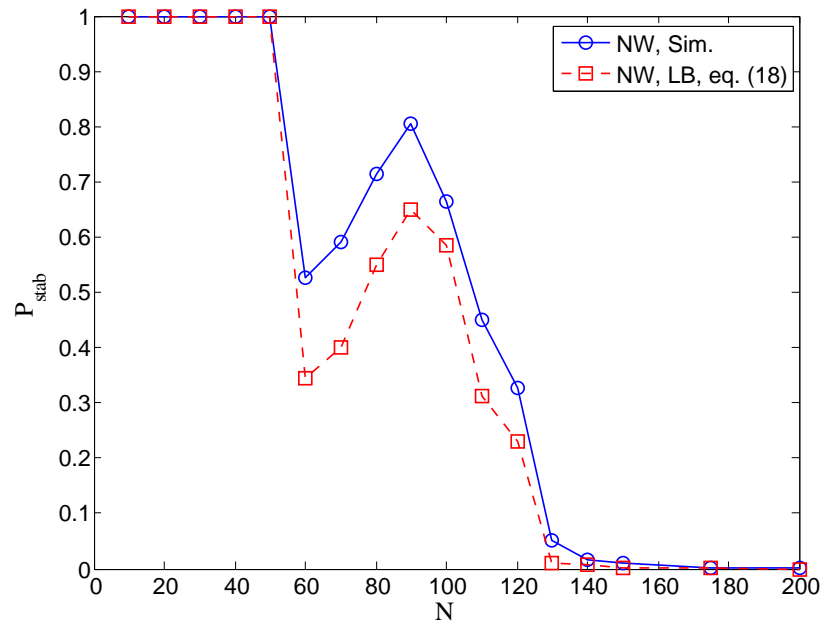
Figure 3.6: Probability of stability as a function N, for the Newman-Watts network.

Fig. 3.6 presents the probability of ε-stability for the Newman-Watts network. It is interesting to note the mechanisms at work as N increases: At first, when N is small there are very few added links given a small value of p. Thus, the network has not yet transitioned into a small-world and its algebraic connectivity is still quite close to that of the ring topology. Thus, as the size of the network increases its second smallest eigenvalue decreases. Since the variance of mismatch, $\mathbf{v}$, is constant ($\sigma_b = 3.15\sigma_\gamma$), the probability of stability decreases. As N continues to increase, by adding links in random, sufficient number of long range connections are established and the small-world transition is achieved. Consequently, algebraic connectivity of the network starts to grow rapidly. Hence, λ_i increase and, therefore, $P_{\text{stab}}^{\text{LB}}$ improves. As N continues to increases $\sqrt{K + Np}\sigma_{\theta_2}$ overtakes $3.15\sigma_\gamma$ in the variance of mismatch and its destructive effect surpasses the improvement caused by transition to small-world. Consequently, we observe that $P_{\text{stab}}^{\text{LB}}$ begins to drop.

Figs. 3.7 through 3.9 depict the probability of ε-stability as a function of ε in the considered Ring, Erdös-Réyni, and Newman-Watts networks for different N and $\bar{d}$: ($N = 100, \bar{d} = 10$), ($N = 200, \bar{d} = 10$), and ($N = 200, \bar{d} = 20$), respectively. As it can be seen, the analytical lower bound and the simulation result for the ring network are reasonably close. This is due to the homogeneity of its node degrees, i.e. $d_i = K$, which holds true for the other networks as N approaches infinity. The other point directly observed from these figures is that the rise in the probability of the stability is much sharper in the Erdös-Réyni and Newman-Watts networks, this is because the spread of the spectrum, $[\mu_{\min}, \mu_{\max}]$, for these networks are smaller than that of ring topology. This, in fact, causes the Lyapunov exponents of the traverse modes to be closer to each other and hence the networks become easily and rapidly synchronized. Other interesting observation is that the results for the Erdös-Réyni and Newman-Watts networks are similar. The reason can be sought in the effectiveness of communication in both networks to each other. As it has been shown in [4], even though

small-worlds are strongly locally connected (due to ring substrate), they have almost the same average shortest path length of Erdös-Réyni networks. This results in almost the same communication efficiency in small-worlds as Erdös-Réyni network. Hence, the synchronizability of both types of networks are similar.
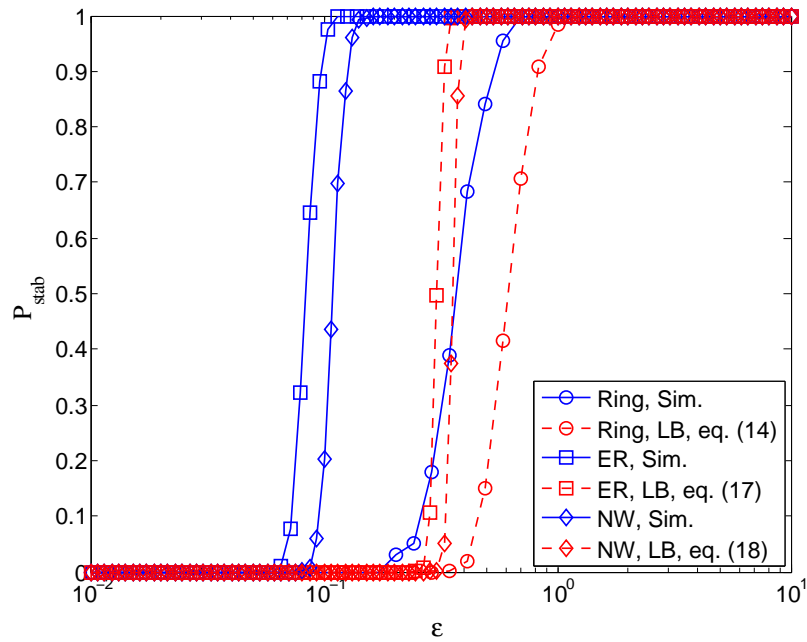
Figure 3.7: P_{stab} as a function of ε for the ring, NW and Erdös-Rényi networks: $N = 100, \bar{d} = 10$.
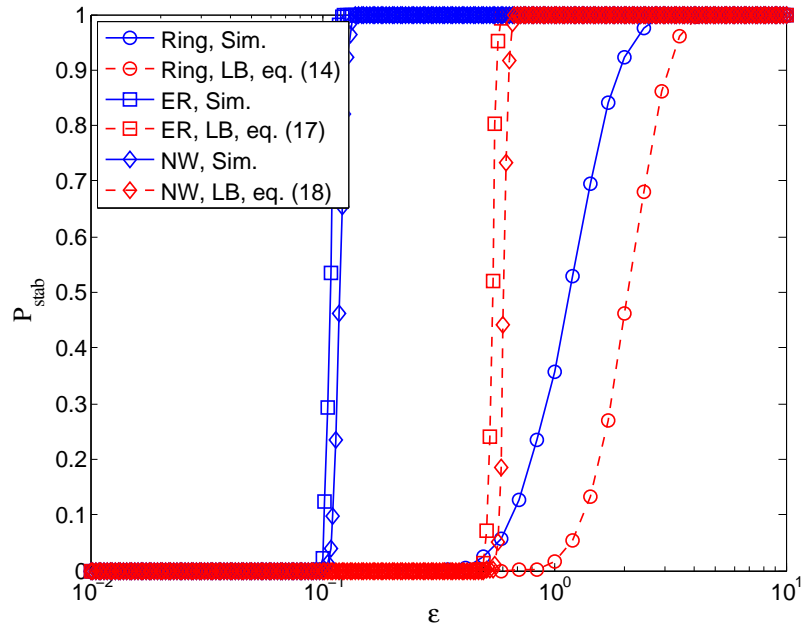
Figure 3.8: P_{stab} as a function of ε for the ring, NW and Erdös-Rényi networks: $N = 200, \bar{d} = 10$.
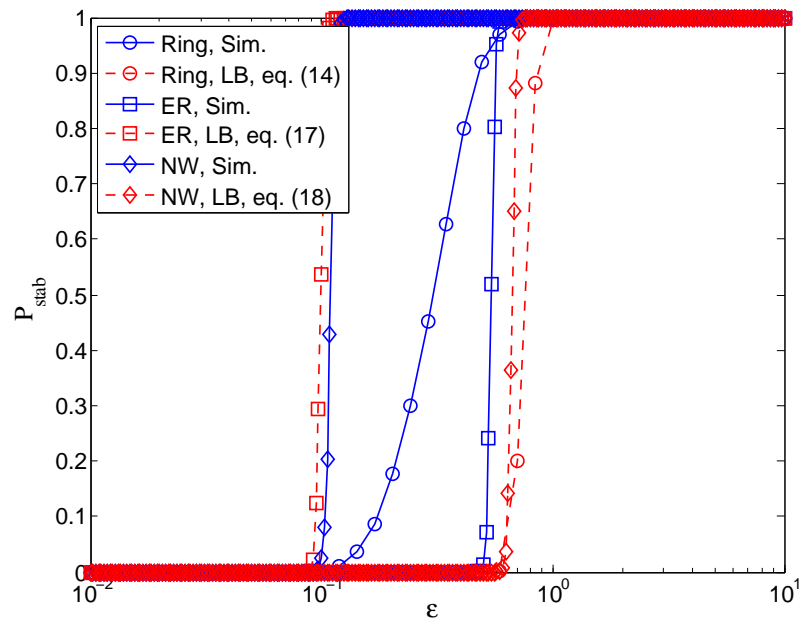
Figure 3.9: P_{stab} as a function of ε for the ring, NW and Erdös-Rényi networks: $N = 200, \bar{d} = 20$.

Conclusion

We had seen that mismatch in either couplings or the local dynamics does not allow perfect synchronization. Rather, the network can only be synchronized to a neighborhood of the synchronization manifold. Considering this relaxed notion of synchronization we have provided a generalized master stability function that takes the mismatches into account. We then used this master stability function to derive lower bounds on the probability of synchronization in regular, Erdös-Rényi, and Newman-Watts networks. We verified our results using numerical examples involving networks of van der Pol oscillators. These examples clearly shows the different phase transition behavior of the different network models.

CHAPTER 4: PINNING CONTROL IN NETWORKS OF DYNAMICAL SYSTEMS

Here, we highlight the effectivity of the pinning control schemes by employing the spectral characteristics of the network. We derive sufficient stability conditions for pinning control of linearly coupled oscillators based on Lyapunov direct method. The introduced stability conditions relate the spectral characteristics of the network to the global stability of synchronization. Based on the derived stability conditions, we introduce an algorithm that achieves global stability of synchronization with a small number of pinning nodes.

Moreover, to the best of our knowledge, all existing studies consider unconstrained controllers in pinning schemes. Since using very large gains in a controller is not practical, we assume that the controller gains are bounded.

System Description

Consider N identical oscillators with phase space equation

$$\dot{\mathbf{x}}_i = \mathbf{A}\mathbf{x}_i + \mathbf{B}\mathbf{f}(\mathbf{C}\mathbf{x}_i), \tag{4.1}$$

$$\mathbf{x}_i(t_0) = \mathbf{x}_{i0}.$$

Now suppose that these oscillators are linearly coupled as

$$\dot{\mathbf{x}}_i = \mathbf{A}\mathbf{x}_i + \mathbf{B}\mathbf{f}(\mathbf{C}\mathbf{x}_i) + c\mathbf{H}\sum_{j=1}^{N} g_{ji}(\mathbf{x}_j - \mathbf{x}_i) + \mathbf{u}_i, \tag{4.2}$$

where $\mathbf{x}_i \in \mathbb{R}^n$ is the state of node i, $\mathbf{A} \in \mathbb{R}^{n \times n}$, $\mathbf{B} \in \mathbb{R}^{n \times m}$ and $\mathbf{C} \in \mathbb{R}^{m \times n}$ are fixed matrices, and $\mathbf{f} : \mathbb{R}^m \to \mathbb{R}^n$ is a nonlinear function. $\mathbf{H} \in \mathbb{R}^{n \times n}$ is the coupling matrix and $c > 0$ is the coupling coefficient. $\mathbf{G} = [g_{ij}] \in \mathbb{R}^{N \times N}$ is the adjacency matrix of the network: $g_{ij} = 0$ indicates that there is no link from node i to node j and $g_{ij} > 0$ indicates a connection from node i to node j with weight g_{ij}. We assume that there are no self-loops, i.e. $g_{ii} = 0$. We also define the Laplacian matrix of the network, $\mathbf{L} \triangleq [l_{ij}]$, as [24]

$$
l_{ij} \triangleq \begin{cases} \sum_{m=1}^{N} g_{mi} & i = j \\ -g_{ij} & i \neq j \end{cases}.
$$

Throughout the paper, we assume that the network is connected and there are no isolated components. In the case of an undirected (bidirectional) network, $\mathbf{L}$ is symmetric and positive semidefinite [24].

Let $\mathbf{s}$ be the solution of

$$
\dot{\mathbf{s}} = \mathbf{As} + \mathbf{Bf}(\mathbf{Cs}), \tag{4.3}
$$

$$
\mathbf{s}(t_0) = \mathbf{s}_0,
$$

where $\mathbf{s}_0 \in \Omega$, and Ω is the set of all initial conditions $\mathbf{x}_0$ such that, $\mathbf{x}(t) \in \Omega$ for all $t \geq t_0$. We know that $\mathbf{s}$ is an invariant manifold of (4.1) [5]. This means that for some choice of initial conditions, $\mathbf{X}(\mathbf{x}_1(t_0), \cdots, \mathbf{x}_N(t_0)) \in \Omega^N$, $\mathbf{S} = [\mathbf{s}, \cdots, \mathbf{s}]^T$ is the synchronous solution of (6.1) [5]. Note that if (4.1) has only fixed points, then $\mathbf{s}$ would be the attracting fixed point, and Ω would be the basin of attraction corresponding to that fixed point. The same goes for limit cycles and chaotic attractors.

Now if we choose $\mathbf{s}$ as a reference signal, the error of trajectory for node i from the invariant

manifold can be defined as

$$\mathbf{e}_i \triangleq \mathbf{x}_i - \mathbf{s}. \tag{4.4}$$

We assume that controller input, $\mathbf{u}_i$, is chosen as linear feedback

$$\mathbf{u}_i = \mathbf{K}_i \mathbf{e}_i. \tag{4.5}$$

Note that since, the pinning approach is decentralized, we only consider the self-feedback in our control rule, and there is no feedback from other nodes in the network.

Suppose that we use $l \leq N$ controllers to achieve synchronization throughout the network. Let $\mathcal{L} \triangleq \{i_1, \cdots, i_l\}$ be the set of pinning points. Then $\forall i \in \mathcal{L}$ we have controller $\mathbf{K}_i \neq \mathbf{0}$ and, $\forall i \notin \mathcal{L}$ we have $\mathbf{K}_i = \mathbf{0}$.

Assumption: There exists a positive semidefinite matrix $\mathbf{M}$ such that

$$\mathbf{e}_i^\dagger \left[\mathbf{f}(\mathbf{x}_i) - \mathbf{f}(\mathbf{s})\right] \leq \mathbf{e}_i^\dagger \mathbf{M} \mathbf{e}_i, \quad \forall \mathbf{x}_i, \mathbf{s} \in \Omega \tag{4.6}$$

where $\dagger$ denotes the Hermitian transpose. Note that this condition is not very restrictive: If all elements of the Jacobian of $\mathbf{f}(\cdot)$ are bounded, there always exists a positive semidefinite matrix $\mathbf{M}$ such that assumption (4.6) holds [19]. This condition is closely related to QUAD condition as discussed in [90]. Unlike QUAD condition, here $\mathbf{M}$ is not necessarily diagonal.

The dynamics of the error terms, $\mathbf{e}_i$, can be found as follows. Starting from (5.4) and substituting (6.1) and (5.3) we have

$$\dot{\mathbf{e}}_i = \dot{\mathbf{x}}_i - \dot{\mathbf{s}}$$

$$= \mathbf{A}\mathbf{e}_i + \mathbf{B}[\mathbf{f}(\mathbf{C}\mathbf{x}_i) - \mathbf{f}(\mathbf{C}\mathbf{s})] + \mathbf{u}_i + \sum_{j=1}^{N} g_{ji}c\mathbf{H}(\mathbf{x}_j - \mathbf{x}_i)$$

$$= \mathbf{A}\mathbf{e}_i + \mathbf{B}[\mathbf{f}(\mathbf{C}\mathbf{x}_i) - \mathbf{f}(\mathbf{C}\mathbf{s})] + \mathbf{u}_i - \sum_{j=1}^{N} l_{ji}c\mathbf{H}\mathbf{x}_j,$$

with the substitution of $\mathbf{u}_i$ from (5.5) we get

$$\dot{\mathbf{e}}_i = \mathbf{A}\mathbf{e}_i + \mathbf{B}[\mathbf{f}(\mathbf{C}\mathbf{x}_i) - \mathbf{f}(\mathbf{C}\mathbf{s})] + \mathbf{K}_i\mathbf{e}_i - \sum_{j=1}^{N} l_{ji}c\mathbf{H}\mathbf{x}_j.$$

Since $\sum_j l_{ji} = 0$, we can add $\sum_j l_{ji}\mathbf{H}\mathbf{s} = \mathbf{0}$, to the right hand side without violating the equality

$$\dot{\mathbf{e}}_i = \mathbf{A}\mathbf{e}_i + \mathbf{B}[\mathbf{f}(\mathbf{C}\mathbf{x}_i) - \mathbf{f}(\mathbf{C}\mathbf{s})] + \mathbf{K}_i\mathbf{e}_i + \sum_{j=1}^{N} l_{ji}c\mathbf{H}\mathbf{s} - \sum_{j=1}^{N} l_{ji}c\mathbf{H}\mathbf{x}_j$$

$$= \mathbf{A}\mathbf{e}_i + \mathbf{B}[\mathbf{f}(\mathbf{C}\mathbf{x}_i) - \mathbf{f}(\mathbf{C}\mathbf{s})] + \mathbf{K}_i\mathbf{e}_i - \sum_{j} l_{ji}c\mathbf{H}\mathbf{e}_j. \tag{4.7}$$

Theorem: If assumption (4.6) holds, synchronization in the network of identical oscillators is asymptotically stable if $\mathbf{K}_i$ satisfy the following set of linear matrix inequalities (LMI)

$$\mathbf{A} - \lambda_i c\mathbf{H} + \mathbf{B}^T\mathbf{C}^T\mathbf{M}\mathbf{C}\mathbf{B} + \sum_{j\in\mathcal{L}} |q_{ij}|^2\mathbf{K}_j \prec \mathbf{0}, \tag{4.8}$$

83

for all $i \in \mathcal{N} = \{1, \cdots, N\}$, where λ_i is the ith eigenvalue of the Laplacian matrix $\mathbf{L}$, and $\mathbf{Q} = [q_{ij}]$ is a unitary matrix associated with Schur decomposition of $\mathbf{L}$. That is $\mathbf{L} = \mathbf{Q}^\dagger \mathbf{\Lambda} \mathbf{Q}$ and λ_i are the diagonal entries of $\mathbf{\Lambda}$. Moreover, $\mathbf{\Lambda}$ is diagonal if $\mathbf{L}$ has N distinct eigenvalues. Otherwise it is upper triangular.

Proof. Consider the Lyapunov function

$$v \triangleq \frac{1}{2}\mathbf{e}^\dagger \mathbf{e} = \frac{1}{2}\sum_i \mathbf{e}_i^\dagger \mathbf{e}_i.$$

where $\mathbf{e} = [\mathbf{e}_1^T \; \cdots \; \mathbf{e}_N^T]^T$. Thus, we can write (5.7) as

$$\dot{\mathbf{e}} = (\mathbf{I}_N \otimes \mathbf{A})\mathbf{e} + (\mathbf{I} \otimes \mathbf{B}) \begin{bmatrix} \mathbf{f}(\mathbf{Cx}_1) - \mathbf{f}(\mathbf{Cs}) \\ \vdots \\ \mathbf{f}(\mathbf{Cx}_N) - \mathbf{f}(\mathbf{Cs}) \end{bmatrix} - c(\mathbf{L} \otimes \mathbf{H})\mathbf{e} + \mathrm{diag}([\mathbf{K}_1, \cdots, \mathbf{K}_N])\mathbf{e}. \quad (4.9)$$

The derivative of the Lyapunov function can be calculated as

$$\dot{v} = \mathbf{e}^\dagger \dot{\mathbf{e}} = \sum_{i \in \mathcal{N}} \mathbf{e}_i^\dagger \dot{\mathbf{e}}_i. \quad (4.10)$$

Substituting (4.9) in (4.10) the derivative of Lyapunov function is

$$\begin{aligned} \dot{v} =& \mathbf{e}^\dagger \left(\mathbf{I} \otimes \mathbf{A} - c\mathbf{L} \otimes \mathbf{H} + \mathrm{diag}([\mathbf{K}_1, \cdots, \mathbf{K}_N]) \right) \mathbf{e} \\ &+ \mathbf{e}^\dagger (\mathbf{I} \otimes \mathbf{B}) \begin{bmatrix} \mathbf{f}(\mathbf{Cx}_1) - \mathbf{f}(\mathbf{Cs}) \\ \vdots \\ \mathbf{f}(\mathbf{Cx}_N) - \mathbf{f}(\mathbf{Cs}) \end{bmatrix} \end{aligned}$$

defining $\boldsymbol{\eta} \triangleq (\mathbf{Q} \otimes \mathbf{I})\mathbf{e}$, or $\boldsymbol{\eta}_i = \sum_{j \in \mathcal{N}} q_{ij}\mathbf{e}_j$, and using the Kronecker product properties, we

84

have $v = 1/2\boldsymbol{\eta}^\dagger\boldsymbol{\eta}$, and

$$\dot{v} = \boldsymbol{\eta}^\dagger\left\{\mathbf{I}\otimes\mathbf{A} - c\boldsymbol{\Lambda}\otimes\mathbf{H} + \mathrm{diag}\left(\left[\sum_{j\in\mathcal{L}}q_{ij}^2\mathbf{K}_j\right]\right)\right\}\boldsymbol{\eta} + \boldsymbol{\eta}^\dagger(\mathbf{Q}\otimes\mathbf{I})(\mathbf{I}\otimes\mathbf{B})\begin{bmatrix}\mathbf{f}(\mathbf{Cx}_1) - \mathbf{f}(\mathbf{Cs})\\ \vdots\\ \mathbf{f}(\mathbf{Cx}_N) - \mathbf{f}(\mathbf{Cs})\end{bmatrix}$$

$$\leq \boldsymbol{\eta}^\dagger\left\{\mathbf{I}\otimes\mathbf{A} - c\boldsymbol{\Lambda}\otimes\mathbf{H} + \mathrm{diag}\left(\left[\sum_{j\in\mathcal{L}}q_{ij}^2\mathbf{K}_j\right]\right)\right\}\boldsymbol{\eta} + \boldsymbol{\eta}^\dagger(\mathbf{I}\otimes(\mathbf{B}^T\mathbf{MC}^T\mathbf{CB}))\boldsymbol{\eta}$$

$$= \boldsymbol{\eta}^\dagger\left\{\mathbf{I}\otimes\mathbf{A} - c\boldsymbol{\Lambda}\otimes\mathbf{H} + \mathrm{diag}\left(\left[\sum_{j\in\mathcal{L}}q_{ij}^2\mathbf{K}_j\right]\right) + \mathbf{I}\otimes(\mathbf{B}^T\mathbf{C}^T\mathbf{MCB})\right\}\boldsymbol{\eta}$$

$$= \sum_{i\in\mathcal{N}}\boldsymbol{\eta}_i^\dagger\left(\mathbf{A} - \lambda_i c\mathbf{H} + \sum_{j\in\mathcal{L}}q_{ij}^2\mathbf{K}_j + \mathbf{B}^T\mathbf{C}^T\mathbf{MCB}\right)\boldsymbol{\eta}_i,$$

Thus, having

$$\mathbf{A} - \lambda_i c\mathbf{H} + \sum_{j\in\mathcal{L}}q_{ij}^2\mathbf{K}_j + \mathbf{B}^T\mathbf{C}^T\mathbf{MCB} \prec \mathbf{0}$$

for all $i \in \mathcal{N}$ guarantees that $\dot{v} < 0$, which mean that the synchronization is stable. $\qquad\square$

Corollary: If assumption (4.6) holds, the set of controllers $\mathbf{u}_i = \mathbf{K}_i\mathbf{e}_i = -ck_i\mathbf{He}_i$ for $i \in \mathcal{L}$ globally asymptotically stabilizes the synchronization in the network, if k_i satisfy

$$\mathbf{A} - c\left(\lambda_i + \sum_{j\in\mathcal{L}}|q_{ij}|^2 k_j\right)\mathbf{H} + \mathbf{B}^T\mathbf{C}^T\mathbf{MCB} \prec \mathbf{0}, \tag{4.11}$$

for all $i \in \mathcal{N}$.

This corollary is more effective when $\mathbf{H}$ is positive definite. Hereafter, we limit ourselves to the case of positive definite $\mathbf{H}$, as assumed in [17] [19] [49].

Remark 1: It is clear from (4.11) that the dynamics of the oscillators can be stabilized

around the synchronization manifold by utilizing one controller with a very large control gain, as long as there exists a Schur decomposition such that $\mathbf{Q}$ has at least one nonzero column.

While the synchronization can be stabilized with a single controller, it is also clear from (4.11) requires a large controller gain. However, in most real world applications having a controller with a large gain is not desirable. To address this issue we seek to stabilize the network with small number of controllers, $|\mathcal{L}|$, under the constraint

$$||\mathbf{K}_i|| < p \quad \forall i \in \mathcal{L}. \tag{4.12}$$

Following the corollary, we form the following function

$$\Psi(\mu) = \mathrm{Re}\{\lambda_{\max}(\mathbf{A} + \mathbf{B}^T\mathbf{C}^T\mathbf{MCB} - \mu c\mathbf{H})\}, \tag{4.13}$$

where $\mathrm{Re}\{\cdot\}$ returns the real part of the argument. Since the coupling matrix is assumed to be positive definite, $\Psi(\mu)$ is a strictly decreasing function of μ. Thus, there exist μ^* such that $\mu > \mu^*$ satisfies $\Psi(\mu) < 0$; or

$$\mu^* = \text{minimize } \mu$$

$$\text{subject to } \Psi(\mu) \leq 0.$$

In other words, if the network has a larger algebraic connectivity [31] than μ^*, it will achieve stability. Thus, if LMI's in (4.8) or (4.11) are not all satisfied, it will be due to the smaller eigenvalues.

Remark 2: It has been shown that for unweighted-undirected networks, if λ_i and d_i are

sorted in descending order, λ_i majorize d_i [31], *i.e.*

$$\sum_{j=1}^{r} \lambda_j \geq \sum_{j=1}^{r} d_j \quad 1 \leq r \leq N,$$

Also we know that $\text{trace}(\mathbf{L}) = \sum_{i=1}^{N} d_i = \sum_{i=1}^{N} \lambda_i$. Therefore,

$$\sum_{j=1}^{r} \lambda_{N-j} \leq \sum_{j=1}^{r} d_{N-j} \quad 1 \leq r \leq N.$$

Hence, lower degrees are more closely linked to the smaller eigenvalues compared to higher degrees. This suggests that lower degree nodes are more susceptible to instability than the higher degree nodes. Thus, pinning the lower degrees is more effective than pinning other nodes. This also has been shown in [19].

Pinning Algorithm

It is clear from (4.11) that larger controller gains help stability. Therefore, when a node is assigned to be a pinning point, one would like to maximize its feedback gain, as allowed by the constraint. Thus, we set

$$k_i = \frac{p}{c||\mathbf{H}||} a_i,$$

where $a_i = 1$ indicates that i is a pinning point ($i \in \mathcal{L}$) and $a_i = 0$ means $i \notin \mathcal{L}$. Hence, the stability conditions can be written as

$$\mu^* - \lambda_i \leq \frac{p}{c||\mathbf{H}||} \sum_{j \in \mathcal{L}} |q_{ij}|^2 \tag{4.14}$$

for all $i \in \mathcal{N}$.

Thus, the problem of finding minimum number of pinning controllers is reduced to

$$\begin{aligned}
\text{minimize} \quad & \sum_{i \in \mathcal{N}} a_i \\
\text{subject to} \quad & \mu^* - \lambda_i \le \frac{p}{c\|\mathbf{H}\|} \sum_{j=1}^{N} a_j |q_{ij}|^2 \quad \forall i \in \mathcal{N}_0.
\end{aligned} \tag{4.15}$$

Here $\mathcal{N}_0$ contains all $i \in \mathcal{N}$ for which the condition in (4.14) is not satisfied.

This is a standard binary linear program, which is known to be NP-hard in general. In the following we propose a suboptimal heuristic algorithm to assign pinning points. Our algorithm is based on the observation that the constraints with smaller eigenvalues requires more effective gain, $\sum_{j=1}^{N} |q_{ij}|^2 k_i$, to be satisfied. Thus, we start with condition with the smallest eigenvalue and proceed to satisfy the conditions until we reach the condition with largest eigenvalue that is not yet satisfied. The following outlines the algorithm:

1. Sort $\lambda_i \ \forall i \in \mathcal{N}_0$ such that $0 = \lambda_{i_0} < \lambda_{i_1} \le \cdots \le \lambda_{i_{N_0-1}}$.

2. Set $v := 0$, and $\mathcal{L} := \emptyset$.

3. If $\mathcal{N}_v = \emptyset$

   - Done

   else go to 4.

4. Add j^* to $\mathcal{L}$ where $j^* = \arg\max_{j \notin \mathcal{L}} |q_{i_v j}|^2$.

5. If (4.14) is satisfied for i_v

   - $v := v + 1$.

   - Set $\mathcal{N}_v$ to include i for which (4.14) is not satisfied.

   - Go to 3.

else, go to 4.

This algorithm provides the suboptimal solution in polynomial time.

Numerical Example

In this section we study a numerical example using the well-known Lorenz chaotic attractor [19]. Consider the state space equation of Lorenz attractor

$$\dot{x}_1 = -35x_1 + 35x_2$$

$$\dot{x}_2 = -7x_1 + 28x_2 - x_1x_3 \tag{4.16}$$

$$\dot{x}_3 = x_1x_2 - 3x_3.$$

We can write these equations in the form (6.1) with $\mathbf{B} = \mathbf{C} = \mathbf{I}_3$, $\mathbf{f}([x_1 \ x_2 \ x_3]^T) = [0 \ -x_1x_3 \ x_1x_2]^T$, and

$$\mathbf{A} = \begin{bmatrix} -35 & 35 & 0 \\ -7 & 28 & 0 \\ 0 & 0 & -3 \end{bmatrix}.$$

Now, we find $\mathbf{M}$ in (4.6) as

$$\mathbf{e}_i^T[\mathbf{f}(\mathbf{x}_i) - \mathbf{f}(\mathbf{s})] = e_{i3}(x_{i1}x_{i2} - s_1s_2) - e_{i2}(x_{i1}x_{i3} - s_1s_3)$$

$$= e_{i3}(s_1e_{i2} + x_{i2}e_{i1}) - e_{i2}(s_1e_{i3} + x_{i3}e_{i1})$$

$$= -x_{i3}e_{i1}e_{i2} + x_{i2}e_{i1}e_{i3}, \tag{4.17}$$

Since $\mathbf{x}_i \in \Omega$ is bounded, absolute value of its mth component $|x_{i,m}|$ can be bounded by M_m. In this example, we can find these bounds numerically to be $|x_{i,1}| \leq M_1 = 23$, $|x_{i,2}| \leq M_2 =$

32, $|x_{i,3}| \le M_3 = 61$. Using the Cauchy-Schwartz inequality, $2e_ie_j \le e_i^2 + e_j^2$, we have

$$\mathbf{e}_i^T[\mathbf{f}(\mathbf{x}_i) - \mathbf{f}(\mathbf{s})] \le \frac{1}{2}(e_{i1}^2 + e_{i2}^2)|x_{i3}| + \frac{1}{2}(e_{i1}^2 + e_{i3}^2)|x_{i2}|$$
$$\le \frac{M_3}{2}e_{i1}^2 + \frac{M_3 + M_2}{2}e_{i2}^2 + \frac{M_2}{2}e_{i3}^2. \qquad (4.18)$$

Thus,

$$\mathbf{M} = \frac{1}{2}\begin{bmatrix} M_3 & 0 & 0 \\ 0 & M_2 + M_3 & 0 \\ 0 & 0 & M_2 \end{bmatrix} = \begin{bmatrix} 30.5 & 0 & 0 \\ 0 & 46.5 & 0 \\ 0 & 0 & 16.0 \end{bmatrix}$$

satisfies (4.6).

We assume the coupling matrix

$$\mathbf{H} = \frac{1}{2}\begin{bmatrix} 1 & 0 & 0 \\ 0 & 2 & 0 \\ 0 & 0 & 1 \end{bmatrix}. \qquad (4.19)$$

We have chosen $\mathbf{H}$ such that $||\mathbf{H}|| = 1$ so that the coupling strength is only determined by coupling coefficient c.

Threshold value of (4.13), scaled by coupling coefficient, is found to be $\mu^*c = 68.17$.

For the simulation purposes, here we adopt the Newman's method to construct a scale-free network [25]. This method, in contrast to the well known random rewiring approach of Watts and Strogatz [4], only adds links randomly between vertices of a regular network with a small probability, ρ. The regular network considered here is a ring network with coordination number m.
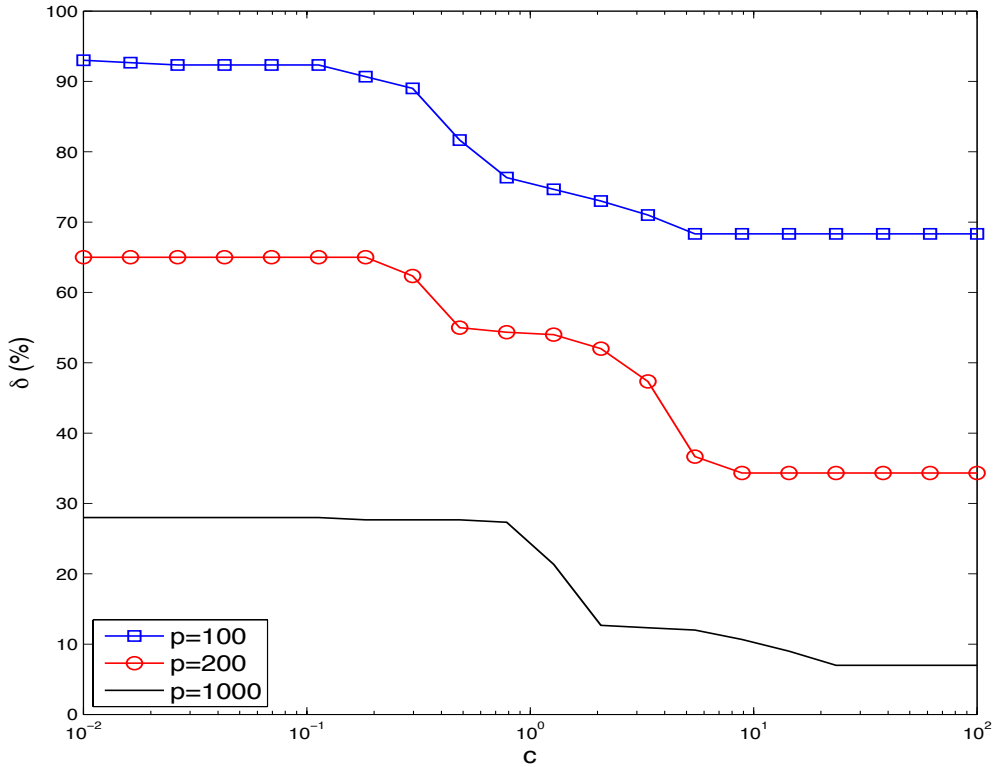
Figure 4.1: Percentage of required pinning points ($\delta = l/N$) versus coupling strength, c, for different values of controller gain constraint, p, in a scale- free network ($N = 300$, $m = 10$ and $\rho = 0.005$), using our proposed method.

The ratio of required number of controllers to the network size, $\delta = l/N$, versus coupling strength, c, for different constraint values, p, is given in Fig. 4.1. It is clear that the performance of the proposed scheme strongly depends on the value of constraint on controllers' gain. More importantly, it can be seen that our approach can stabilize the network for even for very small coupling strengths. In contrast, other schemes such as [19] and [69], cannot

stabilize the synchronization for small coupling coefficients. Also in Fig. 4.1, we see a step-like descending of required ratio of controllers as coupling strength increases. The reason for this behavior is that when c increases, the unstable modes become stable one by one and they no longer contribute to the constraint in (4.15). Due to high clustering coefficient in scale-free networks, eigenvalues appear as bundles close to each other (Fig. 4.2). Consequently, when c crosses each bundle, δ decreases quickly. Then, it remains flat until it reaches another bundle of eigenvalues.
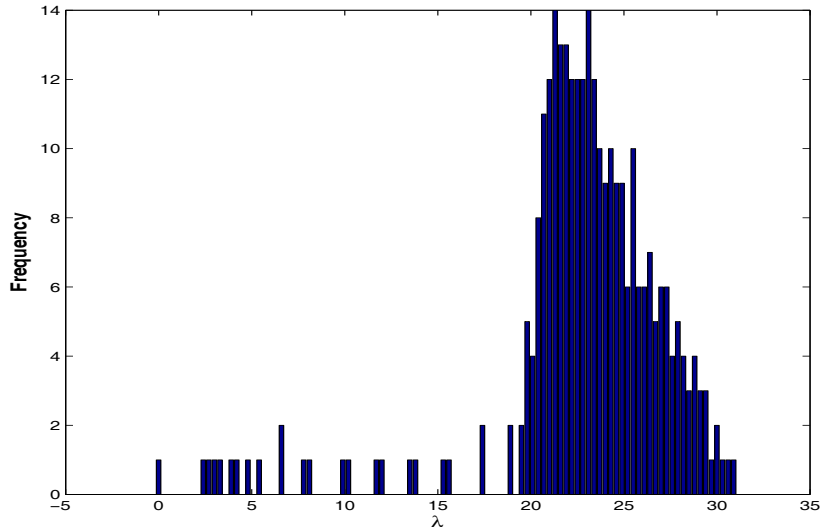
Figure 4.2: Histogram of eigenvalues of Laplacian matrix of a scale-free network ($N = 300$, $m = 10$ and $\rho = 0.005$), for one realization.
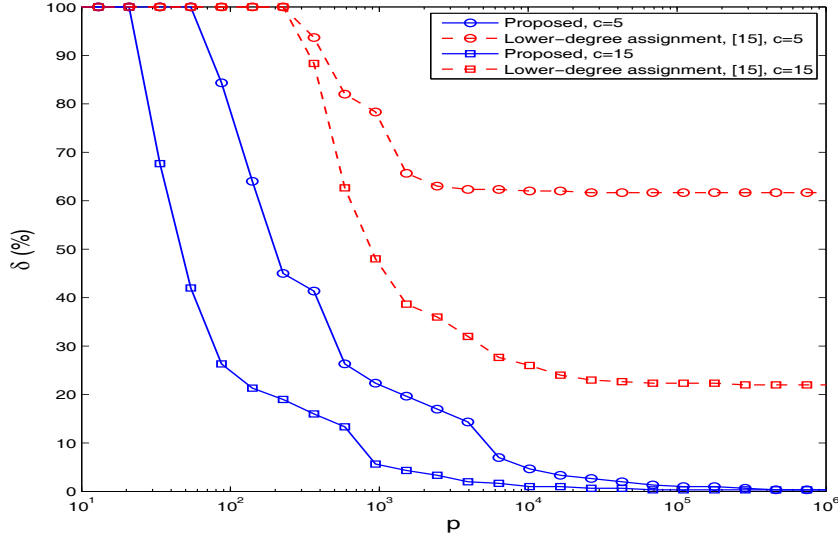
Figure 4.3: Percentage of required pinning points ($\delta = l/N$) versus coupling strength, c, proposed method for different values of controller gains, p, in a scale-free network ($N = 300$, $m = 10$ and $\rho = 0.005$).

Fig. 4.3 shows the percentage of required pinning controllers for stabilization of synchronization versus constraint p with low degree assignment approach of [19] and our proposed scheme, with different coupling strengths. The simulations are performed for both methods under the same constraint on the controller gains. As it can be seen, our method guarantees stability with a smaller number of pinning controllers than the lower-degree assignment proposed in [19]. It is worth noting that when the coupling matrix is positive definite, it has been shown in [19] that lower degree assignment requires fewer nodes to be pinned in comparison to random and higher degree assignments studied in [69].

It is clear that as the constraint on the controller gains is loosened, our scheme uses fewer controllers to stabilize the synchronization throughout the network. In the extreme, if the

constraint is sufficiently relaxed, our approach coincides with that of [17] where the stabilization is accomplished using a single pinning controller.

Another issue of the interest is the total power consumed by the controllers. Fig. 4.4 shows the normalized total required power, lp^2, as a function of the constraint, p, for different coupling strengths, c. We can see that using multiple controllers results in lower total required power compared to single controller pinning method. The overlapped part of the plots corresponding to the proposed method is due to requiring the pinning of all the nodes to achieve stabilization in lower gains. Also, it is clear that our algorithm outperforms the approach in [19] in the sense of required total power to stabilize the network.
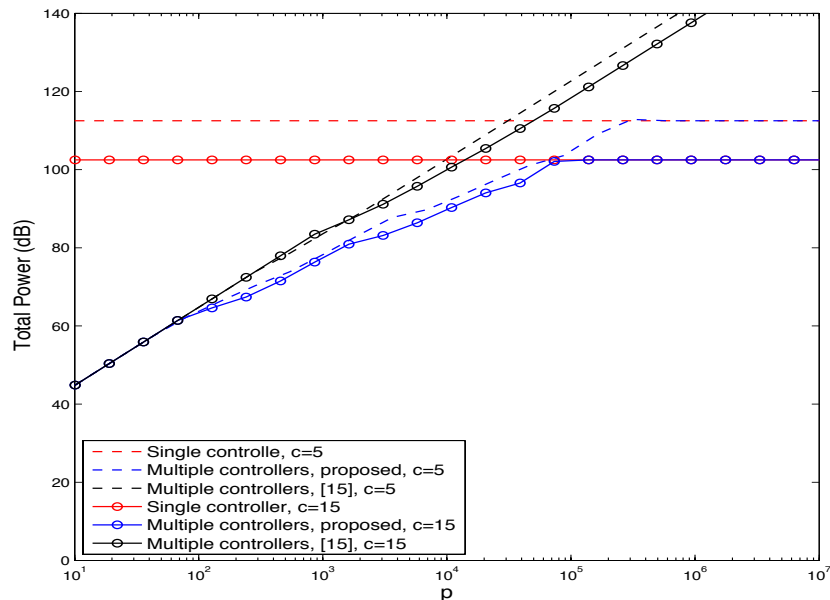
Figure 4.4: Total required power consumed by controllers in a scale-free network for different coupling strengths.

Conclusion

We introduced a pinning algorithm based on spectrum of the network, and assuming constrained controller gains. The proposed algorithm identifies the spectral modes where the network is susceptible to instability. With a numerical example we have shown how the required ratio of pinning changes in terms of structure of scale-free networks. We have also shown that our scheme outperforms the existing controller-assignments such as random, higher-degree or lower-degree assignments, in the sense of using fewer controllers under the same conditions. We have argued that if the constraint on the controller gains is relaxed sufficiently, our algorithm can pin the network by a single controller. Also we demonstrated that our method is more efficient than the existing methods in terms of total power.

CHAPTER 5: PINNING CONTROL IN FAST SWITCHING NETWORKS

Motivated by increasing interest in stabilization of switching networks, here, we employ the pinning control approach to stabilize a switching network of oscillators. We find the smallest ratio of pinned nodes required to guarantee stability of synchronization. We then relate the maximum allowable feedback gain to minimum pinning ratio.

Notations and System Description

Notation

The set of real n-vectors is denoted by $\mathbb{R}^n$ and the set of real $m \times n$ matrices is denoted by $\mathbb{R}^{m \times n}$. Matrices and vectors are denoted by capital and lower-case bold letters, respectively. Identity matrix of size m is denoted by $\mathbf{I}_m$ and all one matrix of size $m \times n$ by $\mathbf{1}_{m \times n}$.

Table I summarizes the variables used frequently in the paper.

Table 5.1: Frequently used variables

Variable	Description
$\mathbf{x}_i$	State vector of node i
$\mathbf{u}_i$	Input vector of node i
$\mathbf{s}$	Reference signal
$\mathbf{e}_i$	Error of trajectory from reference signal for node i
$\mathbf{F}$	Jacobian matrix of local dynamics
$\mathbf{H}$	Coupling matrix between two nodes in the dynamic network
c	Coupling strength in dynamics network
N	Network size
$\mathbf{A} = [a_{ij}]$	Adjacency matrix of the network
$\mathbf{L} = [l_{ij}]$	Laplacian matrix of the network

System Description

Consider N diffusively coupled identical oscillators

$$\dot{\mathbf{x}}_i = \mathbf{f}(\mathbf{x}_i) + c \sum_{j=1}^{N} a_{ij}(t)\mathbf{H}(\mathbf{x}_j - \mathbf{x}_i) + \mathbf{u}_i, \tag{5.1}$$

$$\mathbf{x}_i(t_0) = \mathbf{x}_{i0},$$

where $\mathbf{x}_i \in \mathbb{R}^n$ is the state of node i, $\mathbf{f} : \mathbb{R}^n \to \mathbb{R}^n$ is a nonlinear function describing the dynamics of the oscillators, $\mathbf{H}$ is the coupling matrix, and $c > 0$ is the coupling strength.

$\mathbf{A} = [a_{ij}(t)]$ is the binary adjacency matrix of the network: $a_{ij}(t) = 0$ indicates that there is no coupling from node i to node j and $a_{ij}(t) = 1$ indicates a connection from node i to node j. We assume that the network is undirected, i.e. $\mathbf{A}$ is symmetric. Moreover, we assume that there are no self-loops, i.e. $a_{ii}(t) = 0$ for all t. Furthermore, we assume that with period T_s, $a_{ij}(t)$ takes a new binary value, independent of its previous values and of other links. In other words, the graph is constant over time intervals of length T_s, and when a switching occurs, the new graph is an Erdös-Rényi graph, independent of all past graphs, with edge probability p.Moreover, it is assumed that $a_{ij}(t)$ takes the value 1 with probability p and 0 with probability of $1 - p$. The Laplacian matrix of the network, $\mathbf{L}(t) \triangleq [l_{ij}(t)]$, is defined as

$$l_{ij}(t) \triangleq \begin{cases} \sum_{m=1}^{N} a_{mi}(t) & i = j \\ -a_{ij}(t) & i \neq j \end{cases}. \tag{5.2}$$

Let $\mathbf{s}$ be the solution of

$$\dot{\mathbf{s}} = \mathbf{f}(\mathbf{s}), \tag{5.3}$$
$$\mathbf{s}(t_0) = \mathbf{s}_0,$$

where $\mathbf{s}_0 \in \Omega$, and Ω is the set of all initial states $\mathbf{x}_0$ such that, $\mathbf{x}(t) \in \Omega$ for all $t \geq t_0$. In [5] it is shown that $\mathbf{s}$ is an invariant manifold of (6.1). This means that for some choice of initial conditions, $(\mathbf{x}_{1,0}, \cdots, \mathbf{x}_{N,0}) \in \Omega^N$, $(\mathbf{s}, \cdots, \mathbf{s})$ is the synchronous solution of (6.1) [5]. Note that if (5.3) only has fixed points, then $\mathbf{s}$ will be an attracting fixed point, and Ω will be the basin of attraction corresponding to that fixed point. The same goes for limit cycles and chaotic attractors.

Now, if we choose $\mathbf{s}$ as a reference signal, the error of trajectory of node i from the invariant

manifold can be defined as

$$\mathbf{e}_i \triangleq \mathbf{x}_i - \mathbf{s}. \tag{5.4}$$

We assume that the control input, $\mathbf{u}_i$, is chosen as linear feedback

$$\mathbf{u}_i = -\zeta_i k \mathbf{H} \mathbf{e}_i, \tag{5.5}$$

where k is the feedback gain and ζ_i is a binary variable, where $\zeta_i = 1$ indicates that node i is pinned. Note that since the pinning approach is decentralized, we only consider the self-feedback in our control rule, and there is no feedback from other nodes in the network.

Analysis

The dynamics of the error terms, $\mathbf{e}_i$, can be found as follows. Starting from (5.4) and substituting (6.1) and (5.3) we have

$$\dot{\mathbf{e}}_i = \dot{\mathbf{x}}_i - \dot{\mathbf{s}}$$
$$= \mathbf{F}\mathbf{e}_i + \mathbf{u}_i + \sum_{j=1}^{N} a_{ji} c \mathbf{H}(\mathbf{x}_j - \mathbf{x}_i)$$
$$= \mathbf{F}\mathbf{e}_i + \mathbf{u}_i - \sum_{j=1}^{N} l_{ji} c \mathbf{H}\mathbf{x}_j.$$

With the substitution of $\mathbf{u}_i$ from (5.5) we get

$$\dot{\mathbf{e}}_i = \mathbf{F}\mathbf{e}_i - k\zeta_i \mathbf{H}\mathbf{e}_i - \sum_{j=1}^{N} l_{ji} c \mathbf{H}\mathbf{x}_j.$$

Since $\sum_j l_{ji} = 0$, we can add $\sum_j l_{ji} \mathbf{H} \mathbf{s} = \mathbf{0}$, to the right hand side without violating the equality

$$\dot{\mathbf{e}}_i = \mathbf{F} \mathbf{e}_i - k \zeta_i \mathbf{H} \mathbf{e}_i + \sum_{j=1}^{N} l_{ji} c \mathbf{H} \mathbf{s} - \sum_{j=1}^{N} l_{ji} c \mathbf{H} \mathbf{x}_j$$

$$= \mathbf{F} \mathbf{e}_i - k \zeta_i \mathbf{H} \mathbf{e}_i - \sum_j l_{ji} c \mathbf{H} \mathbf{e}_j. \tag{5.6}$$

Now, stacking $\mathbf{e}_i$ yields

$$\dot{\mathbf{e}} = \left(\mathbf{I}_N \otimes \mathbf{F} - \left[k \operatorname{diag}(\zeta_1 \ \cdots \ \zeta_N) + c \mathbf{L}(t) \right] \otimes \mathbf{H} \right) \mathbf{e}, \tag{5.7}$$

where $\mathbf{e} = [\mathbf{e}_1^T \ \mathbf{e}_2^T \cdots \mathbf{e}_N^T]^T$. If we define matrix $\mathbf{M}(t) = [m_{ij}(t)]$ by

$$m_{ij}(t) = \begin{cases} l_{ij}(t) & i \neq j \, \& \, 1 \leq i, j \leq N \\ l_{ii}(t) + \zeta_i k / c & i = j \, \& \, 1 \leq i \leq N \\ 0 & i = N + 1 \\ -\zeta_i k / c & j = N + 1 \, \& \, 1 \leq i \leq N \end{cases}, \tag{5.8}$$

then (5.7) can be written as

$$\dot{\mathbf{y}} = (\mathbf{I}_{N+1} \otimes \mathbf{F} - c \mathbf{M}(t) \otimes \mathbf{H}) \mathbf{y}, \tag{5.9}$$

where $\mathbf{y} = [\mathbf{e}^T \ \mathbf{s}^T]^T$.

To study the stability of the system (5.9) with the fast switching condition [43, 52, 57], we will use the following theorem:

Theorem 1 [52]: Consider the dynamical system

$$\dot{\mathbf{e}} = (\mathbf{I} \otimes \mathbf{F}(t) + \bar{\mathbf{L}} \otimes \mathbf{H})\mathbf{e}, \quad \mathbf{e}(t_0) = \mathbf{e}_0, \qquad \forall t \geq t_0 \qquad (5.10)$$

where

$$\bar{\mathbf{L}} = \mathbb{E}[\mathbf{L}(t)],$$

and $\mathbb{E}[\cdot]$ is the expected value operator. Assuming that

1. $\mathbf{F}(t)$ is bounded and continuous in $\mathbb{R}_+$, and

2. switching of $\mathbf{L}(t)$ is ergodic, and

3. system (5.10) is uniformly asymptotically stable,

then there exists $T_d > 0$ such that for all $0 < T_s \leq T_d$, the stochastic system

$$\dot{\mathbf{z}} = (\mathbf{I} \otimes \mathbf{F}(t) + \mathbf{L}(t/T_s) \otimes \mathbf{H})\mathbf{z}, \quad \mathbf{z}(t_0) = \mathbf{z}_0, \qquad \forall t \geq t_0$$

is uniformly asymptotically stable almost surely.

Based on this theorem, there exists a dwelling time T_d such that if $T_s < T_d$, then the stability of the system (5.9) can be investigated by considering the expected value of $\mathbf{M}(t)$, denoted by $\bar{\mathbf{M}}$, and we can carry out the stability analysis by using master stability function as in [5].

To use the results in Theorem 1, first we calculate the expected value of the Laplacian matrix

of the system in (5.9)

$$\bar{\mathbf{M}} = p \begin{bmatrix} (N-1) + \frac{k}{cp}\zeta_1 & -1 & \cdots & -1 & -\frac{k}{cp}\zeta_1 \\ -1 & (N-1) + \frac{k}{cp}\zeta_2 & \cdots & -1 & -\frac{k}{cp}\zeta_2 \\ \vdots & \vdots & \ddots & \vdots & \vdots \\ -1 & -1 & \cdots & (N-1) + \frac{k}{cp}\zeta_N & -\frac{k}{cp}\zeta_N \\ 0 & 0 & \cdots & 0 & 0 \end{bmatrix}. \qquad (5.11)$$

Now we proceed to calculate the eigenvalues of $\bar{\mathbf{M}}$ to determine the stability of the network by the available results from static networks. The following Lemma provides the eigenvalues of $\bar{\mathbf{M}}$.

Lemma 4. *Eigenvalues of matrix $\bar{\mathbf{M}}$ are*

$$\lambda_{N+1} = 0$$

$$\lambda_N = \frac{1}{2}\left(pN + \frac{k}{c} - \sqrt{\left(pN + \frac{k}{c}\right)^2 - \frac{4pmk}{c}}\right)$$

$$\lambda_{N-1} = \cdots = \lambda_{m+1} = pN$$

$$\lambda_m = \frac{1}{2}\left(pN + \frac{k}{c} + \sqrt{(pN + \frac{k}{c})^2 - 4pm\frac{k}{c}}\right)$$

$$\lambda_{m-1} = \cdots = \lambda_1 = \frac{k}{c} + pN,$$

where m is the number of pinning nodes.

Proof. We can write $\bar{\mathbf{M}}$ as

$$\bar{\mathbf{M}} = p \begin{bmatrix} k'\mathbf{I}_m + \mathbf{K}_m & -\mathbf{1}_{m \times N-m} & 1/p\mathbf{1}_{m \times 1} \\ -\mathbf{1}_{m \times N-m}^T & m\mathbf{I}_{N-m} + \mathbf{K}_{N-m} & \mathbf{0} \\ 0 & \cdots & 0 \end{bmatrix},$$

where $k' = k/cp + N - m$ and

$$\mathbf{K}_n = \begin{bmatrix} (n-1) & -1 & \cdots & -1 \\ -1 & (n-1) & \cdots & -1 \\ \vdots & \vdots & \ddots & \vdots \\ -1 & -1 & \cdots & (n-1) \end{bmatrix}_{n \times n},$$

is the Laplacian of a complete network of size n. The characteristic polynomial of matrix $\mathbf{K}_n$ is [24]

$$\phi_{\mathbf{K}_n}(\lambda) = \lambda(\lambda - n)^{n-1}. \tag{5.12}$$

Now we calculate the characteristic polynomial of $\bar{\mathbf{M}}' = \bar{\mathbf{M}}/p$:

$$\phi_{\mathbf{M}'}(\lambda) = |\lambda\mathbf{I}_{N+1} - \bar{\mathbf{M}}/p|$$

$$= \lambda \times \begin{vmatrix} (\lambda - k')\mathbf{I}_m - \mathbf{K}_m & \mathbf{1}_{m \times N-m} \\ \mathbf{1}_{m \times N-m}^T & (\lambda - m)\mathbf{I}_{N-m} - \mathbf{K}_{N-m} \end{vmatrix}$$

Using Schur formula for block matrices, we have

$$\phi_{\mathbf{M}'}(\lambda) = \lambda \times |(\lambda - k')\mathbf{I}_m - \mathbf{K}_m| \times |(\lambda - m)\mathbf{I}_{N-m} - \mathbf{K}_{N-m}$$

$$-\mathbf{1}_{m \times N-m}^T[(\lambda - k')\mathbf{I}_m - \mathbf{K}_m]^{-1}\mathbf{1}_{m \times N-m}|$$

$$= \lambda \times \phi_{\mathbf{K}_m}(\lambda - k') \times \left|(\lambda - m)\mathbf{I}_{N-m} - \mathbf{K}_{N-m} - \frac{m}{\lambda - k'}\mathbf{1}_{N-m \times N-m}\right|$$

where the last equality is due to

$$\mathbf{1}_{m \times n}(\lambda \mathbf{I}_n - \mathbf{K}_n)^{-1}\mathbf{1}_{n \times m} = \frac{n}{\lambda}\mathbf{1}_{m \times m}.$$

Since $(\lambda - pm)\mathbf{I}_{N-m} - \mathbf{K}_{N-m}$ is invertible we have

$$\phi_{\mathbf{M}'}(\lambda) = \lambda \times \phi_{\mathbf{K}_m}(\lambda - k') \times \left|\mathbf{I}_{N-m} - \frac{m}{\lambda - k'}[(\lambda - m)\mathbf{I}_{N-m} - \mathbf{K}_{N-m}]^{-1}\mathbf{1}_{N-m \times N-m}\right|.$$

Since $\mathbf{1}_{m \times m} = \mathbf{1}_{m \times 1}\mathbf{1}_{1 \times m}$, using Sylvester's determinant theorem the second term can be written as

$$1 - \frac{N-m}{\lambda - m}\mathbf{1}_{1 \times N-m}[(\lambda - m)\mathbf{I}_{N-m} - \mathbf{K}_{N-m}]^{-1}\mathbf{1}_{N-m \times 1} = \left(1 - \frac{m}{\lambda - k'}\frac{N-m}{\lambda - m}\right)\phi_{\mathbf{K}_{N-m}}(\lambda - m).$$

Substituting the characteristic polynomial of Laplacian of a complete network of size m in (5.12), the characteristic polynomial for $\bar{\mathbf{M}}$ can be obtained as

$$\phi_{\bar{\mathbf{M}}}(\lambda) = \lambda(\lambda - \frac{k}{c} - pN)^{m-1}(\lambda - pN)^{N-m-1}\left(\lambda^2 - (\frac{k}{c} + pN)\lambda + \frac{mk}{c}\right).$$

□

Now if we apply the results of Lemma 1 to the type 1 and 2 MSF, we reach the following

results:

Theorem 2: Network is stabilizable by m pinning controllers with gain k if

1. the network has type 2 MSF, and

$$\alpha_1 \leq c\lambda_N = \frac{1}{2}\left(cpN + k - \sqrt{(cpN + k)^2 - 4cpmk}\right),$$

2. the network has type 3 MSF, and the controller gain and the number of pinning controllers satisfy

$$\alpha_1 \leq c\lambda_N = \frac{1}{2}\left(cpN + k - \sqrt{(cpN + k)^2 - 4cpmk}\right)$$

and,

$$c\lambda_1 = k + cpN \leq \alpha_2.$$

Proof: Follows directly from Lemma 1 and the MSF being negative.

Let us define pinning ratio as $\rho = m/N$ and average coupling strength as $\bar{c} = cp$.

Remark 5. *Based on Theorem 2, regardless of whether the MSF is of type 1 or 2, we must have $c\lambda_N \geq \alpha_1$ which using Lemma 1 yields*

$$m \geq \frac{\alpha_1(\bar{c}N + k) - \alpha_1^2}{\bar{c}k}.$$

In other words, given k, the smallest number pinning controllers that can stabilize the network

105

is

$$m_{\min} = \left\lceil \frac{\alpha_1(\bar{c}N + k) - \alpha_1^2}{\bar{c}k} \right\rceil,$$

and the smallest ratio of pinning nodes is

$$\rho_{\min} = \frac{1}{N} \left\lceil \frac{\alpha_1(\bar{c}N + k) - \alpha_1^2}{\bar{c}k} \right\rceil.$$

Remark 6. *If for systems with type 2 MSF, the control gain, k, can be chosen to be suffi-ciently large, the smallest number of pinning controllers and the smallest ratio of controllers can only be improved to*

$$m_{\min}^{\star} = \left\lceil \frac{\alpha_1}{\bar{c}} \right\rceil,$$

and

$$\rho_{\min}^{\star} = \frac{1}{N} \left\lceil \frac{\alpha_1}{\bar{c}} \right\rceil.$$

Remark 7. *For systems with type 3 MSF, the second condition is $\lambda_1 \leq \alpha_2/c$ which using Lemma 1 yields*

$$k \leq \alpha_2 - \bar{c}N = k_{\max}$$

Thus, the smallest number of pinning controllers and the smallest ratio of controllers can be improved to

$$m_{\min}^{\star} = \left\lceil \frac{\alpha_1\alpha_2 - \alpha_1^2}{\bar{c}\alpha_2 - \bar{c}^2N} \right\rceil,$$

and the smallest ratio of pinning nodes is

$$\rho^{\star}_{\min} = \frac{1}{N} \left\lceil \frac{\alpha_1 \alpha_2 - \alpha_1^2}{\bar{c}\alpha_2 - \bar{c}^2 N} \right\rceil .$$

It is interesting to note that $\rho^{\star}_{\min}$ is lower bounded by the dynamical parameters of the system, namely α_1 and α_2

$$\rho^{\star}_{\min} \geq \frac{1}{N} \left\lceil \frac{4N(\alpha_1 \alpha_2 - \alpha_2^2)}{\alpha_2^2} \right\rceil \approx \frac{4\alpha_1}{\alpha_2}.$$

which can be achieved if $\bar{c} = \alpha_2/2N$ and $k = \alpha_2/2$.

Corollary 2. *A system with type 3 MSF can be stabilized by pinning technique if and only if*

$$\frac{\alpha_2 - |\alpha_2 - 2\alpha_1|}{2N} \leq \bar{c} \leq \frac{\alpha_2 + |\alpha_2 - 2\alpha_1|}{2N}.$$

Proof: *Follows directly from the combination of the two inequalities of Theorem 2 part 2.*

Numerical Example

In this section we study a numerical example using the well-known Rössler chaotic attractor [43]. Consider the state space equation of Rössler attractor

$$
\begin{aligned}
\dot{x}_1 &= x_1 - x_2 \\
\dot{x}_2 &= x_1 + \theta x_2 \\
\dot{x}_3 &= \beta + x_3(x_1 - \gamma).
\end{aligned}
\tag{5.13}
$$

where $\theta = 0.2$, $\beta = 0.2$, and $\gamma = 7$.

We assume the coupling matrix

$$\mathbf{H} = \begin{bmatrix} 1 & 0 & 0 \\ 0 & 0 & 0 \\ 0 & 0 & 0 \end{bmatrix}.$$

With the choice of oscillator parameters in (5.13), the system has a type 3 MSF and we have $\alpha_1 = 0.2$ and $\alpha_2 = 4.8$.
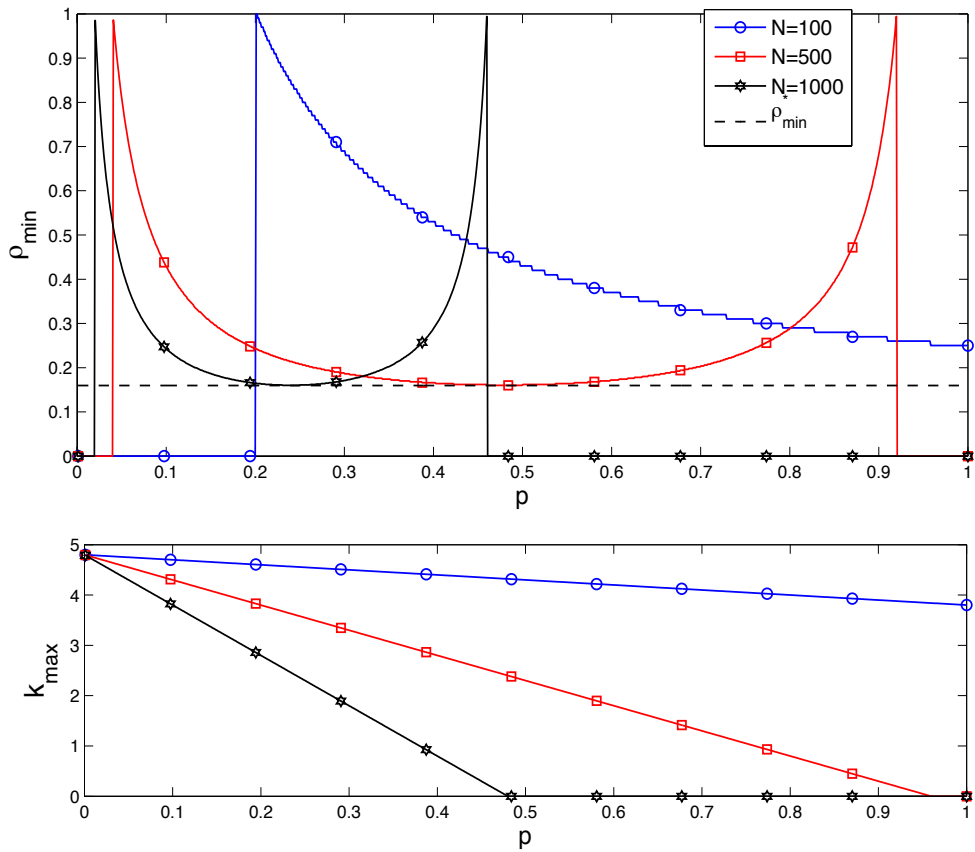
Figure 5.1: Pinning ratio ρ and controller gain k as a function p for different network sizes.

Fig. 5.1 shows the ratio of the pinning nodes and maximum controller gain k required to reach the stable convergence to the reference signal, $\mathbf{s}$, versus p, for several network sizes, N. Here we have assumed that the coupling strength is $c = 0.01$. The switching parameter p controls the average degree of the nodes, pN. As it is illustrated, network can be stabilized if $20 < pN < 460$ which is a direct result of corollary 1. Also, we observe that as p increases the pinning ratio drops until it reaches a minimum of $\rho^{\star}_{\min} \approx 0.16$ (dashed line) at $p^{\star} = \alpha_2/(2cN) = 240/N$. It is very interesting that the minimum pinning ratio is almost independent of the network size. As p exceeds $p^{\star}$, the pinning ratio increases until reaches 1. After that network becomes unstable since average coupling, $\bar{c}$ reaches α_2. Hence the magnitude of controller gain becomes too small to stabilize the network, $k \leq \alpha_2 - cpN$. This constraint on controller gain is the reason for increase in pinning ratio in larger networks as p grows, since as smaller controller gain is available for controllers, it should be compensated by the increase in the number of employed controllers, hence m increases.

Fig. 5.2 illustrates the the ratio of the pinning nodes and controller gain k required to reach the stability of synchronization versus network size N, for different values of p. As it can be observed, for $20 < pN < 460$ network can be stabilized and outside this interval, the evolution of the network to $\mathbf{s}$ is improbable. Also as N grows the same linear decline in the maximum employable controller gain is observed which is predicted by the Theorem 2.

Conclusion

We have analyzed the effectiveness of pinning control under the assumption of fast switching. Bounds on average coupling strength where this strategy can be utilized to achieve stable synchronization are given. We have also calculated the minimum ratio of pinning nodes to achieve the stability based on the type of the master stability function describing the network.
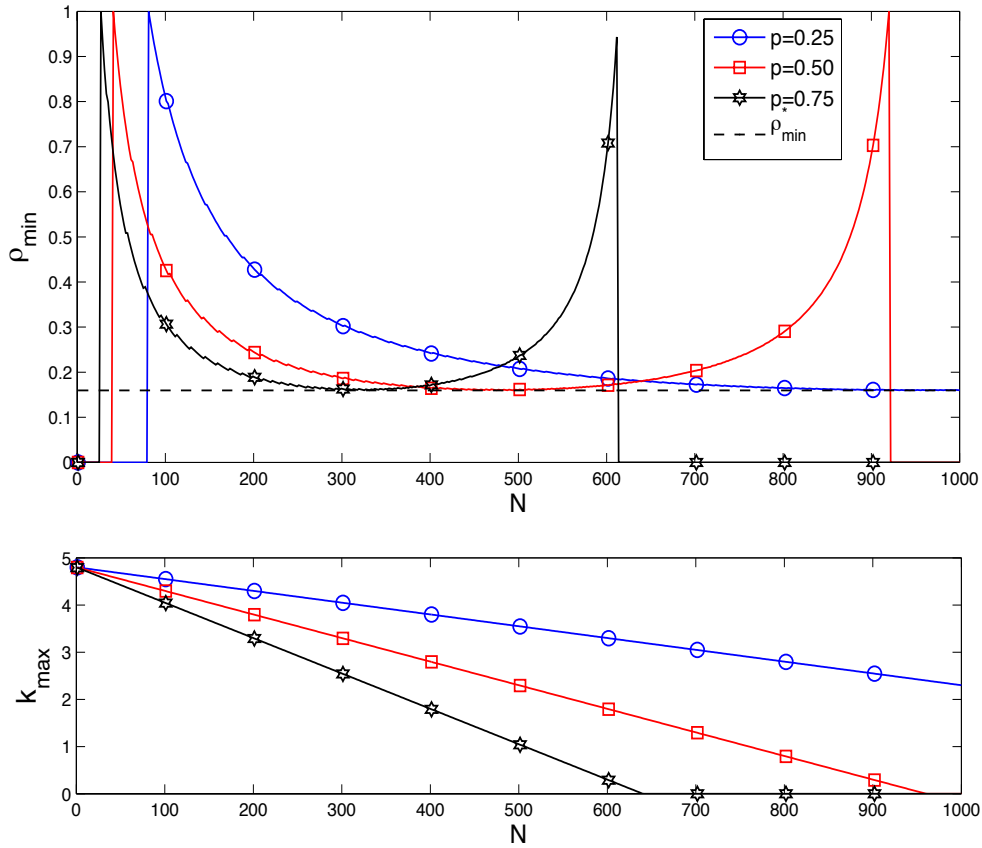
Figure 5.2: Pinning ratio ρ and controller gain k as a function N for some values of p.

We have demonstrated that if a system has type 3 master stability function then the controller gain is bounded. We have also shown that if the constraint on the gain controller is satisfied, in case of type 3 master stability function, the ratio of pinning controllers is almost inversely related to controller gain.

CHAPTER 6: STABILIZING A RANDOM DYNAMICAL NETWORK WITH RANDOM FEEDBACK NETWORK

Although there have been many efforts in the study of the distributed control [73, 75], the impact of topological characteristics of the network on its stability is largely under-studied.

Here, we aim to address some aspects of this problem for large networks. Since considering large networks with non-identical dynamics renders the analysis intractable, here we consider all plants, couplings and controllers to be identical. Moreover, to gain insight into the behavior of large networks without being limited to one particular topology, we take our results further by assuming random networks. To do this we utilize the results in [91], derived for an arbitrary dynamics network, and adapt it to the case where all nodes and coupling dynamics are identical. Then, assuming a random network model, for both dynamics and communications networks, we analyze the probability that the stability condition is satisfied. We then use these results to study asymptotic behavior of large random networks.

Notations and System Description

Notations

The set of real n-vectors is denoted by $\mathbb{R}^n$ and the set of real $m \times n$ matrices is denoted by $\mathbb{R}^{m \times n}$. Matrices and vectors are denoted by capital and lower-case bold letters, respectively. The Euclidean ($\mathcal{L}_2$) vector norm is represented by $||\cdot||$. When applied to a matrix $||\cdot||$ denotes the $\mathcal{L}_2$ induced matrix norm, $||\mathbf{A}|| = \lambda_{\max}(\mathbf{A}^T \mathbf{A})$. Also, we denote a graph corresponding to a network with $\mathcal{G}$, and vector $\mathbf{d}$ denotes the corresponding degree sequence of the graph.

Table 6.1: Frequently used variables

Variable	Description
$\mathbf{x}_i$	State vector of node i
$\mathbf{u}_i$	Input vector of node i
$\mathbf{A}$	Plant dynamics matrix
$\mathbf{H}$	Coupling matrix between two nodes in the dynamic network
$\mathbf{B}$	Plant input matrix
$\mathbf{K}$	Local feedback gain
$\mathbf{L}$	Inter-plant feedback gain
c	Coupling strength in dynamics network
N	Plant network size
$\mathcal{G}_D$	Dynamics network graph
$\mathbf{G} = [g_{ij}]$	Adjacency matrix of $\mathcal{G}_D$
$\mathbf{d}_D = [d_{D,i}]$	Degree sequence of $\mathcal{G}_D$
$\mathcal{G}_C$	Communications (control) network graph
$\mathbf{F} = [f_{ij}]$	Adjacency matrix of $\mathcal{G}_C$
$\mathbf{d}_C = [d_{C,i}]$	Degree sequence of $\mathcal{G}_C$
p	Randomness parameter of dynamics network
q	Conditional randomness parameter of communications network

Table I summarizes the variables used frequently in the rest of this chapter.

System Description

We consider a dynamics network, consisting of N identical linear time-invariant plants described by

$$\dot{\mathbf{x}}_i(t) = \mathbf{A}\mathbf{x}_i(t) + \mathbf{B}\mathbf{u}_i(t) + c\sum_{j=1}^{N} g_{ji}\mathbf{H}\mathbf{x}_j(t), \tag{6.1}$$

$$\mathbf{x}_i(0) = \mathbf{x}_{i0}$$

where $\mathbf{x}_i \in \mathbb{R}^n$ is the state of the ith node, $\mathbf{u}_i \in \mathbb{R}^m$ is the input signal of ith node, and $\mathbf{A} \in \mathbb{R}^{n \times n}$, $\mathbf{B} \in \mathbb{R}^{n \times m}$ and $\mathbf{H} \in \mathbb{R}^{n \times n}$ are the node dynamics, input, and coupling matrices, respectively. c is the coupling strength and $\mathbf{G} = [g_{ij}] \in \mathbb{R}^{N \times N}$ is the binary adjacency matrix associated with the dynamics network (graph) $\mathcal{G}_D$ with no self loops, i.e. $g_{ii} = 0$.

We assume that the isolated nodes are asymptotically stabilizable with local state feedback $\mathbf{u}_i = \mathbf{K}\mathbf{x}_i$. That is, there exist $\mathbf{K}$, and positive definite matrices $\mathbf{P}, \mathbf{Q} \in \mathbb{R}^{n \times n}$ that satisfy the Lyapunov equation

$$(\mathbf{A} + \mathbf{B}\mathbf{K})^T \mathbf{P} + \mathbf{P}(\mathbf{A} + \mathbf{B}\mathbf{K}) = -\mathbf{Q}. \tag{6.2}$$

Furthermore, we assume that the communications network provides the control input vector for node i

$$\mathbf{u}_i = \mathbf{K}\mathbf{x}_i + c \sum_{j=1}^{N} f_{ji} \mathbf{L}\mathbf{x}_j, \tag{6.3}$$

where $\mathbf{K}$ is the local feedback gain, $\mathbf{L}$ is feedback gain from other subsystems, and $\mathbf{F} = [f_{ij}]$ is the binary adjacency matrix corresponding to the communications network, $\mathcal{G}_C$. Again, we assume that there are no self loops, i.e. $f_{ii} = 0$.

Network Stability Condition

In this section, we provide a stability condition for a networked system using Lyapunov direct method for directed networks.

The network is asymptotically stable if there exists a Lyapunov function, $V(\cdot)$, of the network state vectors, which has negative derivative with respect to time.

Following (6.2), we know that $V_{\text{node}}(\mathbf{x}_i) = \mathbf{x}_i^T \mathbf{P} \mathbf{x}_i$ is a Lyapunov function for the isolated nodes. Therefore, one reasonable choice of the Lyapunov function candidate for the whole network is

$$V(\mathbf{x}_1, \cdots, \mathbf{x}_N) = \sum_{i=1}^{N} V_{\text{node}}(\mathbf{x}_i) = \sum_{i=1}^{N} \mathbf{x}_i^T \mathbf{P} \mathbf{x}_i. \tag{6.4}$$

Theorem 9. *Network* (6.1) *with controller* (6.3) *is asymptotically stable if*

$$c^2 \sum_{j=1}^{N} \frac{||\mathbf{P}(f_{ji}\mathbf{BL} + g_{ji}\mathbf{H})||^2}{\delta_{ji}} + \sum_{j=1}^{N} g_{ij}\delta_{ij} < \lambda_{min}(\mathbf{Q}) \tag{6.5}$$

for all i, where δ_{ij} are arbitrary positive reals.

Proof. Follows directly from Theorem 1 in [91]. □

Inspecting (6.5), we observe that if we include feedbacks from subsystems which are not connected in the dynamics network ($f_{ji} = 1$ and $g_{ji} = 0$), we add unnecessary positive terms to the left side of the stability conditions, which makes the conditions harder to satisfy. Therefore, the communications network should be a subset of the dynamics network, *i.e.* $\mathcal{G}_C \subseteq \mathcal{G}_D$ or $f_{ij} = 0$ if $g_{ij} = 0$.

To gain the largest convergence rate for each node, we choose $\mathbf{Q}$ to be the identity matrix of consistent size [59]. From (6.5), it is clear that the norm of the closed loop gain from other nodes, $||\mathbf{P}(\mathbf{BL} + \mathbf{H})||$, should be chosen to be as small as possible. Ideally, if $\mathbf{L}$ exists such that $||\mathbf{P}(\mathbf{BL} + \mathbf{H})|| = 0$ (known as matching condition [73]), the stability conditions in (6.5) are satisfied with $\delta_{ij} < 1/N$ and $f_{ij} = g_{ij}$ or $\mathcal{G}_C = \mathcal{G}_D$. However, It is desirable to use a $\mathcal{G}_C$ that is smaller than $\mathcal{G}_D$, if possible. Furthermore, in general, the matching condition may

not be satisfied. In this case one would want to choose $\mathbf{L}$ that minimizes the norm or

$$\mathbf{L}^\star = \arg \min_{\mathbf{L}} ||\mathbf{P}(\mathbf{BL} + \mathbf{H})||. \tag{6.6}$$

The norm of the closed loop gain will then be $||\mathbf{P}(\mathbf{BL}^\star + \mathbf{H})||$. We note that the optimization problem in (6.6) reduces to a standard semidefinite program (SDP), which can be readily solved (see [91] and Ch.4 in [92]).

Theorem 10. *Let $\delta_{ij} = \delta_o$ if $f_{ij} = 0$ and $\delta_{ij} = \delta_c$ if $f_{ij} = 1$, then the network in (6.1) with controller (6.3) is stable if*

$$\frac{\alpha_i}{\delta_o} + \beta_i \delta_o + \frac{\gamma_i}{\delta_c} + \zeta_i \delta_c < 1, \tag{6.7}$$

where

$$\alpha_i = c^2 \rho_1 \left(\sum_{j=1}^N g_{ji} - \sum_{j=1}^N g_{ji} f_{ji} \right) = c^2 \rho_1 \left(d_{D,i}^{in} - d_{C,i}^{in} \right),$$

$$\beta_i = \sum_{j=1}^N g_{ij} - \sum_{j=1}^N g_{ij} f_{ij} = d_{D,i}^{out} - d_{C,i}^{out},$$

$$\gamma_i = c^2 \rho_2 \sum_{j=1}^N g_{ji} f_{ji} = c^2 \rho_2 d_{C,i}^{in},$$

$$\zeta_i = \sum_{j=1}^N g_{ij} f_{ij} = d_{C,i}^{out},$$

and $d_{D,i}^{in}$ and $d_{C,i}^{in}$ are the in-degrees of node i in $\mathcal{G}_D$ and $\mathcal{G}_C$, respectively. Similarly, $d_{D,i}^{out}$ and $d_{C,i}^{out}$ are the out-degrees of node i in $\mathcal{G}_D$ and $\mathcal{G}_C$, respectively. And $\rho_1 = ||\mathbf{PH}||^2$ and $\rho_2 = ||\mathbf{P}(\mathbf{H} + \mathbf{BL}^\star)||^2$.

Proof. We can write

$$\delta_{ij} = (1 - f_{ij})\delta_o + f_{ij}\delta_c \tag{6.8}$$

115

and

$$\frac{1}{\delta_{ij}} = \frac{1 - f_{ij}}{\delta_o} + \frac{f_{ij}}{\delta_c}. \tag{6.9}$$

Also, considering the fact that $\mathcal{G}_C \subseteq \mathcal{G}_D$, the stability conditions in (6.5) can be expressed as

$$c^2 \rho_1 \sum_{j=1}^{N} \frac{g_{ji}}{\delta_{ji}} + c^2 (\rho_2 - \rho_1) \sum_{j=1}^{N} \frac{g_{ji} f_{ji}}{\delta_{ji}} + \sum_{j=1}^{N} \delta_{ij} g_{ij} < 1. \tag{6.10}$$

Hence, substituting (6.8) and (6.9) in (6.10), yields (6.7). □

Corollary 3. *If we choose $\delta_o = c\sqrt{\rho_1}$ and $\delta_c = c\sqrt{\rho_2}$, the network (6.1) with controller (6.3) is stable if*

$$d_{D,i} \geq d_{C,i} > \eta \sqrt{\rho_1} d_{D,i} - \frac{\eta}{c}, \tag{6.11}$$

where $d_{D,i} = d_{D,i}^{in} + d_{D,i}^{out}$, $d_{C,i} = d_{C,i}^{in} + d_{C,i}^{out}$, and

$$\eta = \frac{1}{\sqrt{\rho_1} - \sqrt{\rho_2}}. \tag{6.12}$$

Proof. Substituting the values of δ_o and δ_c in (6.7),

$$\sqrt{\rho_1} \left(d_{D,i}^{in} + d_{D,i}^{out} \right) - \left(\sqrt{\rho_1} - \sqrt{\rho_2} \right) \left(d_{C,i}^{in} + d_{C,i}^{out} \right) < \frac{1}{c}.$$

□

Corollary 4. *If the matching condition, $\|\mathbf{P}(\mathbf{H} + \mathbf{BL}^*)\| = 0$, is satisfied, (6.11) reduces to*

$$d_{D,i} \geq d_{C,i} > d_{D,i} - \frac{1}{c\sqrt{\rho_1}}. \tag{6.13}$$

The constraints on $d_{C,i}$ derived above guarantee the stability of the network. However, except for the trivial cases (e.g. if the two bounds in (6.11) force $d_{C,i} = d_{D,i}$), given the network $\mathcal{G}_D$ it is not easy to find a small $\mathcal{G}_C$ such that these conditions are satisfied. In fact, finding the smallest $\mathcal{G}_C$ reduces to a linear integer program, which in general is NP-hard.

In the following, to get further insight into the problem, we assume that the communications network, $\mathcal{G}_C$, is a random sub-graph of the dynamics network, $\mathcal{G}_D$. In other words, we assume that with probability q, there is a connection from node i to node j if in the dynamics network there is such a link. That is,

$$
f_{ij} = \begin{cases} 1 & \text{with probability } q \text{ if } g_{ij} = 1 \\ 0 & \text{otherwise} \end{cases}.
\tag{6.14}
$$

Note that, here, we make no assumption about the topology of the dynamics Network.

With a random sub-graph as the communications network, the question of interest is: *Given $\mathcal{G}_D$ and q, what is the probability that the network is stable?*

Degree distribution of random subgraph $\mathcal{G}_C$

Since the in-degree and out-degree of each node are summations of independent Bernoulli random variables with success probability q, their distributions are binomial. That is

$$
d_{C,i}^{in} \sim \mathcal{B}(d_{D,i}^{in}, q), \ d_{C,i}^{out} \sim \mathcal{B}(d_{D,i}^{out}, q).
$$

Since $d_{C,i}^{in}$ and $d_{C,i}^{out}$ are independent random variables and have the same success probability, their sum also has a binomial distribution. That is

$$d_{C,i} \sim \mathcal{B}(d_{D,i}, q). \tag{6.15}$$

If pN is large enough, we can approximate the distribution of $d_{C,i}$ with a Gaussian distribution with mean [93]

$$\mu_i = q d_{D,i}. \tag{6.16}$$

Lemma 5. *Covariance of $d_{C,i}$ in* (6.15) *is*

$$\sigma_{ij}^2 = \begin{cases} q(1-q)d_{D,i} & i = j \\ q(1-q)(g_{ij} + g_{ji}) & i \neq j \end{cases}. \tag{6.17}$$

Proof. We know that

$$d_{C,i} = \sum_{k=1}^{N}(f_{ik}g_{ik} + f_{ki})g_{ki}. \tag{6.18}$$

118

From definition of covariance, we have

$$
\begin{aligned}
\sigma_{ij}^2 &= \mathbb{E}[d_{C,i}d_{C,j}] - q^2 d_{D,i}d_{D,j} \\
&= \sum_{k,l}(f_{ik}g_{ik} + f_{ki}g_{ki})(f_{jl}g_{jl} + f_{lj}g_{lj}) - q^2 d_{D,i}d_{D,j} \\
&= \sum_{k,l} g_{ik}g_{jl}(q(1-q)1_{i=j}1_{k=l} + q^2) \\
&\quad + \sum_{k,l} g_{ik}g_{lj}(q(1-q)1_{i=l}1_{j=k} + q^2) \\
&\quad + \sum_{k,l} g_{ki}g_{jl}(q(1-q)1_{i=l}1_{j=k} + q^2) \\
&\quad + \sum_{k,l} g_{ik}g_{jl}(q(1-q)1_{i=j}1_{k=l} + q^2) - q^2 d_{D,i}d_{D,j}
\end{aligned}
$$

where 1_x is the indicator function of x. Thus,

$$
\begin{aligned}
\sigma_{ij}^2 &= q(1-q)1_{i=j}d_{D,i}^{\text{out}} + q^2 d_{D,i}^{in}d_{D,j}^{in} + \sum_{k,l}(g_{ik}g_{lj} + g_{ki}g_{jl})(q(1-q)1_{j=k}1_{i=l} + q^2) \\
&\quad + q(1-q)1_{i=j}d_{D,i}^{in} + q^2 d_{D,i}^{in}d_{D,j}^{in} - q^2 d_{D,i}d_{D,j}
\end{aligned}
$$

or

$$
\begin{aligned}
\sigma_{ij}^2 &= q(1-q)1_{i=j}d_{D,i} + q^2 d_{D,i}^{\text{out}}d_{D,j}^{\text{out}} + q^2 d_{D,i}^{\text{out}}d_{D,j}^{in} + q^2 d_{D,i}^{in}d_{D,j}^{\text{out}} + q^2 d_{D,i}^{in}d_{D,j}^{in} - q^2 d_{D,i}d_{D,j} \\
&= q(1-q)(g_{ij} + g_{ji}) + q(1-q)1_{i=j}d_{D,i}.
\end{aligned}
$$

Thus, if $i \neq j$

$$
\sigma_{ij}^2 = q(1-q)(g_{ij} + g_{ji}),
$$

and if $i = j$

$$\sigma_{ii}^2 = q(1-q)d_{D,i}.$$

□

It is clear from (6.17) that if $d_{D,i} \gg 2 \geq g_{ij} + g_{ji}$, $d_{C,i}$ can be approximated to be independent, and hence, jointly Gaussian. That is

$$\mathbf{d}_C \sim \mathcal{N}(q\mathbf{d}_D, q(1-q)\mathrm{diag}(\mathbf{d}_D)), \tag{6.19}$$

where $\mathbf{d}_C = \begin{bmatrix} d_{C,1} & \cdots & d_{C,N} \end{bmatrix}^T$ and $\mathbf{d}_D = \begin{bmatrix} d_{D,1} & \cdots & d_{D,N} \end{bmatrix}^T$.

Probability of Stability

The probability that the stability condition associated with node i is satisfied can be approximated as

$$P\left(d_{C,i} \geq \phi_i\right) \approx Q\left(\frac{\phi_i - \mu_i}{\sigma_{ii}}\right), \tag{6.20}$$

where

$$\phi_i = \eta\sqrt{\rho_1}d_{D,i} - \frac{\eta}{c}, \tag{6.21}$$

and

$$Q(x) = \frac{1}{\sqrt{2\pi}}\int_x^{+\infty} e^{-\frac{y^2}{2}}\,dy. \tag{6.22}$$

Since the degrees are almost independent, the probability of stability with random commu-

nications network can be approximated as

$$P_{\text{stab}} \approx \Pi_{i=1}^{N} Q\left(\frac{\phi_i - \mu_i}{\sigma_i}\right)$$

$$= \Pi_{i=1}^{N} Q\left(\frac{\eta\sqrt{\rho_1} - q}{\sqrt{q(1-q)}}\sqrt{d_{D,i}} - \frac{\eta}{\sqrt{q(1-q)}}\frac{1}{c\sqrt{d_{D,i}}}\right)$$

$$= \Pi_{i=1}^{N} Q\left(\frac{\eta\sqrt{\rho_1}d_{D,i} - \frac{\eta}{c} - qd_{D,i}}{\sqrt{q(1-q)d_{D,i}}}\right). \tag{6.23}$$

Erdös-Rényi Dynamics Network

So far we have assumed that the dynamics network is arbitrary and the communications network is random. Now, let us assume that the dynamics network is also a directed Erdös-Rényi random network [23] with randomness parameter p. Then, for large N, we can assume that $d_{D,i} \approx 2pN$ [23]. Thus, (6.23) becomes

$$P_{\text{stab}} \approx Q^N\left(\frac{2\eta\sqrt{\rho_1}pN - \frac{\eta}{c} - 2pqN}{\sqrt{2pq(1-q)N}}\right). \tag{6.24}$$

If in (6.11), we use the approximations $d_{D,i} \approx 2pN$ and $d_{C,i} \approx qd_{D,i} = 2pqN$, which are valid for large N, the stability condition for a random network with a random communications network reduces to

$$q > \eta\sqrt{\rho_1} - \frac{\eta}{2cpN}. \tag{6.25}$$

We can now use this result to study asymptotic network stability trends.

We can see that as the network size, N, increases and c is kept constant, the last term on the right hand side of (6.25) decreases. Since $\eta\sqrt{\rho_1} > 1$, a random network tends to become unstable if the ratio of number of links in the communications network to that

of the dynamics network, q, is kept fixed. To sustain the stability of the network as the network size grows under the aforementioned condition, either the coupling strength, c, or the randomness parameter of the dynamics network, p, must decrease, at least as $1/N$. This means that a larger dynamics network must either be more weakly $(c = \mathcal{O}(1/N))$, or more sparsely $(p = \mathcal{O}(1/N))$, connected, if it is to be stable. Either way, to keep the overall network stable with a fixed q, the overall effect of all other nodes on a particular node, must not be allowed to increase. In the case of fixed network size, to have a stable network as p increases, coupling strength must decrease at least as $1/p$. This is intuitively justifiable since the mean and variance of dynamics at each node have linear and quadratic relations with both coupling strength and randomness parameter, respectively.

For reasonably large pN, due to multiplication of large number of terms in (6.24), the probability of stability has a sharp roll-off as a function of q. To quantify where these sharp transitions take place, we can look at

$$q_c = P_{\text{stab}}^{-1}\left(\frac{1}{2}\right).$$

From (6.24), we can calculate q_c as

$$q_c = \frac{2\eta(2c\sqrt{\rho_1}pN - 1) + cz^2}{2c(2pN + z^2)} - \frac{z}{2(2pN + z^2)}\sqrt{z^2 + 4\eta\left(2\sqrt{\rho_1}pN - \frac{1}{c}\right) - \frac{2\eta^2(2c\sqrt{\rho_1}pN - 1)^2}{c^2pN}}$$

$$(6.26)$$

where $z = Q^{-1}\left(2^{-\frac{1}{N}}\right)$.

Numerical Results

In this section, we verify the validity of our results with a numerical example. Here, we consider a dynamics network with

$$\mathbf{A} = \begin{bmatrix} 0 & 1 \\ \frac{5}{2} & 0 \end{bmatrix},$$

and

$$\mathbf{B} = \begin{bmatrix} 0 \\ \frac{1}{4} \end{bmatrix}.$$

These nodes are assumed to be coupled by

$$\mathbf{H} = \begin{bmatrix} 0 & \frac{1}{4} \\ 1 & 0 \end{bmatrix}.$$

By setting the desired poles of isolated nodes at -1, -2, and using the method proposed in [91], we can calculate the local feedback gain as

$$\mathbf{K} = -\begin{bmatrix} 18 & 12 \end{bmatrix}.$$

The solution of problem (6.6) is

$$\mathbf{L}^{\star} = -\begin{bmatrix} 4 & 0 \end{bmatrix},$$

and the solution of the Lyapunov equation is

$$\mathbf{P} = \begin{bmatrix} 1 & -\frac{1}{2} \\ -\frac{1}{2} & \frac{1}{2} \end{bmatrix}.$$

Consequently, we have $\rho_1 = 0.841$ and $\rho_2 = 0.1$.
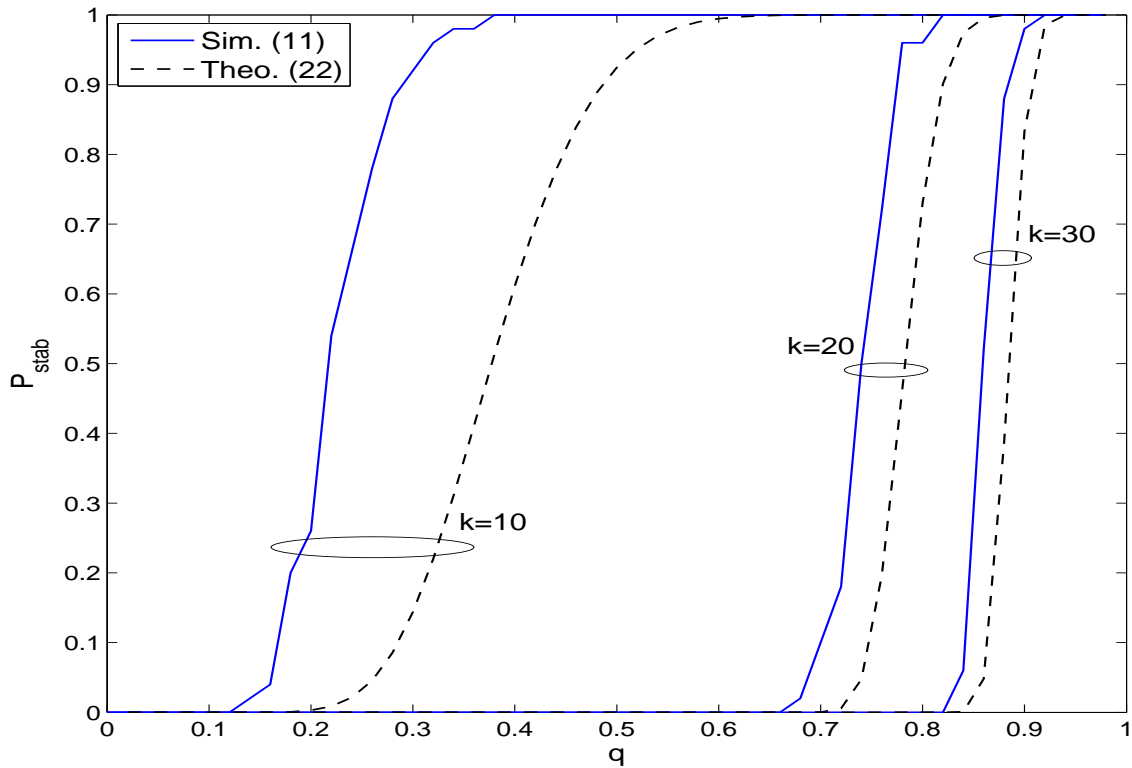
Figure 6.1: Probability of stability versus randomness parameter q, in the ring configuration of different coordination numbers, k, for dynamics network and $N = 100$, and coupling strength of $c = 0.05$.

Fig. 6.1 shows the probability of the stability as a function of conditional randomness parameter of the communications network, q. Here the dynamics network is assumed to

have a ring configuration with coordination number k, i.e., every vertex is connected to $2k$ of its closest vertices in the ring. As it can be seen the approximations are reasonable. More interestingly, they are closer to simulations for larger coordination numbers. The reason for this phenomenon is that the average number of links in the communications network is $2kq$, and for higher k the Gaussian approximation for the node degrees is more accurate. Also, Fig. 6.1 shows that as number of links in the dynamics network increases, so does the average number of links in the communications network required to stabilize the overall network. This is also predicted by (6.23).
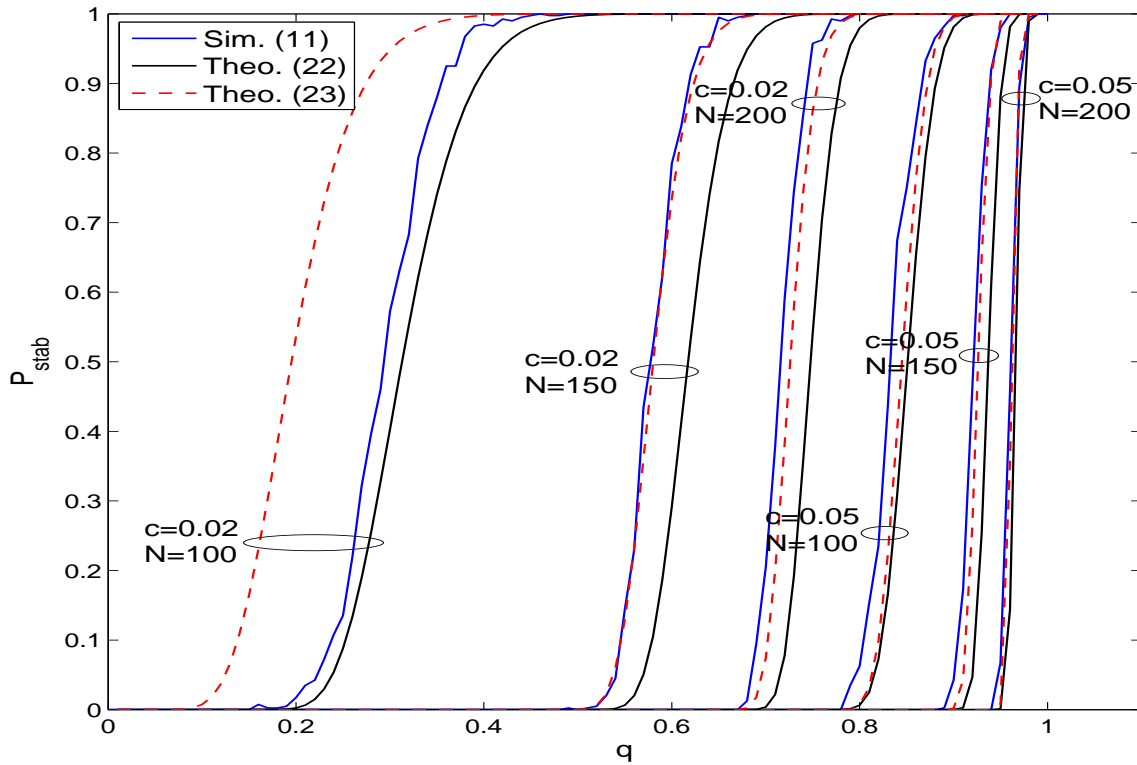
Figure 6.2: Probability of stability as a function of randomness parameter q of the communications network for different network size, N and coupling strength, c.
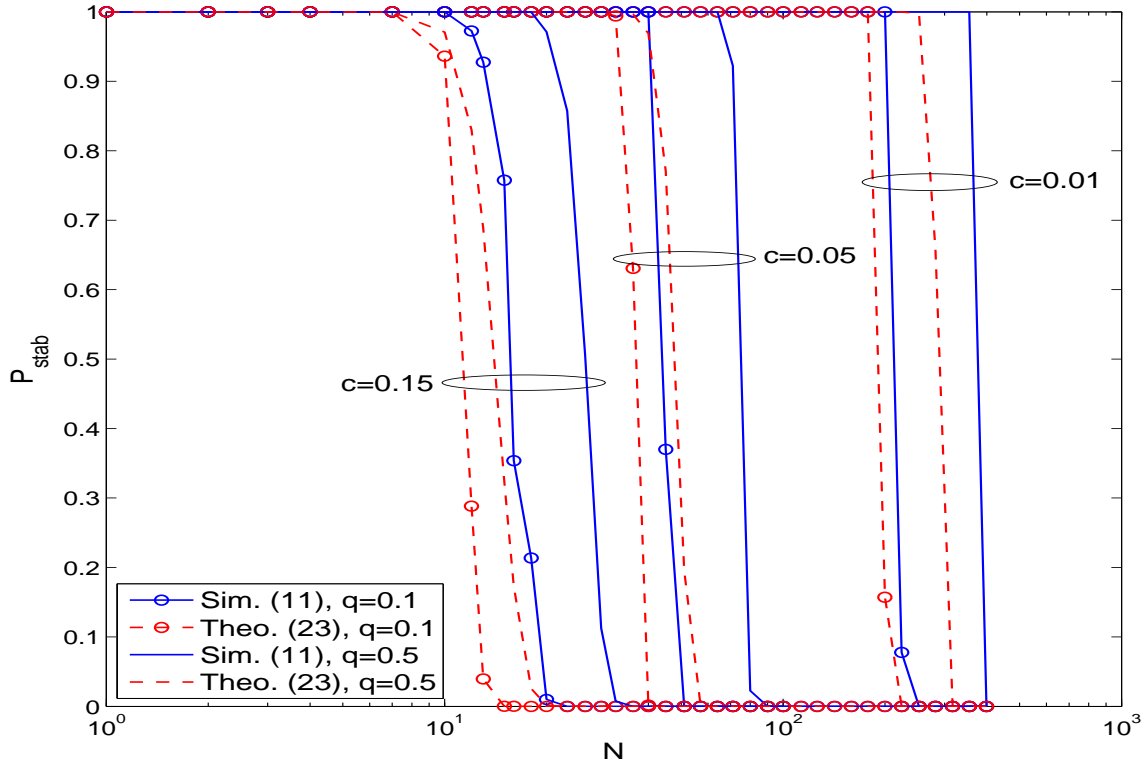
Figure 6.3: Probability of stability versus network size, N, in Erdös-Rényi network for different values of c and q.

The probability of stability for large Erdös-Rényi dynamics network with randomness parameter of $p = 0.25$ is shown in Fig. 6.2. As it can be observed, the approximations in (6.23) and (6.24) are reasonable in comparison to the simulation results.

Fig. 6.3 depicts the probability of stability as a function of network size N for different values of q and c. We see that for weaker couplings and higher randomness values for the communications network, the overall network tends to be stabilized for larger network sizes.
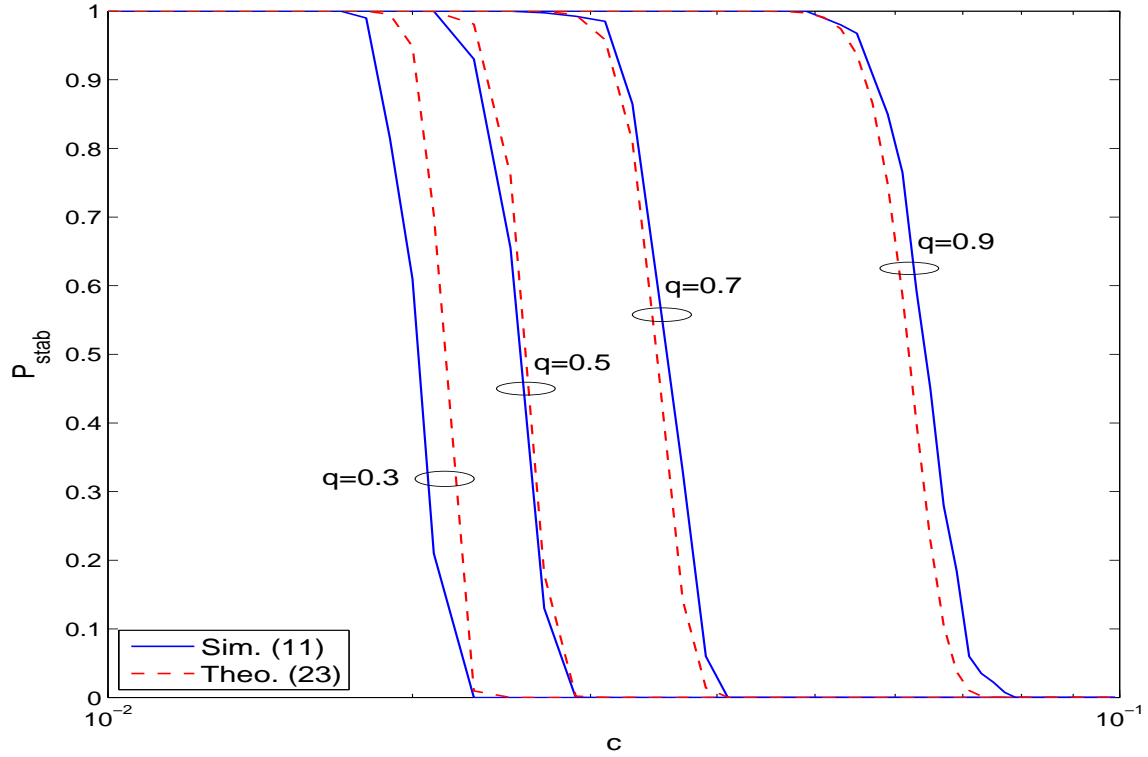
Figure 6.4: Probability of stability versus coupling strength, c, in Erdös-Rényi dynamics network for different q and network size $N = 100$.

This behavior can be predicted from (6.25), which can be rewritten as

$$N < \frac{\eta}{2cp(\eta\sqrt{\rho_1} - q)}. \tag{6.27}$$

Thus, weaker couplings or richer connected communications network makes the network more stable.

Fig. 6.4 shows the probability of stability as a function of coupling strength, c, in an Erdös-Rényi dynamics network for different randomness values of communications network, q. As

it can be seen, a larger q results in stabilization of the stronger connected networks.

Conclusion

We have presented a network stability condition for an arbitrary dynamics network with identical plants, controllers and couplings. Using this condition, we have derived approximate probability of stability, assuming that the communications network is a random sub-network of the dynamics network. We have further studied our network stability condition and probability of stability for the case where the dynamics network is an Erdös-Rényi network. Using these result, we have studied the asymptotic trends in stability of the network, when network parameters take extreme values. A numerical example shows that our analytical results have reasonable accuracy.

CHAPTER 7: SWITCHING CONTROL OF LINEAR TIME-VARYING NETWORKED SYSTEMS WITH SPARSE OBSERVER-CONTROLLER NETWORKS

In this chapter, a set of stability conditions for linear time-varying networked control systems with arbitrary topologies using a piecewise quadratic switching stabilization approach with multiple quadratic Lyapunov functions is provided. This set of stability conditions is used to provide a novel iterative low-complexity algorithm that must be updated and optimized in discrete time for the design of a sparse observer-controller network, for a given plant network with an arbitrary topology. The distributed observers is employed by utilizing the output of other subsystems to improve the stability of each observer. To avoid unbounded growth of controller and observer gains,the bounds on the norms of the gains are imposed.

Introduction

Networked control systems (NCS) have been the subject of much interest due to the fact that they have a wide range of applications, including electric power networks, transportation networks, factory automation, tele-operations and sensor and actuator networks, and the fact that they pose interesting unsolved problems in control theory. A centralized architecture is traditionally employed to control spatially distributed systems in which the components were connected via dedicated hard-wired links carrying the information from the sensors to a central location, where control signals were computed and sent to the actuators. However, the centralized architecture is not scalable. Moreover, it does not meet many new requirements such as modularity, resiliency, integrated diagnostics, and efficient maintenance. Distributed

or decentralized networked control systems meet these requirements through reduction in the required communications and distribution of the computational power across the system. Consequently, these approaches can be scalable. More recently, the distributed and decentralized architectures have been made feasible due to relative maturity in communication and computing technologies, enabling their convergence with control.

In general, a NCS consists of a number of subsystems, each comprised of a plant and a controller, coupled together in some network topology. The interaction of plants with one another forms the *plant network*. Measurements and control signals are communicated using the *control network*, a.k.a. information, communications, or feedback network (Fig. 7.1). This generalization covers the full range of architectures from decentralized, when the control network has no links, to centralized, when the control network is complete (i.e. all information is available to all controllers). For each architecture both the dynamics of each subsystem and the topology of plant network, play important roles in the stability of the entire interconnected system.

A key aspect in designing a particular NCS is the amount of information exchange. Typically, the all-to-all information exchange required for a centralized architecture is not feasible due to cost and complexity of the required communication. On the other end of the spectrum, ideally, one would have a decentralized controller [94] [95] [96]. It can be shown that even if each subsystem is asymptotically stable in isolation, the entire interconnected system may be unstable. Therefore, a decentralized architecture is usually inadequate to satisfy the performance requirements or even to stabilize the plant network. Thus, often the best solution is a distributed architecture, where some information is exchanged with neighbors [97]- [101].
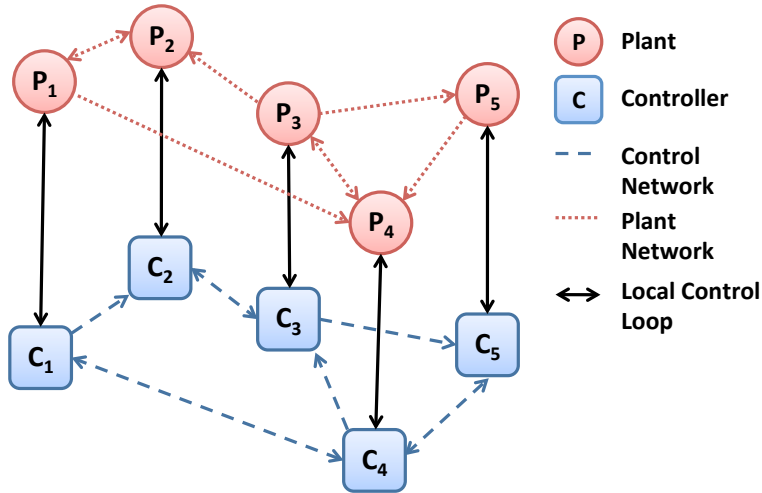
Figure 7.1: A Networked Control System (NCS)

The networked control literature can be classified into two main groups. The first group as illustrated in [102]- [76] studies different factors, including bandwidth, packet dropout and disorder, data quantization, time-varying sampling intervals, and time delays, all of which are imposed by imperfections and limitations of communication channels and can degrade the system performance or even destabilize the system. The second group, which this paper also falls into, considers the topological network effects, and investigates how the topology of the plant network affects the entire interconnected system stability and other performance metrics.

The problem of imposing *a priori* constraints on the controller has been arisen in previous articles on decentralized and distributed control of a general linear time-invariant (LTI) system. These constraints often are called the information constraints, and specify what information is available to which controller and manifests itself as sparsity or delay constraints. In [110]- [113], the authors have shown the convexification problem of finding optimal controller in order to minimize a norm of the closed loop map under a structural condition,

namely *quadratic invariance*, which is an algebraic condition relating the plant and the constraint set. The works in [114, 115] have shown similar results, conditioned on the plant network being a partially ordered set (poset) which is based on poset information structure (acyclic information flow) among subsystems. This constraint is closely related to quadratic invariance, however, it can lead to more computationally efficient solutions and is applicable to a more general class of problems.

While these results are elegant and important, they impose restrictions on the topology of the plant network of LTI systems. The key question in the design of control network for NCSs with arbitrary plant network topologies is one of *topological information requirements* and can be framed as the question: *Which subsystems should be given the input and output information of a particular subsystem, in order for the local controllers to be able to satisfy a global control objective?* This is a critical question in the design of massively distributed control systems, such as the Smart Grid [116]- [119].

In this paper, we extend our LTI NCS results [120] by considering a linear time-varying (LTV) NCS with an arbitrary topology and provide a methodology to design an iterative sparse observer and controller network which updates in discrete time. As in our previous work [120] here we also assume that the communication links do not have any bandwidth limitation, data loss or induced network delays.

We first use multiple quadratic Lyapunov functions to develop a set of stability conditions that guarantee global asymptotic stability using the piecewise quadratic switching stabilization method [121]- [124]. We then use these stability conditions to design an iterative sparse observer-controller network for a given plant network with an arbitrary topology. We take a broader look at the topological information requirements by taking into account the distributed state estimation problem, which is generally neglected in existing work.

Notation and Problem Definition

Notation

The set of real (column) n-vectors is denoted by $\mathbb{R}^n$ and the set of real $m \times n$ matrices is denoted by $\mathbb{R}^{m \times n}$. We use $\mathbb{R}_+$ and $\mathbb{Z}_+$ to denote the sets of non-negative real and non-negative integers respectively. Matrices and vectors are denoted by capital and lower-case bold letters, respectively. Generalized matrix inequality, $\prec$, is defined by the positive definite cone between symmetric matrices. The Euclidean (l_2) vector norm and the induced l_2 matrix norm are represented by $\|\cdot\|$ and the Frobenius matrix norm is denoted by $\|\cdot\|_F$. By $\lambda_{\min}(\cdot)$, $\lambda_{\max}(\cdot)$ and $\sigma_{\max}(\cdot)$ we denote the smallest and largest eigenvalue and the largest singular value of the argument, respectively. The Schur (Hadamard) product is represented by $\circ$ and the $m \times n$ unit matrix consisting of all ones is denoted by $\mathbf{1}^{m \times n}$. We let $\mathcal{N} = \{1, \ldots, N\}$ and $\mathcal{N}_i = \mathcal{N} - \{i\}$. The indicator function of x is represented by 1_x and column-stacking operator is denoted by $\text{vec}(\cdot)$.

In the following subsection, we address the problem statement by employing the same methodology similar to that of [120].

Problem Definition

Consider a network of N coupled LTV subsystems, each consisting of a plant and a controller. The state of the ith plant, $\mathbf{x}_i(t) \in \mathbb{R}^{n_i}$, is governed by

$$\dot{\mathbf{x}}_i(t) = \mathbf{A}_i(t)\mathbf{x}_i(t) + \mathbf{B}_i(t)\mathbf{u}_i(t) + \sum_{j \in \mathcal{N}_i} \mathbf{H}_{ij}(t)\mathbf{x}_j(t)$$

$$\mathbf{y}_i(t) = \mathbf{C}_i(t)\mathbf{x}_i(t), \tag{7.1}$$

where $\mathbf{u}_i(t) \in \mathbb{R}^{m_i}$ and $\mathbf{y}_i(t) \in \mathbb{R}^{r_i}$ are input and output of the ith subsystem, and $\mathbf{A}_i(t)$, $\mathbf{B}_i(t)$, $\mathbf{C}_i(t)$ and $\mathbf{H}_{ij}(t)$ are known matrices. We assume that subsystem (7.1) is both completely controllable and completely observable for all i. We consider an arbitrary directed network without self-loops. That is, $\mathbf{H}_{ii}(t) \equiv \mathbf{0}$, and $\mathbf{H}_{ij}(t)$ and $\mathbf{H}_{ji}(t)$ are not necessarily equal. We look for a distributed stabilizing observer-based controller of the form

$$\dot{\hat{\mathbf{x}}}_i(t) = \mathbf{A}_i(t)\hat{\mathbf{x}}_i(t) + \mathbf{B}_i(t)\mathbf{u}_i(t) + \sum_{j \in \mathcal{N}_i} \mathbf{H}_{ij}(t)\hat{\mathbf{x}}_j(t) + \mathbf{M}_i(t)(\mathbf{C}_i(t)\hat{\mathbf{x}}_i(t) - \mathbf{y}_i(t))$$

$$+ \sum_{j \in \mathcal{N}_i} \mathbf{O}_{ij}(t)(\mathbf{C}_j(t)\hat{\mathbf{x}}_j(t) - \mathbf{y}_j(t)),$$

$$\mathbf{u}_i(t) = \mathbf{K}_i(t)\hat{\mathbf{x}}_i(t) + \sum_{j \in \mathcal{N}_i} \mathbf{L}_{ij}(t)\hat{\mathbf{x}}_j(t), \tag{7.2}$$

where $\hat{\mathbf{x}}_i(t)$ is the estimate of $\mathbf{x}_i(t)$, $\mathbf{K}_i(t)$ and $\mathbf{L}_{ij}(t)$ are local and coupling controller gains, and $\mathbf{M}_i(t)$ and $\mathbf{O}_{ij}(t)$ are local and coupling observer gains, respectively. Note that to estimate $\mathbf{x}_i(t)$, we not only use output of subsystem i, but also outputs of (potentially) all other subsystems. This is dual to the concept of distributed control. Our objective is to find distributed observer-based control law (7.2), using feedback from (potentially) all other subsystems to stabilize the plant network with a sparse control network. That is, we aim to find $\mathbf{K}_i(t), \mathbf{M}_i(t), \mathbf{L}_{ij}(t)$ and $\mathbf{O}_{ij}(t)$, such that the entire interconnected system is globally asymptotically stable and that the number of links in the control network (number of non-zero coupling gains $\mathbf{L}_{ij}(t)$ and $\mathbf{O}_{ij}(t)$) is minimized. We also impose constraints

$$\|\mathbf{K}_i(t)\| \leq \kappa_i, \tag{7.3a}$$

$$\|\mathbf{M}_i(t)\| \leq \mu_i, \tag{7.3b}$$

$$\|\mathbf{L}_{ij}(t)\| \leq \iota_{ij}, \tag{7.3c}$$

$$\|\mathbf{O}_{ij}(t)\| \leq \omega_{ij}, \tag{7.3d}$$

134

to avoid undesirably large gains.

Defining $\mathbf{x}(t) = \text{vec}(\mathbf{x}_i(t))$, $\mathbf{u}(t) = \text{vec}(\mathbf{u}_i(t))$, $\mathbf{y}(t) = \text{vec}(\mathbf{y}_i(t))$, (7.1) reduces to

$$\dot{\mathbf{x}}(t) = \mathbf{A}(t)\mathbf{x}(t) + \mathbf{B}(t)\mathbf{u}(t) + \mathbf{H}(t)\mathbf{x}(t),$$

$$\mathbf{y}(t) = \mathbf{C}(t)\mathbf{x}(t), \tag{7.4}$$

where $\mathbf{A}(t) = \text{diag}(\mathbf{A}_i(t))$, $\mathbf{B}(t) = \text{diag}(\mathbf{B}_i(t))$, $\mathbf{C}(t) = \text{diag}(\mathbf{C}_i(t))$ and $\mathbf{H}(t) = [\mathbf{H}_{ij}(t)]$.

Moreover, (7.2) yields

$$\dot{\hat{\mathbf{x}}}(t) = \mathbf{A}(t)\hat{\mathbf{x}}(t) + \mathbf{B}(t)\mathbf{u}(t) + \mathbf{H}(t)\hat{\mathbf{x}}(t) + \mathbf{M}(t)(\mathbf{C}(t)\hat{\mathbf{x}}(t) - \mathbf{y}(t)) + \mathbf{O}(t)(\mathbf{C}(t)\hat{\mathbf{x}}(t) - \mathbf{y}(t)),$$

$$\mathbf{u}(t) = \mathbf{K}(t)\hat{\mathbf{x}}(t) + \mathbf{L}(t)\hat{\mathbf{x}}(t), \tag{7.5}$$

where $\mathbf{K}(t) = \text{diag}(\mathbf{K}_i(t))$, $\mathbf{M}(t) = \text{diag}(\mathbf{M}_i(t))$, $\mathbf{L}(t) = [\mathbf{L}_{ij}(t)]$, with $\mathbf{L}_{ii}(t) \equiv \mathbf{0}$ and $\mathbf{O}(t) = [\mathbf{O}_{ij}(t)]$, with $\mathbf{O}_{ii}(t) \equiv \mathbf{0}$.

Defining error $\mathbf{e}(t) \triangleq \hat{\mathbf{x}}(t) - \mathbf{x}(t)$ reduces (7.4) and (7.5) to

$$\dot{\mathbf{x}}(t) = [\mathbf{A}(t) + \mathbf{H}(t) + \mathbf{B}(t)(\mathbf{K}(t) + \mathbf{L}(t))]\,\mathbf{x}(t) + \mathbf{B}(t)(\mathbf{K}(t) + \mathbf{L}(t))\mathbf{e}(t), \tag{7.6}$$

$$\dot{\mathbf{e}}(t) = [\mathbf{A}(t) + \mathbf{H}(t) + (\mathbf{M}(t) + \mathbf{O}(t))\mathbf{C}(t)]\,\mathbf{e}(t). \tag{7.7}$$

This is an LTV networked linear cascade dynamical system with the equilibrium point $(\mathbf{x}, \mathbf{e}) \equiv (\mathbf{0}, \mathbf{0})$.

Assumption 3. *Matrices* $\mathbf{A}(t), \mathbf{B}(t), \mathbf{C}(t)$ *and* $\mathbf{H}(t)$ *are continuously differentiable and have*

bounded derivatives:

$$\|\dot{\mathbf{A}}(t)\| \le a, \ \|\dot{\mathbf{B}}(t)\| \le b, \ \|\dot{\mathbf{C}}(t)\| \le c, \ \|\dot{\mathbf{H}}(t)\| \le h. \tag{7.8}$$

Under Assumption 3, for all $t, t' \in \mathbb{R}_+$ we have [125]

$$\|\mathbf{A}(t) - \mathbf{A}(t')\| \le a|t - t'|, \ \|\mathbf{B}(t) - \mathbf{B}(t')\| \le b|t - t'|,$$

$$\|\mathbf{C}(t) - \mathbf{C}(t')\| \le c|t - t'|, \ \|\mathbf{H}(t) - \mathbf{H}(t')\| \le h|t - t'|. \tag{7.9}$$

Piecewise Quadratic Switching Stabilization

As the nature of problem is time-varying, and analytical design approaches are intractable (due to the generality of the network topology), one needs to take a numerical design approach. Thus, the design must be updated and optimized at discrete times. Consider the discrete series $0 = t_0 < t_1 < \cdots < t_k < \cdots$. If a sample-and-hold control approach over intervals $[t_k, t_{k+1})$ is used, system (7.6) and (7.7) will become

$$\dot{\mathbf{x}}(t) = [\mathbf{A}(t) + \mathbf{H}(t) + \mathbf{B}(t)(\mathbf{K}_k + \mathbf{L}_k)]\,\mathbf{x}(t) + \mathbf{B}(t)(\mathbf{K}_k + \mathbf{L}_k)\mathbf{e}(t), \tag{7.10}$$

$$\dot{\mathbf{e}}(t) = [\mathbf{A}(t) + \mathbf{H}(t) + (\mathbf{M}_k + \mathbf{O}_k)\mathbf{C}(t)]\,\mathbf{e}(t), \tag{7.11}$$

for $t \in [t_k, t_{k+1})$.

Assumption 4. *For every $k \in \mathbb{Z}_+$, there exists constant $T_{\min} > 0$ such that*

$$T_k \triangleq t_{k+1} - t_k \ge T_{\min}. \tag{7.12}$$

136

Later, in Corollary 5 we will find a lower bound for $T_{\min}$.

Theorem 1. *The equilibrium point,* $\mathbf{x} \equiv \mathbf{0}$, *of the system*

$$\dot{\mathbf{x}}(t) = \left[\mathbf{A}(t) + \mathbf{H}(t) + \mathbf{B}(t)(\mathbf{K}_k + \mathbf{L}_k) \right] \mathbf{x}(t), \qquad (7.13)$$

is globally asymptotically stable, if for every $k \in \mathbb{Z}_+$ *and* $t \in [t_k, t_{k+1})$, *there exist* $\mathbf{K}_k$, $\mathbf{L}_k$, $\mathbf{P}_k$, $\beta_i > 0$, *and* $\epsilon_i > 0$ *such that*

$$2\boldsymbol{\beta} \circ \mathbf{P}_k + \left[\mathbf{A}(t) + \mathbf{H}(t) + \mathbf{B}(t)(\mathbf{K}_k + \mathbf{L}_k) \right]^T \mathbf{P}_k$$

$$+ \mathbf{P}_k \left[\mathbf{A}(t) + \mathbf{H}(t) + \mathbf{B}(t)(\mathbf{K}_k + \mathbf{L}_k) \right] \preceq \mathbf{0} \qquad (7.14a)$$

$$\mathbf{P}_k - \boldsymbol{\epsilon} \succeq \mathbf{0} \qquad (7.14b)$$

$$\mathbf{P}_{k-1} - \mathbf{P}_k \succeq \mathbf{0} \qquad (7.14c)$$

are satisfied for all $k \geq 1$ *and* (7.14a), (7.14b) *are satisfied for* $k = 0$, *where* $\mathbf{P}_k = diag(\mathbf{P}_{k,i})$, $\boldsymbol{\beta} = diag\left(\beta_i \mathbf{1}^{n_i \times n_i}\right)$, *and* $\boldsymbol{\epsilon} = diag(\epsilon_i \mathbf{I}_{n_i})$.

Proof. Consider multiple quadratic Lyapunov functions [124] $V_k(\mathbf{x}(t)) = \mathbf{x}^T(t)\mathbf{P}_k\mathbf{x}(t)$, $t \in [t_k, t_{k+1})$, and let $V(\mathbf{x}(t)) = V_k(\mathbf{x}(t))$ when $t \in [t_k, t_{k+1})$. Since $\mathbf{P}_k \succ \mathbf{0}$, to show that $\mathbf{x}(t) \to 0$, it suffices to show that $V(\mathbf{x}(t)) \to 0$. Condition (7.14a) yields

$$\dot{V}_k(\mathbf{x}(t)) = \mathbf{x}^T(t) \left[\mathbf{A}(t) + \mathbf{H}(t) + \mathbf{B}(t)(\mathbf{K}_k + \mathbf{L}_k) \right]^T \mathbf{P}_k \mathbf{x}(t)$$

$$+ \mathbf{x}^T(t) \mathbf{P}_k \left[\mathbf{A}(t) + \mathbf{H}(t) + \mathbf{B}(t)(\mathbf{K}_k + \mathbf{L}_k) \right] \mathbf{x}(t)$$

$$\leq -2 \mathbf{x}^T(t) \boldsymbol{\beta} \circ \mathbf{P}_k \mathbf{x}(t)$$

$$= -2 \sum_{i \in \mathcal{N}} \beta_i \mathbf{x}_i^T(t) \mathbf{P}_{k,i} \mathbf{x}_i(t)$$

$$\leq -2\beta \sum_{i \in \mathcal{N}} \mathbf{x}_i^T(t) \mathbf{P}_{k,i} \mathbf{x}_i(t)$$

$$= -2\beta V_k(\mathbf{x}(t)), \tag{7.15}$$

for $t \in [t_k, t_{k+1})$, where $\beta = \min_i \beta_i$. This means that $\dot{V}(\mathbf{x}(t)) = \dot{V}_k(\mathbf{x}(t))$ is negative definite over $t \in [t_k, t_{k+1})$. Moreover, since $\mathbf{x}(t)$ is continuous, condition (7.14c) implies that $V(\mathbf{x}(t))$ is decreasing over all t. Thus, since $V(\mathbf{x}(t))$ is positive definite, if we show that its samples, $V(\mathbf{x}(t_k)) = V_k(\mathbf{x}(t_k))$, converge to zero we have $V(\mathbf{x}(t)) \to 0$ as well. Since the sequence $V_k(\mathbf{x}(t_k))$ is monotonically decreasing and positive definite, it converges to some value $v \geq 0$. To show that $v = 0$, first we note that due to the comparison lemma [125], (7.15) yields

$$V_k(\mathbf{x}(t)) \leq V_k(\mathbf{x}(t_k)) e^{-2\beta(t - t_k)}, t \in [t_k, t_{k+1}). \tag{7.16}$$

Now, we can write

$$
\begin{aligned}
0 = v - v \\
&= \lim_{k \to \infty} V_{k+1}(\mathbf{x}(t_{k+1})) - \lim_{k \to \infty} V_k(\mathbf{x}(t_k)) \\
&= \lim_{k \to \infty} \left[V_{k+1}(\mathbf{x}(t_{k+1})) - V_k(\mathbf{x}(t_{k+1}^-)) \right] + \lim_{k \to \infty} \left[V_k(\mathbf{x}(t_{k+1}^-)) - V_k(\mathbf{x}(t_k)) \right] \\
&= \lim_{k \to \infty} \left[\mathbf{x}^T(t_{k+1}) \left(\mathbf{P}_{k+1} - \mathbf{P}_k \right) \mathbf{x}(t_{k+1}) \right] + \lim_{k \to \infty} \left[V_k(\mathbf{x}(t_k)) \left(e^{-2\beta(t_{k+1}^- - t_k)} - 1 \right) \right] \\
&\leq \lim_{k \to \infty} \left[V_k(\mathbf{x}(t_k)) \left(e^{-2\beta(t_{k+1}^- - t_k)} - 1 \right) \right] \\
&\leq - \left(1 - e^{-2\beta T_{\min}} \right) \lim_{k \to \infty} V_k(\mathbf{x}(t_k)) \\
&\leq - \left(1 - e^{-2\beta T_{\min}} \right) \lim_{k \to \infty} \left[\lambda_{\min}(\mathbf{P}_k) \| \mathbf{x}(t_k) \|^2 \right] \\
&\leq - \epsilon \left(1 - e^{-2\beta T_{\min}} \right) \lim_{k \to \infty} \| \mathbf{x}(t_k) \|^2 \\
&\leq 0, && (7.17)
\end{aligned}
$$

where $\epsilon = \min_i \epsilon_i > 0$. This implies that

$$
\epsilon \left(1 - e^{-2\beta T_{\min}} \right) \lim_{k \to \infty} \| \mathbf{x}(t_k) \|^2 = 0. \qquad (7.18)
$$

which requires that $\lim_{k \to \infty} \mathbf{x}(t_k) \to 0$, and $\lim_{k \to \infty} V_k(\mathbf{x}(t_k)) \to 0$. In other words, the system (7.13) is globally asymptotically stable. $\qquad \square$

Theorem 2. *The equilibrium point of the system in (7.6) and (7.7), $(\mathbf{x}, \mathbf{e}) \equiv (\mathbf{0}, \mathbf{0})$, is globally asymptotically stable, if for every $k \in \mathbb{Z}_+$ and $t \in [t_k, t_{k+1})$, there exist $\mathbf{K}_k$, $\mathbf{L}_k$, $\mathbf{P}_k$,*

$\mathbf{M}_k$, $\mathbf{O}_k$, $\hat{\mathbf{P}}_k$, $\beta_i > 0$, *and* $\epsilon_i > 0$ *such that*

$$2\boldsymbol{\beta} \circ \mathbf{P}_k + [\mathbf{A}(t) + \mathbf{H}(t) + \mathbf{B}(t)(\mathbf{K}_k + \mathbf{L}_k)]^T \mathbf{P}_k$$

$$+\mathbf{P}_k [\mathbf{A}(t) + \mathbf{H}(t) + \mathbf{B}(t)(\mathbf{K}_k + \mathbf{L}_k)] \preceq \mathbf{0} \tag{7.19a}$$

$$2\boldsymbol{\beta} \circ \hat{\mathbf{P}}_k + [\mathbf{A}(t) + \mathbf{H}(t) + (\mathbf{M}_k + \mathbf{O}_k)\mathbf{C}(t)]^T \hat{\mathbf{P}}_k$$

$$+\hat{\mathbf{P}}_k [\mathbf{A}(t) + \mathbf{H}(t) + (\mathbf{M}_k + \mathbf{O}_k)\mathbf{C}(t)] \preceq \mathbf{0} \tag{7.19b}$$

$$\mathbf{P}_k - \boldsymbol{\epsilon} \succeq \mathbf{0} \tag{7.19c}$$

$$\hat{\mathbf{P}}_k - \boldsymbol{\epsilon} \succeq \mathbf{0} \tag{7.19d}$$

$$\mathbf{P}_{k-1} - \mathbf{P}_k \succeq \mathbf{0} \tag{7.19e}$$

$$\hat{\mathbf{P}}_{k-1} - \hat{\mathbf{P}}_k \succeq \mathbf{0} \tag{7.19f}$$

are satisfied for all $k \geq 1$ *and* (7.19a) *to* (7.19d) *are satisfied for* $k = 0$, *where* $\mathbf{P}_k = diag(\mathbf{P}_{k,i})$, $\hat{\mathbf{P}}_k = diag(\hat{\mathbf{P}}_{k,i})$, $\boldsymbol{\beta} = diag(\beta_i \mathbf{1}^{n_i \times n_i})$, *and* $\boldsymbol{\epsilon} = diag(\epsilon_i \mathbf{I}_{n_i})$.

Proof. By Theorem 1, conditions (7.19a), (7.19c) and (7.19e) imply that the unforced system (7.10) is globally asymptotically stable and, consequently, (7.10) is input-to-state stable. Similarly, (7.19b), (7.19d) and (7.19f) guarantee global asymptotical stability of (7.11). Hence the equilibrium point of cascaded dynamical system (7.10) and (7.11), $(\mathbf{x}, \mathbf{e}) \equiv (\mathbf{0}, \mathbf{0})$, is globally asymptotically stable [125]. $\qquad\square$

We note that conditions (7.19a) and (7.19b) are the requirement that the energy in the system is decreasing in every interval while conditions (7.19c) and (7.19d) guarantee positive definiteness of multiple quadratic Lyapunov functions. Conditions (7.19e) and (7.19f) are necessary to guarantee multiple quadratic Lyapunov functions form a non-increasing sequence when entering the next interval.

Theorem 2 provides a set of stability conditions based on which the controllers and observers can be designed. However, these conditions are not convex. This is important since a solution must be found iteratively at each t_k. The following theorem provides a set of convex, albeit more conservative, stability conditions. It also incorporates bounds (7.3).

Theorem 3. *System (7.1) with controller (7.2) is globally asymptotically stable, and bounds (7.3) are satisfied, if the following convex constraints have a feasible point, such that*

$$\mathbf{F}_k + \mathbf{F}_k^T + \gamma\mathbf{I}_n \preceq \mathbf{0} \tag{7.20a}$$

$$\hat{\mathbf{F}}_k + \hat{\mathbf{F}}_k^T + \gamma\mathbf{I}_n \preceq \mathbf{0} \tag{7.20b}$$

$$\epsilon^{-1} \succeq \mathbf{Z}_k \succ \mathbf{0} \tag{7.20c}$$

$$\hat{\mathbf{P}}_k - \epsilon \succeq \mathbf{0} \tag{7.20d}$$

$$\mathbf{Z}_k - \mathbf{Z}_{k-1} \succeq \mathbf{0} \tag{7.20e}$$

$$\hat{\mathbf{P}}_{k-1} - \hat{\mathbf{P}}_k \succeq \mathbf{0} \tag{7.20f}$$

$$\kappa_i\lambda_{min}(\mathbf{Z}_{k,i}) - \sigma_{max}(\mathbf{W}_{k,i}) \geq 0 \tag{7.20g}$$

$$\iota_{ij}\lambda_{min}(\mathbf{Z}_{k,j}) - \sigma_{max}(\mathbf{Y}_{k,ij}) \geq 0 \tag{7.20h}$$

$$\mu_i\lambda_{min}(\hat{\mathbf{P}}_{k,i}) - \sigma_{max}(\hat{\mathbf{W}}_{k,i}) \geq 0 \tag{7.20i}$$

$$\omega_{ij}\lambda_{min}(\hat{\mathbf{P}}_{k,i}) - \sigma_{max}(\hat{\mathbf{Y}}_{k,ij}) \geq 0 \tag{7.20j}$$

are satisfied for all $i, j \in \mathcal{N}$, $\gamma > 0$, $k \geq 1$ and (7.20a)-(7.20d) and (7.20g)-(7.20j) are satisfied for $k = 0$, where

$$\mathbf{F}_k = (\mathbf{A}_k + \mathbf{H}_k)\mathbf{Z}_k + \mathbf{B}_k(\mathbf{W}_k + \mathbf{Y}_k) + \boldsymbol{\beta} \circ \mathbf{Z}_k,$$

$$\hat{\mathbf{F}}_k = \hat{\mathbf{P}}_k(\mathbf{A}_k + \mathbf{H}_k) + (\hat{\mathbf{W}}_k + \hat{\mathbf{Y}}_k)\mathbf{C}_k + \boldsymbol{\beta} \circ \hat{\mathbf{P}}_k,$$

$\mathbf{Z}_k = diag(\mathbf{Z}_{k,i})$, $\hat{\mathbf{P}}_k = diag(\hat{\mathbf{P}}_{k,i})$, $\mathbf{W}_k = diag(\mathbf{W}_{k,i})$, $\hat{\mathbf{W}}_k = diag(\hat{\mathbf{W}}_{k,i})$, $\mathbf{Y}_k = [\mathbf{Y}_{k,ij}]$ *and*

141

$\hat{\mathbf{Y}}_k = [\hat{\mathbf{Y}}_{k,ij}]$ *with* $\mathbf{Y}_{k,ii} = \hat{\mathbf{Y}}_{k,ii} \equiv \mathbf{0}$.

Furthermore, if $\mathbf{Z}_{k,i}^\star, \hat{\mathbf{P}}_{k,i}^\star, \mathbf{W}_{k,i}^\star, \hat{\mathbf{W}}_{k,i}^\star, \mathbf{Y}_{k,ij}^\star, \hat{\mathbf{Y}}_{k,ij}^\star$ *is a solution of* (7.20), *the controller and observer gains are*

$$\begin{aligned}
\mathbf{K}_{k,i}^\star &= \mathbf{W}_{k,i}^\star \mathbf{Z}_{k,i}^{\star\,-1}, \quad \mathbf{L}_{k,ij}^\star = \mathbf{Y}_{k,ij}^\star \mathbf{Z}_{k,j}^{\star\,-1}, \\
\mathbf{M}_{k,i}^\star &= \hat{\mathbf{P}}_{k,i}^{\star\,-1} \hat{\mathbf{W}}_{k,i}^\star, \quad \mathbf{O}_{k,ij}^\star = \hat{\mathbf{P}}_{k,i}^{\star\,-1} \hat{\mathbf{Y}}_{k,ij}^\star,
\end{aligned} \tag{7.21}$$

for all $t \in [t_k, t_{k+1})$ *and the next switching time is* $t_{k+1} = t_k + T_k$ *where*

$$T_k = \frac{1}{2} \min \left\{ \frac{-\lambda_{max}(\mathbf{F}_k + \mathbf{F}_k^T)}{(a+h)\|\mathbf{Z}_k\| + b\|\mathbf{W}_k + \mathbf{Y}_k\|}, \frac{-\lambda_{max}(\hat{\mathbf{F}}_k + \hat{\mathbf{F}}_k^T)}{(a+h)\|\hat{\mathbf{P}}_k\| + c\|\hat{\mathbf{W}}_k + \hat{\mathbf{Y}}_k\|} \right\}. \tag{7.22}$$

Proof. We will show that the conditions of Theorem 2, namely (7.19a)-(7.19f), are satisfied if (7.20a)-(7.20f) hold. Defining new variables $\mathbf{Z}_k \triangleq \mathbf{P}_k^{-1}$, $\mathbf{W}_k \triangleq \mathbf{K}_k \mathbf{P}_k^{-1}$, and $\mathbf{Y}_k \triangleq \mathbf{L}_k \mathbf{P}_k^{-1}$, reveals that (7.19a), (7.19c) and (7.19e) are equivalent to

$$2\boldsymbol{\beta} \circ \mathbf{Z}_k + [(\mathbf{A}(t) + \mathbf{H}(t))\mathbf{Z}_k + \mathbf{B}(t)(\mathbf{W}_k + \mathbf{Y}_k)]^T$$
$$+ [(\mathbf{A}(t) + \mathbf{H}(t))\mathbf{Z}_k + \mathbf{B}(t)(\mathbf{W}_k + \mathbf{Y}_k)] \preceq \mathbf{0}, \tag{7.23a}$$

$$\boldsymbol{\epsilon}^{-1} \succeq \mathbf{Z}_k \succ \mathbf{0}, \tag{7.23b}$$

$$\mathbf{Z}_k - \mathbf{Z}_{k-1} \succeq \mathbf{0}, \tag{7.23c}$$

Clearly, (7.23b) and (7.23c) are (7.20c) and (7.20e). To show that (7.23a) yields (7.20a), we first note that

$$\begin{aligned}
(\mathbf{A}(t) + \mathbf{H}(t))\mathbf{Z}_k &= (\mathbf{A}_k + \mathbf{H}_k)\mathbf{Z}_k + (\triangle\mathbf{A}(t) + \triangle\mathbf{H}(t))\mathbf{Z}_k \\
&\preceq (\mathbf{A}_k + \mathbf{H}_k)\mathbf{Z}_k + \|(\triangle\mathbf{A}(t) + \triangle\mathbf{H}(t))\mathbf{Z}_k\| \, \mathbf{I}_n \\
&\preceq (\mathbf{A}_k + \mathbf{H}_k)\mathbf{Z}_k + T_k(a+h)\|\mathbf{Z}_k\|\mathbf{I}_n,
\end{aligned} \tag{7.24}$$

where $\triangle \mathbf{A}(t) = \mathbf{A}(t) - \mathbf{A}_k$ and $\triangle \mathbf{H}(t) = \mathbf{H}(t) - \mathbf{H}_k$, and the last inequality is due to Assumption 3. Similarly, we can show that

$$\mathbf{B}(t)(\mathbf{W}_k + \mathbf{Y}_k) \preceq \mathbf{B}_k(\mathbf{W}_k + \mathbf{Y}_k) + T_k b \|\mathbf{W}_k + \mathbf{Y}_k\| \mathbf{I}_n. \tag{7.25}$$

Thus, the left hand side of (7.23a) can be upper bounded by

$$\mathbf{F}_k + \mathbf{F}_k^T + 2T_k[(a+h)\|\mathbf{Z}_k\| + b\|\mathbf{W}_k + \mathbf{Y}_k\|]\mathbf{I}_n. \tag{7.26}$$

In other words, if (7.26) is negative semidefinite, (7.19a) holds. Upper bound (7.26) is negative semidefinite, if there exist $\gamma > 0$ such that

$$\mathbf{F}_k + \mathbf{F}_k^T + \gamma \mathbf{I}_n \preceq \mathbf{0}, \tag{7.27}$$

which is (7.20a) and

$$T_k \leq \frac{1}{2} \frac{-\lambda_{\max}(\mathbf{F}_k + \mathbf{F}_k^T)}{(a+h)\|\mathbf{Z}_k\| + b\|\mathbf{W}_k + \mathbf{Y}_k\|}, \tag{7.28}$$

which is guaranteed by (7.22). A similar argument, omitted for brevity, shows that (7.19b), (7.19d) and (7.19f) are satisfied if (7.20b), (7.20d), (7.20f) and (7.22) hold.

For (7.3a) we note that we can upper bound the norm of $\mathbf{K}_i$ as

$$
\begin{aligned}
\|\mathbf{K}_{k,i}\| &= \|\mathbf{W}_{k,i}\mathbf{Z}_{k,i}^{-1}\| \\
&\leq \|\mathbf{W}_{k,i}\|\|\mathbf{Z}_{k,i}^{-1}\| \\
&= \sigma_{\max}(\mathbf{W}_{k,i})\lambda_{\max}(\mathbf{Z}_{k,i}^{-1}) \\
&= \frac{\sigma_{\max}(\mathbf{W}_{k,i})}{\lambda_{\min}(\mathbf{Z}_{k,i})}.
\end{aligned} \tag{7.29}
$$

Thus, forcing (7.3a) will be forced if

$$\|\mathbf{K}_{k,i}\| \leq \frac{\sigma_{\max}(\mathbf{W}_{k,i})}{\lambda_{\min}(\mathbf{Z}_{k,i})} \leq \kappa_i, \tag{7.30}$$

or equivalently $\kappa_i \lambda_{\min}(\mathbf{Z}_{k,i}) - \sigma_{\max}(\mathbf{W}_{k,i}) \geq 0$, which is (7.20g). Similarly, (7.3b)-(7.3d) are forced if (7.20h)-(7.20j) hold.

Finally, we note that the original variables can then be found from $\mathbf{P}_k = \mathbf{Z}_k^{-1}$, $\mathbf{K}_k = \mathbf{W}_k \mathbf{Z}_k^{-1}$ and $\mathbf{L}_k = \mathbf{Y}_k \mathbf{Z}_k^{-1}$. □

Corollary 5. *If the conditions of Theorem 3 hold, a lower bound for $T_{\min}$ in Assumption 2 is*

$$T_{\min} = \min_k T_k \geq \frac{1}{2} \min \left\{ \frac{\epsilon \gamma}{a + h + b\,(\kappa + \iota)}, \; \frac{1}{\|\hat{\mathbf{P}}_0\|} \frac{\gamma}{a + h + c\,(\mu + \omega)} \right\} \tag{7.31}$$

where $\epsilon = \min_i \epsilon_i > 0$, $\gamma > 0$ are the margins in inequalities (7.20a) and (7.20b) and $\kappa = \sum_{i \in \mathcal{N}} \sqrt{\min\{m_i, n_i\}} \kappa_i$, $\iota = \sum_{i,j \in \mathcal{N}} \sqrt{\min\{m_i, n_j\}} \iota_{ij}$, $\mu = \sum_{i \in \mathcal{N}} \sqrt{\min\{n_i, r_i\}} \mu_i$ and $\omega = \sum_{i,j \in \mathcal{N}} \sqrt{\min\{n_i, r_j\}} \omega_{ij}$.

Proof. Equation (7.20a) gives us $\lambda_{\max}(\mathbf{F}_k + \mathbf{F}_k^T) \leq -\gamma$. From (7.28), we have

$$
\begin{aligned}
T_k &= -\frac{1}{2}\frac{\lambda_{\max}(\mathbf{F}_k + \mathbf{F}_k^T)}{(a+h)\|\mathbf{Z}_k\| + b\|\mathbf{W}_k + \mathbf{Y}_k\|} \\
&= -\frac{1}{2}\frac{\lambda_{\max}(\mathbf{F}_k + \mathbf{F}_k^T)}{(a+h)\|\mathbf{Z}_k\| + b\|\mathbf{K}_k\mathbf{Z}_k + \mathbf{L}_k\mathbf{Z}_k\|} \\
&\geq \frac{1}{2\|\mathbf{Z}_k\|}\frac{\gamma}{a + h + b\|\mathbf{K}_k + \mathbf{L}_k\|} \\
&\geq \frac{1}{2}\frac{\epsilon\gamma}{a + h + b\|\mathbf{K}_k + \mathbf{L}_k\|_F} \\
&\geq \frac{1}{2}\frac{\epsilon\gamma}{a + h + b\left(\|\mathbf{K}_k\|_F + \|\mathbf{L}_k\|_F\right)} \\
&\geq \frac{1}{2}\frac{\epsilon\gamma}{a + h + b\left(\kappa + \iota\right)}.
\end{aligned}
\tag{7.32}
$$

The last four inequalities are satisfied because for any $\mathbf{D} \in \mathbb{R}^{m\times n}$, the Frobenius and Euclidian norms satisfy $\|\mathbf{D}\| \leq \|\mathbf{D}\|_F \leq \sqrt{\min\{m,n\}}\|\mathbf{D}\|$.

Similarly, we have

$$
\begin{aligned}
T_k &= -\frac{1}{2}\frac{\lambda_{\max}(\hat{\mathbf{F}}_k + \hat{\mathbf{F}}_k^T)}{(a+h)\|\hat{\mathbf{P}}_k\| + c\|\hat{\mathbf{W}}_k + \hat{\mathbf{Y}}_k\|} \\
&= -\frac{1}{2}\frac{\lambda_{\max}(\hat{\mathbf{F}}_k + \hat{\mathbf{F}}_k^T)}{(a+h)\|\hat{\mathbf{P}}_k\| + c\|\hat{\mathbf{P}}_k\mathbf{M}_k + \hat{\mathbf{P}}_k\mathbf{O}_k\|} \\
&\geq \frac{1}{2\|\hat{\mathbf{P}}_k\|}\frac{\gamma}{a + h + c\|\mathbf{M}_k + \mathbf{O}_k\|} \\
&\geq \frac{1}{2\|\hat{\mathbf{P}}_0\|}\frac{\gamma}{a + h + c\|\mathbf{M}_k + \mathbf{O}_k\|_F} \\
&\geq \frac{1}{2\|\hat{\mathbf{P}}_0\|}\frac{\gamma}{a + h + c\left(\mu + \omega\right)}.
\end{aligned}
\tag{7.33}
$$

$\square$

Sparse Control Network Design

To design a sparse control network, we seek a set of $\mathbf{L}_{k,ij}$ and $\mathbf{O}_{k,ij}$ that guarantee stability, with a small number links. Note that if link ij is used it can carry both $\mathbf{L}_{k,ij}\hat{\mathbf{x}}_j(t)$ and $\mathbf{O}_{k,ij}\mathbf{y}_j(t)$. Thus, the use of a link from node i to node j at time k can be encoded in binary variables $\alpha_{k,ij} \in \{0,1\}$. Then we can write $\mathbf{L}_{k,ij} = \alpha_{k,ij}\mathbf{L}_{k,ij}^\star$ and $\mathbf{O}_{k,ij} = \alpha_{k,ij}\mathbf{O}_{k,ij}^\star$, where $\mathbf{L}_{k,ij}^\star$ and $\mathbf{O}_{k,ij}^\star$ are the optimal link gains, when the link is used. In aggregate, these can be written as $\mathbf{L}_k = \boldsymbol{\alpha}_k \circ \mathbf{L}_k^\star$ and $\mathbf{O}_k = \hat{\boldsymbol{\alpha}}_k \circ \mathbf{O}_k^\star$, where $\boldsymbol{\alpha}_k = [\alpha_{k,ij}\mathbf{1}^{m_i \times n_j}]$ and $\hat{\boldsymbol{\alpha}}_k = [\alpha_{k,ij}\mathbf{1}^{n_i \times r_j}]$ with $\alpha_{k,ii} \equiv 0$.

Now, with the stability conditions provided in (7.20) in hand, our objective is to design a control network with minimum number of links that satisfies stability conditions (7.20). Minimizing the number of communication links is equivalent to minimizing the number of $\alpha_{k,ij} = 1$, or in other words, minimizing the sum of $\alpha_{k,ij}$ subject to constraints in (7.20). Our problem can therefore be formulated as the following convex mixed-binary program:

$$\text{minimize} \sum_{i,j \in \mathcal{N}} \alpha_{k,ij} \tag{7.34a}$$

$$\text{subject to (7.20)} \tag{7.34b}$$

$$\alpha_{k,ij} \in \{0,1\} \tag{7.34c}$$

where $\mathbf{Y}_k = \boldsymbol{\alpha}_k \circ \mathbf{X}_k$ and $\hat{\mathbf{Y}}_k = \hat{\boldsymbol{\alpha}}_k \circ \hat{\mathbf{X}}_k$.

The complexity of solving problem (7.34) is important, since it has to be solved in each iteration. In general a mixed-binary program is NP-hard. In the worst case, one has to solve $\mathcal{O}(2^{N^2})$ convex problems, carrying an exhaustive search on the binary variables. While a variety of exact methods for convex mixed-binary programs are available [126], their com-

putational complexity is prohibitive for large networks, specially since the calculation is to be repeated periodically. Here, we propose a simple suboptimal relaxation-thresholding approach which should be carried out in each iteration:

1. Set $k \leftarrow 0$ and $t_0 \leftarrow 0$.

2. Find a feasible point for (7.34) excluding (7.20e) and (7.20f) to find the initial conditions $\mathbf{Z}_0$ and $\hat{\mathbf{P}}_0$.

3. Initialize $\alpha_{k,ij} \leftarrow 1$ for all $i, j \in \mathcal{N}, i \neq j$.

4. Find a feasible point for (7.34) to yield $\mathbf{Z}_{k,i}, \mathbf{W}_{k,i}, \mathbf{X}_{k,ij}, \hat{\mathbf{P}}_{k,i}, \hat{\mathbf{W}}_{k,i}$ and $\hat{\mathbf{X}}_{k,ij}$. If a feasible solution is found, $\alpha_{k,ij}^{\dagger} \leftarrow \alpha_{k,ij}$. Otherwise go to step 7, unless the problem is infeasible at the first iteration, in which case there is no solution and the design procedure is terminated.

5. Solve (7.34) with (7.34c) relaxed to $\alpha_{k,ij} \in [0,1]$ to obtain solution $\alpha_{k,ij}^{(r)}$ satisfying (7.20a) and (7.20b) and $\mathbf{Z}_{k,i}, \mathbf{W}_{k,i}, \mathbf{X}_{k,ij}, \hat{\mathbf{P}}_{k,i}, \hat{\mathbf{W}}_{k,i}, \hat{\mathbf{X}}_{k,ij}$ are those found in step 4.

6. If all $\alpha_{k,ij}^{(r)} = 0$, set $\alpha_{k,ij}^{\dagger} \leftarrow 0$ and go to step 7. Otherwise, set $\alpha_{k,ij}$ corresponding to the smallest non-zero $\alpha_{k,ij}^{(r)}$ to zero and return to step 4.

7. Return $\alpha_{k,ij}^{\dagger}$.

8. Calculate the next switching time T_k from (7.22).

Note that with the above design procedure, in the worst case, one has to solve $\mathcal{O}(N^2)$ convex problems in each iteration, since it can be solved by using a linear search in a sorted set $\{\alpha_{k,ij}^{(r)}\}$.

To further simplify the procedure we can substitute steps 6 and 7 above with

147

6. Solve

$$\underset{m,l}{\text{maximize}} \quad \tau_k = \alpha^{(r)}_{k,ml}$$

$$\text{subject to} \quad \alpha_{k,ij} = 1_{\alpha^{(r)}_{k,ij} \geq \tau_k}, \text{(7.20a) and (7.20b)}.$$

(7.35)

7. Return $\alpha^{\dagger}_{k,ij} = 1_{\alpha^{(r)}_{k,ij} > \tau^{\star}_k}$, where $\tau^{\star}_k$ is the solution of (7.35).

We note that the maximum number of convex problems that should be solved in (7.35) in each iteration is only $\mathcal{O}(\log N)$, since it can be solved by a binary search on τ_k in a sorted set $\{\alpha^{(r)}_{k,ij}\}$. Of course, this reduction in complexity is at the price of a more conservative solution.

Numerical Example

Consider the system shown in Fig. 7.2, where three inverted pendulums are mounted on coupled carts. Linearizing equations of motions yield [127]

$$\mathbf{A}_i(t) = \begin{bmatrix} 0 & 1 & 0 & 0 \\ \frac{M_i+m}{M_i l}g & 0 & \frac{k_i(t)}{M_i l} & \frac{c_i+b_i(t)}{M_i l} \\ 0 & 0 & 0 & 1 \\ \frac{-m}{M_i}g & 0 & \frac{-k_i(t)}{M_i} & \frac{-c_i-b_i(t)}{M_i} \end{bmatrix}, \mathbf{H}_{ij}(t) = \begin{bmatrix} 0 & 0 & 0 & 0 \\ 0 & 0 & \frac{-k_{ij}(t)}{M_i l} & \frac{-b_{ij}(t)}{M_i l} \\ 0 & 0 & 0 & 0 \\ 0 & 0 & \frac{k_{ij}(t)}{M_i} & \frac{b_{ij}(t)}{M_i} \end{bmatrix},$$

$$\mathbf{B}_i(t) = \begin{bmatrix} 0 & \frac{-1}{M_i l} & 0 & \frac{1}{M_i} \end{bmatrix}^T, \mathbf{C}_i(t) = \begin{bmatrix} 1 & 0 & 0 & 0 \\ 0 & 0 & 1 & 0 \end{bmatrix},$$

(7.36)

for $(i,j) = (1,2),(2,1),(2,3),(3,2)$, where $k_i(t) = \sum_{j \in \mathcal{N}_i} k_{ij}(t)$ and $b_i(t) = \sum_{j \in \mathcal{N}_i} b_{ij}(t)$. Here c_i, $b_{ij}(t) = b_{ji}(t)$, and $k_{ij}(t) = k_{ji}(t)$ are friction, damper and spring coefficients, respectively, and we have assumed the moment of inertia of the pendulums to be zero.
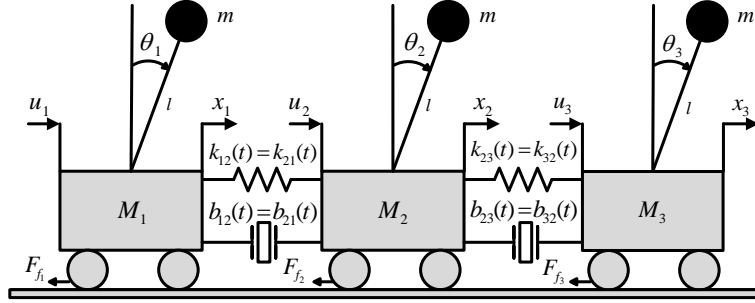
Figure 7.2: Network of three coupled inverted pendulums

Since the subsystems are controllable and observable, we can use the optimization problem (7.34) to design distributed observers and controllers that stabilize the entire network with small number of links in the control network. As design criteria, we assume bounds on the norm of local gains are $\kappa_1 = \kappa_2 = 280$, $\kappa_3 = 480$ and $\mu_i = 40$ and bounds on the norms of coupling gains are $\iota_{ij} = 20$ and $\omega_{ij} = 10$ and the numerical system parameters are $M_1 = 5$, $M_2 = 3$, $M_3 = 7$, $m = 1$, $g = 10$, $l = 1$, $k_{ij}(t) = 1 + 0.5\cos(t)$, $b_{ij}(t) = 1 + 0.5\sin(t)$, $c_1 = 4$, $c_2 = 2$ and $c_3 = 1$. All subsystem matrices are continuously differentiable uniformly bounded with $a = 0.48$, $h = 0.34$ and $b = c = 0$. Hence, Assumption 1 is satisfied. We set $\gamma = 0.2$, $\beta_i = 0.01$ and $\epsilon_i = 0.05$ for all i.

The simulation results are presented in Fig. 7.3(a) to Fig. 7.4(d) for $t = [0, 10\pi]$ seconds where to solve (7.34), we used our proposed simple suboptimal relaxation-thresholding approach with linear search. To show that how this performs well (near optimal), we compare the number of required links with the optimal exhaustive search on binary variables. Fig. 7.3(a) to 7.3(d) depict $\|\mathbf{P}_{k,i}\|$ and $\|\hat{\mathbf{P}}_{k,i}\|$ as a function of t_k. We can see that, as expected they converge as $t_k \to \infty$. The convergence of $\|\mathbf{P}_{k,i}\|$ happens after only one time slot, while $\|\hat{\mathbf{P}}_{k,i}\|$ takes 5 time slots to converge. Fig. 7.3(e) and Fig. 7.3(f), depict $\|\mathbf{K}_{k,i}\|$ and $\|\mathbf{M}_{k,i}\|$, which are the local controller and observer gains, respectively. Similarly, Fig. 7.4(a), and Fig. 7.4(b) depict $\|\mathbf{L}_{k,ij}\|$ and $\|\mathbf{O}_{k,ij}\|$, which are the coupling controller and observer gains,

149

respectively. We observe that whenever a link is not necessary, (i.e., $\alpha_{k,ij} = 0$), the link gain is set to zero. Otherwise, it is assigned the optimal values $\mathbf{L}_{k,ij}^\star$ and $\mathbf{O}_{k,ij}^\star$. We can see that all local and coupling gains are limited as enforced in (7.3).

In Fig. 7.4(c), we plot number of required links in communications network versus t_k for the two cases: (i) proposed simple suboptimal relaxation-thresholding approach and (ii) optimal exhaustive search on binary variables. The suboptimal approach performs very well and as we expected, the optimal search gives better result at the price of more complexity. Fig. 7.4(d) presents the updating times, T_k versus t_k. We see that the fewer number of links indicates the shorter updating time T_k and whenever there is a change in the number of required links, there also is a step change in the updating time T_k.

Concluding Remarks

We have provided an iterative design approach for distributed observer-based controllers that stabilize a given linear time-varying networked control system with an arbitrary directed topology. To measure states of each subsystem, we use the outputs of other subsystems to improve stability of observer dynamics; this approach is the dual of the distributed controller network. Our design approach is based on a set of stability conditions obtained using the piecewise quadratic switching stabilization method with multiple quadratic Lyapunov functions, which must be updated and optimized in discrete time and provides a sparse observer-controller network that guarantees global asymptotic stability. Due to the assumptions made here to maintain tractability, the design has some degree of conservatism. Thus, although the results provide us with significant insight into the problem of designing a sparse observer-controller network, a gap still remains. Further quantification or reduction of this gap will be quite valuable.

We added a free variable to the stability inequalities to avoid spending the entire margin in the stability criteria during the search for a sparse observer-controller network. Optimal distribution of this margin among the inequalities to make the network robust without significantly growing the size of the observer-controller network is, however, unknown. Therefore, further investigation of the tradeoff between the stability margin and the sparsity of the observer-controller network will be interesting.

We believe that the results presented in this chapter provide a foundation for further progress toward understanding these interesting and important problems.
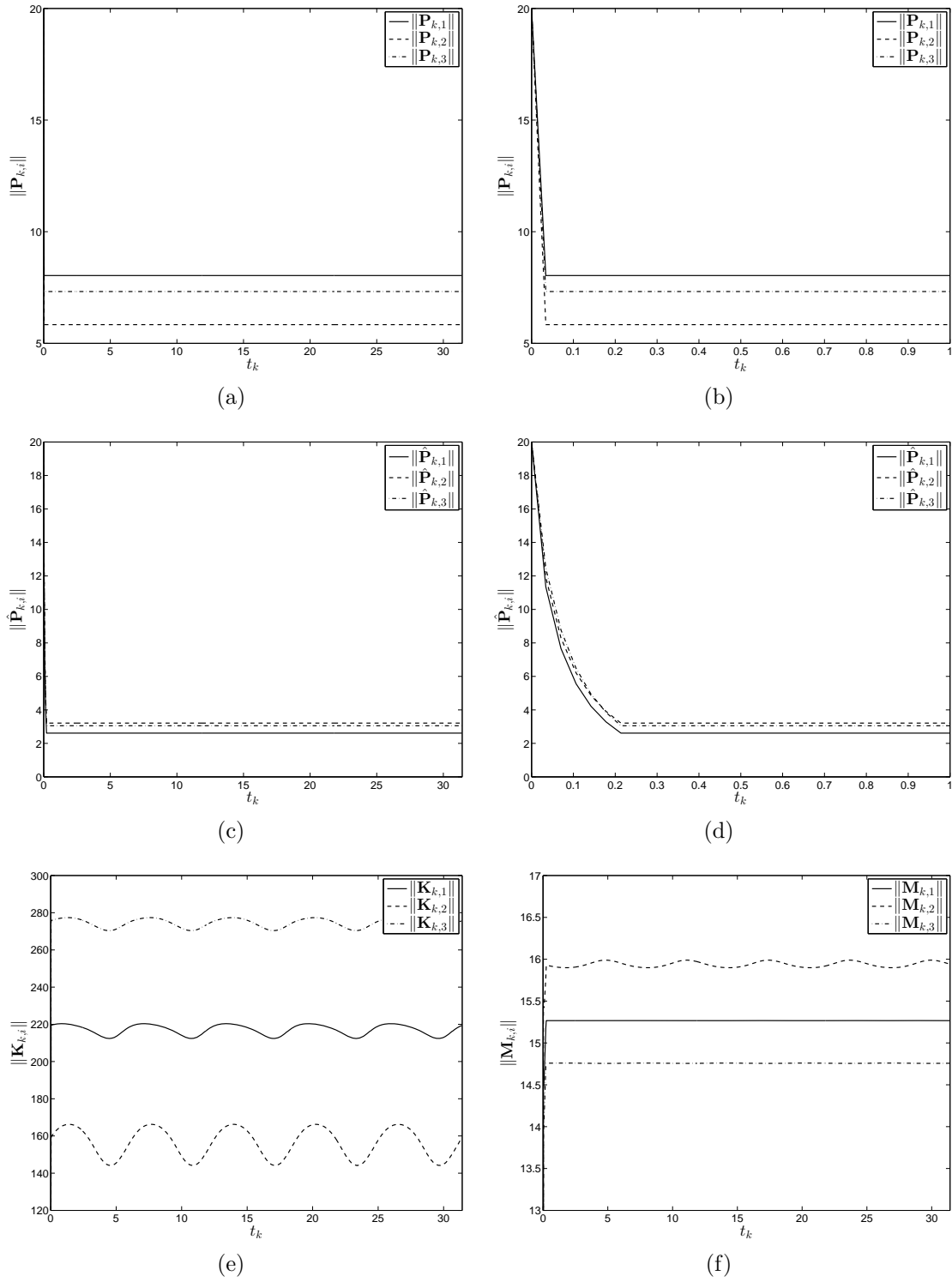
Figure 7.3: (a,b) Norm of $\mathbf{P}_{k,i}$ versus time, (c,d) Norm of $\hat{\mathbf{P}}_{k,i}$ versus time , (e, f) Norm of local controller gains $\mathbf{K}_{k,i}$ and $\mathbf{M}_{k,i}$ versus time.
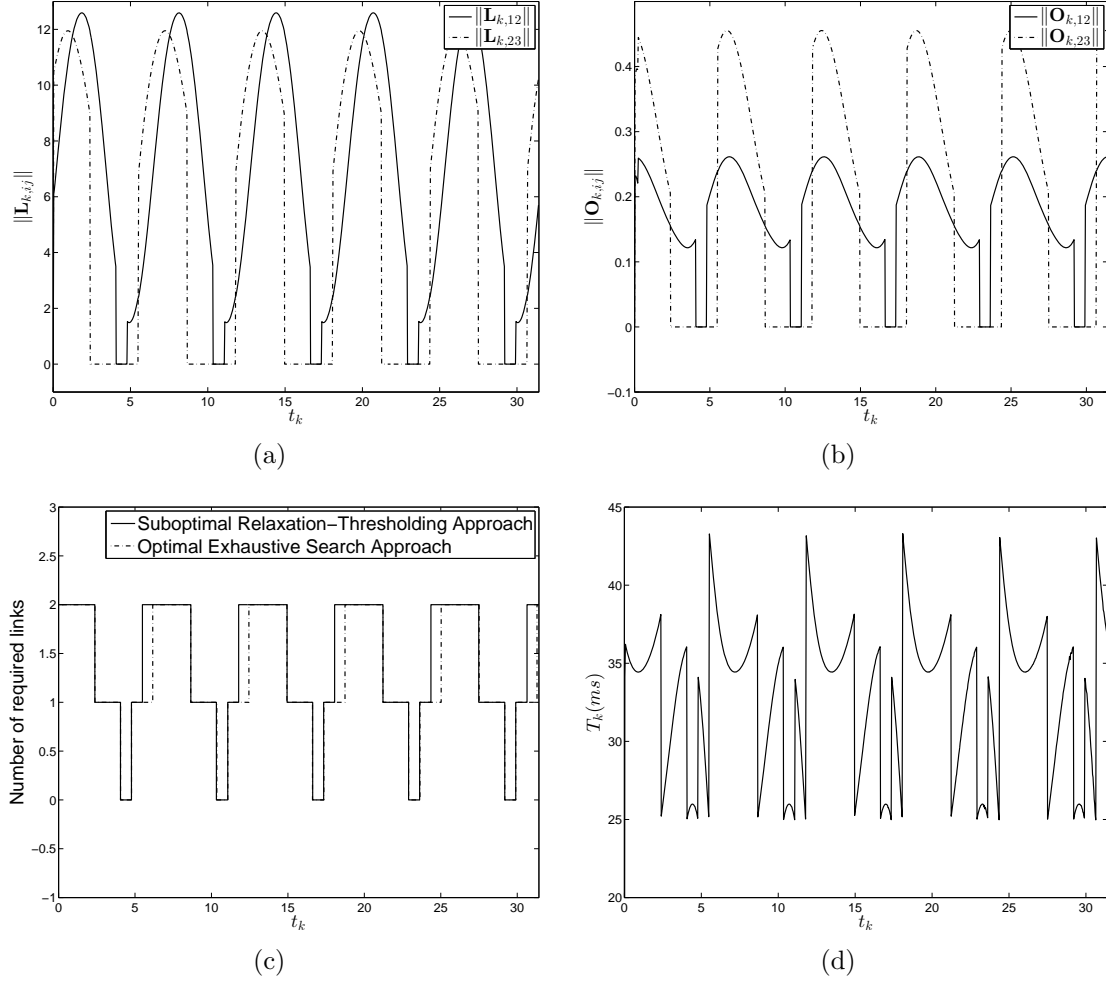
Figure 7.4: (a, b) Norm of coupling controller and observer gains $\mathbf{L}_{k,ij}$ and $\mathbf{O}_{k,ij}$ versus time. Note that the rest of links, i.e., $\mathbf{L}_{k,21} = \mathbf{L}_{k,32} = \mathbf{L}_{k,13} = \mathbf{L}_{k,31} = 0$ and $\mathbf{O}_{k,21} = \mathbf{O}_{k,32} = \mathbf{O}_{k,13} = \mathbf{O}_{k,31} = 0$ for all t_k. (c) Number of required links versus time for the two cases: (i) proposed simple suboptimal relaxation-thresholding approach and (ii) optimal exhaustive search approach, (d) Updating times, T_k.

CHAPTER 8: CONCLUSION

The contribution of this dissertation comes in three major categories. First, the stability of synchronization in complex network of dynamical systems has been analyzed. Using Lyapunov direct method, sufficient conditions on the stability of the synchronization state for wide range of *identical* dynamical systems have been derived. With these conditions which came in the form of master stability condition, the impact of topological effect of the network, i.e., the connections, have been separated from the characteristic behavior of the isolated dynamics of the node, i.e., local dynamics. This enabled the separate study of the connection network and individual dynamics. This analysis unlike most of literatures that have used negativeness of Lyapunov exponents as stability criteria as only necessary condition for stability, produced sufficient global stability. With the very simple and quite effective framework provided by this approach, a thorough analytical treatment of stability in in networks of practical interests, namely, random networks and small-worlds, has been given. The previous works were only based on extensive simulations. In a nutshell, chapter 2 addressed the following series of questions: *I) What are the conditions under which the network is guaranteed to have stable synchronous state? II) What are the conditions that connection network should have to be synchronizable? III) In large complex networks of practical interests, i.e., random networks and small worlds, what would be the required statistical characteristics of the substrate network to achieve the stable synchronization state?*

Next in this category, in chapter 3, the study addressed the following questions: *I)What would be the sufficient conditions under which the network 's error from nominal synchronization state would be bounded and stable? II) What would be the upper bound of that error from the nominal synchronization state?* By removing the condition of absolute similarity of the individual nodes, the bounded stability of the error from nominal synchronization trajectory

154

in presence of mismatches has been analyzed. That is, it has been assumed that although the nodes are similar but they are not identical. The extensive analytical treatment for random networks and small-worlds has been conducted and novel results have been derived.

The next progress made by this study has been to address the problems in decentralized control under more realistic condition on the controller gains. Questions such as *I) Feasibility: What is the minimum number of decentralized controllers to stabilize a network? II) Achievability: which nodes should have controllers to achieve that minimum number of controllers to have a stable synchronous state?* These questions have been addressed in chapter 4. Although the problem of feasibility happened to be NP-Hard with respect to networks size, a heuristic algorithm has been devised which under most circumstances approach the optimum solution and has a complexity of network size order.

Chapter 5 has addressed the following questions in fast switching networks:*I) what is the conditions of stability for the network under the fast switching networks? II) what is the minimum number of controllers to pin a network of fast switching oscillators?* The answer to the first question was proven to be simple: the conditions of stability is the same as previous part of the study if applied to the time/ensemble average of the switching network. The second question has been addressed with a tractable solution and the framework set proved to be useful in the study of the communication networks with fast moving nodes.

Third front of contributions addressed the following questions in distributed control of the networks in linear systems: *I) what is the minimal order of communications network to achieve stability in heterogeneous network of linear time varying systems with partially observable nodes? II) how these results scale for the large networks?* These questions have been addressed in chapter 6 and 7, respectively. By posing the problem as a convex problem, a tractable solution have found for the distributed control networks. The scalability problem

due to complexity of the general question has been addressed to linear time-invariant systems as the network size grows unboundedly. The latter results gave insight to structural effect of the networks and set a lower bound on the performance of the cyber network-design.

LIST OF REFERENCES

[1] S. Boccaletti, V. Latora, Y. Moreno, M. Chavez, and D.-U. Hwang, "Complex networks: Structure and dynamics," *Physics Reports*, vol. 424, pp. 175 – 308, 2006.

[2] R. C. Hilborn, *Chaos and Nonlinear Systems: An Introduction for Scientists and Engineers.* Oxford University Press, 92.

[3] A. Arenas, A. Diaz-Guilera, J. Kurths, Y. Moreno, and C. Zhou, "Synchronization in complex networks," *0805.2976*, vol. 469, no. 3, pp. 93–153, May 2008. [Online]. Available: http://arxiv.org/abs/0805.2976

[4] D. J. Watts and S. H. Strogatz, "Collective dynamics of **"small-world"** networks," *Letters to Nature*, vol. 393, pp. 440–442, 1998.

[5] L. M. Pecora and T. L. Carroll, "Master stability for synchronized coupled system," *Phys. Rev. Lett.*, vol. 80, no. 10, pp. 2109–2112, 1998.

[6] M. E. J. Newman and D. J. Watts, "Renormalization group analysis of the small-world network model," *Physics Letters A*, vol. 263, pp. 341–346, 1999.

[7] A.-L. Barabási and R. Albert, "Emergence of scaling in random networks," *Science*, vol. 286, no. 5439, pp. 509–512, 1999. [Online]. Available: http://www.sciencemag.org/content/286/5439/509.abstract

[8] M. Porfiri, D. Stilwell, and E. Bollt, "Synchronization in random weighted directed networks," *Circuits and Systems I: Regular Papers, IEEE Transactions on*, vol. 55, no. 10, pp. 3170–3177, Nov. 2008.

[9] Y. Hatano and M. Mesbahi, "Agreement over random networks," *IEEE Transactions on Automatic Control,*, vol. 50, no. 11, pp. 1867–1872, 2005.

[10] S. Boyd, A. Ghosh, B. Prabhakar, and D. Shah, "Randomized gossip algorithms," *Information Theory, IEEE Transactions on*, vol. 52, no. 6, pp. 2508–2530, 2006.

[11] V. M. Preciado and G. C. Verghese, "Synchronization in generalized Erdös-Rényi networks of nonlinear oscillators," in *Decision and Control, European Control Conference. CDC-ECC. 44th IEEE Conference on*, dec. 2005, pp. 4628 – 4633.

[12] A. Tahbaz-Salehi and A. Jadbabaie, "A necessary and sufficient condition for consensus over random networks," *Automatic Control, IEEE Transactions on*, vol. 53, no. 3, pp. 791–795, 2008.

[13] B. Shahrasbi and N. Rahnavard, "A clustering-based coordinated spectrum sensing in wideband large-scale cognitive radio networks," in *Globecom 2013 - Cognitive Radio and Networks Symposium (GC13 CogRN)*, Atlanta, USA, Dec. 2013.

[14] A. Sani, A. Abbasfar, and M. Fozooni, "Resource allocation for ofdma downlink with qos consideration," in *Ubiquitous and Future Networks (ICUFN), 2012 Fourth International Conference on*, July 2012, pp. 261–265.

[15] B. Shahrasbi, A. Talari, and N. Rahnavard, "TC-CSBP: Compressive sensing for time-correlated data based on belief propagation,," *2011 Annual Conference on Information Sciences and Systems (CISS'11)*, March 2011.

[16] A. Sani and A. Abbasfar, "Discrete bit-loading for ofdma downlink with qos consideration," in *Telecommunications Network Strategy and Planning Symposium (NETWORKS), 2012 XVth International*, Oct 2012, pp. 1–6.

[17] T. Chen, X. Liu, and W. Lu, "Pinning complex networks by a single controller," *IEEE Transactions on Circuits and Systems I*, vol. 54, no. 6, pp. 1317 –1326, june 2007.

[18] J. Zhou, J. an Lu, and J. Lu, "Pinning adaptive synchronization of a general complex dynamical network," *Automatica*, vol. 44, no. 4, pp. 996 – 1003, 2008.

[19] W. Yu, G. Chen, and J. Lu, "On pinning synchronization of complex dynamical networks," *Automatica*, vol. 45, no. 2, pp. 429 – 435, 2009.

[20] H. K. Khalil, *Nonlinear Systems*. Macmillan, 1992.

[21] G. A. Leonov and N. V. Kuznetsov, "Time-varying linearization and the perron effects," *International Journal of Bifurcation and Chaos*, vol. 17, no. 4, pp. 1079–1107, 2007.

[22] J. P. LaSalle, *The Stability of Dynamical Systems*. Society for Industrial and Applied Mathematics, 1976.

[23] B. Bollobas, *Random Graphs*. Cambridge University Press, 2001.

[24] B. Mohar, *The Laplacian spectrum of graphs*. Wiley, 1991.

[25] M. E. J. Newman, *Networks: An Introduction*. Oxford University Press, 2010.

[26] J. Travers and S. Milgram, "An experimental study of the small world problem," *Sociometry*, vol. 32, p. 425443, 1969.

[27] P. J. Harrison and V. A. West, "Six degrees of separation: on the prior probability that schizophrenia susceptibility genes converge on synapses, glutamate and nmda receptors," *Nature, Molecular Psychiatry*, vol. 11, pp. 981–983, 2006. [Online]. Available: http://www.nature.com/mp/journal/v11/n11/suppinfo/4001886s1.html

[28] N. Wiener, *Cybernetics or Control and Communication in the Animal and the Machine*. MIT press, 1965, vol. 25.

[29] A. T. Winfree, "Biological rhythms and the behavior of populations of coupled oscillators," *Journal of Theoretical Biology*, vol. 16, no. 1, pp. 15 – 42, 1967.

[30] A. E. Motter, "Bounding network spectra for network design," *New Journal of Physics*, vol. 9, no. 6, p. 182, 2007. [Online]. Available: http://stacks.iop.org/1367-2630/9/i=6/a=182

[31] R. Merris, "Laplacian graph eigenvectors," *Linear Algebra and its Applications*, vol. 278, no. 13, pp. 221 – 236, 1998.

[32] M. Barahona and L. M. Pecora, "Synchronization in small-world systems," *Phys. Rev. Lett.*, vol. 89, p. 054101, Jul 2002. [Online]. Available: http://link.aps.org/doi/10.1103/PhysRevLett.89.054101

[33] T. Nishikawa, A. E. Motter, Y.-C. Lai, and F. C. Hoppensteadt, "Heterogeneity in oscillator networks: Are smaller worlds easier to synchronize?" *Phys. Rev. Lett.*, vol. 91, no. 1, p. 014101, Jul 2003.

[34] X. F. Wang and G. Chen, "Synchronization in small-world dynamical networks," *International Journal of Bifurcation and Chaos*, vol. 12, no. 1, pp. 187–192, 2002.

[35] S. C. Manrubia and A. S. Mikhailov, "Mutual synchronization and clustering in randomly coupled chaotic dynamical networks," *Phys. Rev. E*, vol. 60, pp. 1579–1589, Aug 1999.

[36] T. Ichinomiya, "Frequency synchronization in a random oscillator network," *Phys. Rev. E*, vol. 70, p. 026116, Aug 2004.

[37] Y. Wu, Y. Shang, M. Chen, C. Zhou, and J. Kurths, "Synchronization in small-world networks," *Chaos*, vol. 18, no. 3, pp. 157–165, September 2008.

[38] M. Zhao, T. Zhou, B.-H. Wang, G. Yan, H.-J. Yang, and W.-J. Bai, "Relations between average distance, heterogeneity and network synchronizability," *Physica A: Statistical Mechanics and its Applications*, vol. 371, no. 2, pp. 773 – 780, 2006. [Online]. Available: http://www.sciencedirect.com/science/article/pii/S0378437106003815

[39] V. Preciado and A. Jadbabaie, "Moment-based analysis of synchronization in small-world networks of oscillators," in *Decision and Control, 2009 held jointly with the 2009 28th Chinese Control Conference. CDC/CCC 2009. Proceedings of the 48th IEEE Conference on*, 2009, pp. 1690–1695.

[40] M. Chavez, D.-U. Hwang, A. Amann, H. G. E. Hentschel, and S. Boccaletti, "Synchronization is enhanced in weighted complex networks," *Phys. Rev. Lett.*, vol. 94, p. 218701, Jun 2005. [Online]. Available: http://link.aps.org/doi/10.1103/PhysRevLett.94.218701

[41] S.-W. Son, B. J. Kim, H. Hong, and H. Jeong, "Dynamics and directionality in complex networks," *Phys. Rev. Lett.*, vol. 103, p. 228702, Nov 2009. [Online]. Available: http://link.aps.org/doi/10.1103/PhysRevLett.103.228702

[42] C. Zhou, A. E. Motter, and J. Kurths, "Universality in the synchronization of weighted random networks," *Phys. Rev. Lett.*, vol. 96, no. 3, p. 034101, Jan 2006.

[43] M. Frasca, A. Buscarino, A. Rizzo, and L. Fortuna, "Spatial pinning control," *Phys. Rev. Lett.*, vol. 108, p. 204102, May 2012.

[44] J. Lu and G. Chen, "A time-varying complex dynamical network model and its controlled synchronization criteria," *Automatic Control, IEEE Transactions on*, vol. 50, no. 6, pp. 841–846, 2005.

[45] "Synchronization analysis of delayed complex networks with time-varying couplings," *Physica A: Statistical Mechanics and its Applications*, vol. 387, no. 14, pp. 3729 – 3737, 2008.

[46] J. G. Restrepo, E. Ott, and B. R. Hunt, "Spatial patterns of desynchronization bursts in networks," *Phys. Rev. E*, vol. 69, no. 6, p. 066215, Jun 2004.

[47] J. Sun, E. M. Bolit, and T. Nishikawa, "Master stability functions for coupled nearly identical dynamical systems," *Europhysics Letters*, vol. 85, no. 6, pp. 1–5, 2009.

[48] F. Sorrentino and M. Porfiri, "Synchronization of coupled nonidentical dynamical systems," *Europhysics Letters*, vol. 93, no. 5, pp. 1–7, 2011.

[49] J. Xiang and G. Chen, "On the v-stability of complex dynamical networks," *Automatica*, vol. 43, no. 6, pp. 1049 – 1057, 2007.

[50] J. Zhao, D. J. Hill, and T. Liu, "Global bounded synchronization of general dynamical networks with nonidentical nodes," *Transactions on Automatic Control*, vol. 57, no. 10, pp. 2656–2572, October 2012.

[51] S. Acharyya and R. E. Amritkar, "Analysis of parameter mismatches in the master stability function for network synchronization," *Letters Journal Exploring the Frontiers of Physics*, vol. 99, no. 4, pp. 1–7, 2012.

[52] M. Porfiri, D. J. Stilwell, E. M. Bollt, and J. D. Skufca, "Random talk: Random walk and synchronizability in a moving neighborhood network," *Physica D: Nonlinear Phenomena*, vol. 224, no. 1-2, pp. 102 – 113, 2006.

[53] H. Lin and P. Antsaklis, "Stability and stabilizability of switched linear systems: A survey of recent results," *Automatic Control, IEEE Transactions on*, vol. 54, no. 2, pp. 308–322, Feb 2009.

[54] J. Zhao, D. J. Hill, and T. Liu, "Synchronization of complex dynamical networks with switching topology: A switched system point of view," *Automatica*, vol. 45, no. 11, pp. 2502–2511, Nov. 2009. [Online]. Available: http://dx.doi.org/10.1016/j.automatica.2009.07.013

[55] J. Daafouz, P. Riedinger, and C. Iung, "Stability analysis and control synthesis for switched systems: a switched lyapunov function approach," *Automatic Control, IEEE Transactions on*, vol. 47, no. 11, pp. 1883–1887, Nov 2002.

[56] R. DeCarlo, M. Branicky, S. Pettersson, and B. Lennartson, "Perspectives and results on the stability and stabilizability of hybrid systems," *Proceedings of the IEEE*, vol. 88, no. 7, pp. 1069–1082, July 2000.

[57] D. Stilwell, E. Bollt, and D. Roberson, "Sufficient conditions for fast switching synchronization in time-varying network topologies," *SIAM Journal on Applied Dynamical Systems*, vol. 5, no. 1, pp. 140–156, 2006.

[58] M. Porfiri and F. Fiorilli, "Node-to-node pinning control of complex networks," *Chaos: An Interdisciplinary Journal of Nonlinear Science*, vol. 19, no. 1, pp. –, 2009. [Online]. Available: http://scitation.aip.org/content/aip/journal/chaos/19/1/10.1063/1.3080192

[59] J.-J. Slotine and W. Li, *Applied Nonlinear Control*. Prentice Hall, Oct. 1991.

[60] Y.-Y. Liu, J.-J. Slotine, and A. Barabási, "Controllability of complex networks," *Nature*, vol. 473, pp. 167–173, May 2011.

[61] K.-Y. YOU and L.-H. XIE, "Survey of recent progress in networked control systems," *Acta Automatica Sinica*, vol. 39, no. 2, pp. 101 – 117, 2013. [Online]. Available: http://www.sciencedirect.com/science/article/pii/S1874102913600130

163

[62] F. Sorrentino, M. di Bernardo, F. Garofalo, and G. Chen, "Controllability of complex networks via pinning," *Phys. Rev. E*, vol. 75, pp. 1–6, 2007.

[63] Y. Tang, H. Gao, J. Kurths, and J. an Fang, "Evolutionary pinning control and its application in uav coordination," *Industrial Informatics, IEEE Transactions on*, vol. 8, no. 4, pp. 828–838, Nov 2012.

[64] G. Weisbuch, G. Deffuan, and F. Amblard, "Persuasion dynamics," *Physica A*, vol. 353, pp. 555–575, 2005.

[65] X. Wang and M. D. Lemmon, "Decentralized event-triggered broadcasts over networked control systems," in *Proceedings of the 11th international workshop on Hybrid Systems: Computation and Control*, ser. HSCC '08. Berlin, Heidelberg: Springer-Verlag, 2008, pp. 674–677.

[66] ——, "Event-triggering in distributed networked systems with data dropouts and delays," in *Proceedings of the 12th International Conference on Hybrid Systems: Computation and Control*, ser. HSCC '09. Berlin, Heidelberg: Springer-Verlag, 2009, pp. 366–380.

[67] M. J. Mazo, A. Anta, and P. Tabuada, "An iss self-triggered implementation of linear controllers," *Automatica*, vol. 46, no. 8, pp. 1310 – 1314, 2010.

[68] R. O. Grigoriev, M. C. Cross, and H. G. Schuster, "Pinning control of spatiotemporal chaos," *Phys. Rev. Lett.*, vol. 79, pp. 2795–2798, Oct 1997. [Online]. Available: http://link.aps.org/doi/10.1103/PhysRevLett.79.2795

[69] X. Li, X. Wang, and G. Chen, "Pinning a complex dynamical network to its equilibrium," *IEEE Transactions on Circuits and Systems I*, vol. 51, no. 10, pp. 2074 – 2087, oct. 2004.

[70] M. Porfiri and M. di Bernardo, "Criteria for global pinning-controllability of complex networks," *Automatica*, vol. 44, no. 12, pp. 3100 – 3106, 2008.

[71] P. DeLellis, M. di Bernardo, and M. Porfiri, "Pinning control of complex networks via edge snapping," *Chaos: An Interdisciplinary Journal of Nonlinear Science*, vol. 21, no. 3, p. 033119, 2011. [Online]. Available: http://link.aip.org/link/?CHA/21/033119/1

[72] R. Li, Z. Duan, and G. Chen, "Cost and effects of pinning control for network synchronization," *CoRR*, vol. abs/0710.2716, 2007. [Online]. Available: http://dblp.uni-trier.de/db/journals/corr/corr0710.html#abs-0710-2716

[73] X. Wang and M. D. Lemmon, "Event-triggering in distributed networked control systems," *Automatic Control, IEEE Transactions on*, vol. 56, no. 3, pp. 586 –601, march 2011.

[74] J. Hespanha, P. Naghshtabrizi, and Y. Xu, "A survey of recent results in networked control systems," *Proceedings of the IEEE*, vol. 95, no. 1, pp. 138–162, Jan 2007.

[75] X. Wang and M. D. Lemmon, "Event-triggered broadcasting across distributed networked control systems." American Control Conference, 2008, pp. 3139–3144.

[76] L. Zhang, H. Gao, and O. Kaynak, "Network-induced constraints in networked control systems –a survey," *Industrial Informatics, IEEE Transactions on*, vol. 9, no. 1, pp. 403–416, Feb 2013.

[77] M. Shirazi and A. Vosoughi, "Bayesian cramer-rao bound for distributed estimation of correlated data with non-linear observation model," in *Signals, Systems and Computers, 2014 48th Asilomar Conference on*, Nov 2014, pp. 1484–1488.

[78] D. Dimarogonas, E. Frazzoli, and K. Johansson, "Distributed event-triggered control for multi-agent systems," *Automatic Control, IEEE Transactions on*, vol. 57, no. 5, pp. 1291–1297, May 2012.

[79] W. Sun, J. L, S. Chen, and X. Yu, "Pinning impulsive control algorithms for complex network," *Chaos: An Interdisciplinary Journal of Nonlinear Science*, vol. 24, no. 1, pp. –, 2014. [Online]. Available: http://scitation.aip.org/content/aip/journal/chaos/24/1/10.1063/1.4869818

[80] X. Wang and M. Lemmon, "Self-triggered feedback control systems with finite-gain $\mathcal{L}_2$ stability," *Automatic Control, IEEE Transactions on*, vol. 54, no. 3, pp. 452–467, March 2009.

[81] L. C. Martins and L. G. Brunnet, "Multi-state coupled map lattices," *Physica A: Statistical Mechanics and its Applications*, vol. 296, no. 1-2, pp. 119 – 130, 2001.

[82] G. S. Medvedev, "Synchronization of coupled limit cycles," *preprint*, 2010, arXiv:1005.4074v2 [nlin.AO].

[83] W. So, "Commutativity and spectra of hermitian matrices," *Linear Algebra and its Applications*, vol. 212-213, no. 0, pp. 121 – 129, 1994.

[84] J. Lu, X. Yu, G. Chen, and D. Cheng, "Characterizing the synchronizability of small-world dynamical networks," *IEEE Transactions on Circuits and Systems I,*, vol. 51, no. 4, pp. 787–796, 2004.

[85] G. V. Osipov, A. S. Pikovsky, M. G. Rosenblum, and J. Kurths, "Phase synchronization effects in a lattice of nonidentical rössler oscillators," *Phys. Rev. E*, vol. 55, pp. 2353–2361, Mar 1997.

[86] E. P. Wigner, "On the distribution of the roots of certain symmetric matrices," *The Annals of Mathematics*, vol. 67, no. 2, pp. 325–327, 1958.

[87] D. Poland, "Loci of limit cycles," *Physical Review E*, vol. 49, no. 1, pp. 49–57, January 1994.

[88] J. L. Daleckii and M. G. Krein, *Stability of Solutions of Differential Equations in Banach Space*. American Mathematical Society, 1974.

[89] P. Moschopoulos and W. Canada, "The distribution function of a linear combination of chi-squares," *Computers and Mathematics with Applications*, vol. 10, no. 45, pp. 383 – 386, 1984. [Online]. Available: http://www.sciencedirect.com/science/article/pii/089812218490066X

[90] P. D. Lellis, M. di Bernardo, and G. Russo, "On quad, lipschitz, and contracting vector fields for consensus and synchronization of networks," *Circuits and Systems I: Regular Papers, IEEE Transactions on*, vol. 58, no. 3, pp. 576–583, 2011.

[91] M. Razeghi-Jahromi and A. Seyedi, "Stabilization of distributed networked control systems with minimal communications network," in *American Control Conference (ACC)*, July 2011, pp. 515 –520.

[92] S. Boyd and L. Vandenberghe, *Convex Optimization*. Cambridge University Press, Mar. 2004.

[93] A. Papoulis, *Probability, Random Variables, and Stochastic Processes*, 3rd ed. McGraw-Hill, 1991.

[94] D. Siljak, *Decentralized control of complex systems*. Dover Publications, 2012.

[95] A. Zecevic and D. Siljak, "Global low-rank enhancement of decentralized control for large-scale systems," *IEEE Transactions on Automatic Control*, vol. 50, no. 5, pp. 740–744, 2005.

[96] M. Mazo, A. Anta, and P. Tabuada, "An ISS self-triggered implementation of linear controllers," *Automatica*, vol. 46, no. 8, pp. 1310–1314, 2010.

[97] W. Zhang, M. Branicky, and S. Phillips, "Stability of networked control systems," *IEEE Control Systems*, vol. 21, no. 1, pp. 84–99, 2001.

[98] J. Baillieul and P. Antsaklis, "Control and communication challenges in networked real-time systems," *Proceedings of the IEEE*, vol. 95, no. 1, pp. 9–28, 2007.

[99] J. Hespanha, P. Naghshtabrizi, and Y. Xu, "A survey of recent results in networked control systems," *Proceedings of the IEEE*, vol. 95, no. 1, pp. 138–162, 2007.

[100] F. Wang and D. Liu, *Networked control systems: theory and applications.* Springer, 2008.

[101] X. Wang and M. Lemmon, "Event-triggering in distributed networked control systems," *IEEE Transactions on Automatic Control*, vol. 56, no. 3, pp. 586–601, 2011.

[102] L. Montestruque and P. Antsaklis, "Stability of model-based networked control systems with time-varying transmission times," *IEEE Transactions on Automatic Control*, vol. 49, no. 9, pp. 1562–1572, 2004.

[103] D. Nesic and A. Teel, "Input-output stability properties of networked control systems," *IEEE Transactions on Automatic Control*, vol. 49, no. 10, pp. 1650–1667, 2004.

[104] G. Walsh, H. Ye, and L. Bushnell, "Stability analysis of networked control systems," *IEEE Transactions on Control Systems Technology*, vol. 10, no. 3, pp. 438–446, 2002.

[105] P. Seiler and R. Sengupta, "An $\mathcal{H}_\infty$ approach to networked control," *IEEE Transactions on Automatic Control*, vol. 50, no. 3, pp. 356–364, 2005.

[106] M. Yu, L. Wang, T. Chu, and F. Hao, "Stabilization of networked control systems with data packet dropout and transmission delays: continuous-time case," *European Journal of Control*, vol. 11, no. 1, pp. 40–49, 2005.

[107] J. Wu and T. Chen, "Design of networked control systems with packet dropouts," *IEEE Transactions on Automatic Control*, vol. 52, no. 7, pp. 1314–1319, 2007.

[108] E. Witrant, C. Canudas-de Wit, D. Georges, and M. Alamir, "Remote stabilization via communication networks with a distributed control law," *IEEE Transactions on Automatic Control*, vol. 52, no. 8, pp. 1480–1485, 2007.

[109] H. Gao, T. Chen, and J. Lam, "A new delay system approach to network-based control," *Automatica*, vol. 44, no. 1, pp. 39 – 52, 2008.

[110] M. Rotkowitz and S. Lall, "A characterization of convex problems in decentralized control," *IEEE Transactions on Automatic Control*, vol. 51, no. 2, pp. 274–286, 2006.

[111] M. Rotkowitz and N. Martins, "On the closest quadratically invariant constraint," in *Proceedings of the 48th IEEE Conference on Decision and Control*. IEEE, 2009, pp. 1607–1612.

[112] M. Rotkowitz, R. Cogill, and S. Lall, "Convexity of optimal control over networks with delays and arbitrary topology," *International Journal of Systems, Control and Communications*, vol. 2, no. 1, pp. 30–54, 2010.

[113] J. Swigart and S. Lall, "A graph-theoretic approach to distributed control over networks," in *Proceedings of the 48th IEEE Conference on Decision and Control*. IEEE, 2009, pp. 5409–5414.

[114] P. Parrilo, P. Shah *et al.*, "A partial order approach to decentralized control," Ph.D. dissertation, Massachusetts Institute of Technology, 2011.

[115] P. Shah and P. Parrilo, "An optimal controller architecture for poset-causal systems," in *50th IEEE Conference on Decision and Control.* IEEE, 2011, pp. 5522–5528.

[116] S. Amin, "Smart grid: Overview, issues and opportunities. advances and challenges in sensing, modeling, simulation, optimization and control," *European Journal of Control*, vol. 17, no. 5-6, pp. 547–567, 2011.

[117] J. van Schuppen, O. Boutin, P. Kempker, J. Komenda, T. Masopust, N. Pambakian, and A. Ran, "Control of distributed systems: Tutorial and overview," *European Journal of Control*, vol. 17, no. 5, pp. 579–602, 2011.

[118] K. Rudie, S. Lafortune, and F. Lin, "Minimal communication in a distributed discrete-event system," *IEEE Transactions on Automatic Control*, vol. 48, no. 6, pp. 957–975, 2003.

[119] F. Lin, K. Rudie, and S. Lafortune, "Minimal communication for essential transitions in a distributed discrete-event system," *IEEE Transactions on Automatic Control*, vol. 52, no. 8, pp. 1495–1502, 2007.

[120] M. Razeghi-Jahromi and A. Seyedi, "Stabilization of networked control systems with sparse observer-controller networks," *to appear in IEEE Transactions on Automatic Control*, vol. 60, no. 6, 2015, available at arXiv:1303.2280 [math.OC].

[121] D. Liberzon and A. S. Morse, "Basic problems in stability and design of switched systems," *IEEE Control Systems*, vol. 19, no. 5, pp. 59–70, 1999.

[122] D. Liberzon, *Switching in systems and control.* Springer, 2003.

[123] A. N. Michel, "Recent trends in the stability analysis of hybrid dynamical systems," *IEEE Transactions on Circuits and Systems I: Fundamental Theory and Applications*, vol. 46, no. 1, pp. 120–134, 1999.

[124] H. Lin and P. J. Antsaklis, "Stability and stabilizability of switched linear systems: a survey of recent results," *IEEE Transactions on Automatic control*, vol. 54, no. 2, pp. 308–322, 2009.

[125] W. Haddad and V. Chellaboina, *Nonlinear dynamical systems and control: a Lyapunov-based approach.* Princeton University Press, 2011.

[126] I. Grossmann, "Review of nonlinear mixed-integer and disjunctive programming techniques," *Optimization and Engineering*, vol. 3, no. 3, pp. 227–252, 2002.

[127] K. Ogata, *Modern control engineering, 1997.* Prentice-Hall Inc., NJ.